



HEINRICH HEINE  
UNIVERSITÄT DÜSSELDORF

**Enrichment, isolation and molecular  
characterization of circulating tumour cells for  
treatment optimization in metastatic breast cancer**

Inaugural dissertation

for the attainment of the title of doctor  
in the Faculty of Mathematics and Natural Sciences  
at the Heinrich Heine University Düsseldorf

presented by

**Rita Lampignano**  
from Bari, Italy

Düsseldorf, November 2017

from the institute for Obstetrics and Gynaecology  
at the Heinrich Heine University Düsseldorf

Published by permission of the  
Faculty of Mathematics and Natural Sciences at  
Heinrich Heine University Düsseldorf

Supervisor: Prof. Dr. Hans Neubauer  
Co-supervisor: Prof. Dr. Vlada B. Urlacher

Date of the oral examination: 26/04/2018

Part of this thesis was published in:

*“A novel workflow to enrich and isolate patient-matched EpCAM<sup>high</sup> and EpCAM<sup>low/negative</sup> CTCs enables the comparative characterization of the PIK3CA status in metastatic breast cancer”*. **Lampignano R**, Yang L, Neumann MHD, Franken A, Fehm T, Niederacher D, Neubauer H. International Journal of Molecular Sciences. 2017, 18, 1885, doi:10.3390/ijms18091885.

*“EpCAM– and EpCAM+ circulating tumor cells in metastatic breast and prostate cancer patients: a multicentre study”*. de Wit S, Manicone M, Rossi E, Trap EK, **Lampignano R**, Yang L, Oulhen M, Crespo M, Berghuis AMS, Andree KC, Vidotto R, Tzschaschel M, Colomba E, Flohr P, Zamarchi R, Rack B, Alunni-Fabbroni M, Neubauer H, Fehm T, Farace F, de Bono JS, IJzerman MJ, Terstappen LWMM. Scientific Reports. *Submitted*.

*“Diagnostic leukapheresis results in a significant increase in CTC yield in metastatic breast and prostate cancer”*. Andree KC, Mentink A, Swennenhuis JF, Terstappen LWMM, Stoecklein NH, Neves RPL, **Lampignano R**, Neubauer H, Fehm T, Fischer JC, Rossi E, Manicone M, Basso U, Marson P, Zamarchi R, Lorient Y, Lapierre V, Faugeroux V, Oulhen M, Ebbs B, Lambros M, Crespo M, Flohr P, de Bono JS. American Association for Cancer Research Annual Meeting. 2017.

*A Charlie*



# Table of Contents

<b>1. Introduction.....</b>	<b>1</b>
1.1. Hallmarks of (breast) cancer.....	1
1.2. Breast cancer .....	2
1.2.1. Epidemiology and aetiology .....	2
1.2.2. Histopathology .....	3
1.2.3. Clinical subtypes and treatment approaches.....	5
1.2.4. PI3K pathway and PIK3CA mutations.....	6
1.2.4.1. Targeting the PI3K pathway .....	8
1.3. The invasion-metastasis cascade.....	10
1.3.1. Invasion and intravasation .....	10
1.3.1.1. The epithelial-to-mesenchymal transition.....	12
1.3.2. Extravasation and colonization .....	13
1.4. Circulating tumour cells.....	14
1.4.1. Definition and characteristics .....	14
1.4.2. The EpCAM <sup>low/negative</sup> subset of CTCs.....	15
1.4.3. Challenges in CTC-research: rarity and heterogeneity .....	16
1.4.3.1. Label-dependent enrichment strategies .....	16
1.4.3.2. Label-free enrichment strategies.....	17
1.4.3.3. Detecting and isolating CTCs.....	19
1.4.4. Clinical role of CTCs in metastatic breast cancer .....	20
1.4.4.1. Validity of CTC enumeration .....	20
1.4.4.2. Utility of CTC characterization .....	21
1.4.4.3. Clinical relevance of CTCs with epithelial-mesenchymal plasticity .....	22
<b>2. Aim of the study .....</b>	<b>23</b>
<b>3. Materials and Methods.....</b>	<b>25</b>
3.1. Cell lines.....	25
3.1.1. Culture conditions .....	25
3.1.2. Sub-culturing of MCF-7 and T47D cells.....	25
3.1.3. Cryopreservation and re-culturing.....	25
3.2. Cytospins preparation .....	26
3.2.1. MCF-7 and whole blood fixation .....	26

3.2.2.	Isolation of leukocytes from whole blood .....	26
3.2.3.	Cell counting.....	27
3.2.4.	Spinning of cells.....	27
3.3.	Enrichment, detection and isolation of patient-matched EpCAM <sup>high</sup> and EpCAM <sup>low/negative</sup> CTCs combining CellSearch® and VyCAP™ systems.....	28
3.3.1.	Validation of the immunocytostaining.....	29
3.3.1.1.	Immunocytostaining of cytospins.....	30
3.3.1.2.	Epifluorescence microscopy .....	30
3.3.2.	Validation of the workflow.....	31
3.3.2.1.	Immunostaining of cells in suspension .....	31
3.3.2.2.	Cell line spiking experiments .....	31
3.3.2.3.	Immunocytostaining on microsieves .....	32
3.3.3.	Processing mBC patients' blood samples .....	33
3.3.4.	Processing mBC patients' DLA samples .....	33
3.3.5.	Detecting tumour cells: image analysis.....	33
3.4.	Enrichment and isolation of patient-matched EpCAM <sup>high</sup> and EpCAM <sup>low/negative</sup> CTCs combining CellSearch®, Parsortix™ and CellCelector™ systems .....	34
3.4.1.	Validation of the immunocytostaining.....	36
3.4.1.1.	Immunocytostaining of cytospins.....	37
3.4.1.2.	Epifluorescence microscopy .....	37
3.4.2.	Validation of the workflow.....	38
3.4.2.1.	Immunostaining of cells in suspension .....	38
3.4.2.2.	Cell line spiking experiments .....	38
3.4.2.3.	Detection and isolation of tumour cells .....	39
3.4.2.4.	Immunocytostaining in cassette .....	40
3.4.3.	Processing MBC patients' blood samples .....	40
3.4.3.1.	Statistical analysis .....	40
3.5.	Molecular characterization of single patient-matched EpCAM <sup>high</sup> and EpCAM <sup>low/negative</sup> CTCs.....	41
3.5.1.	Whole genome amplification .....	41
3.5.1.1.	Quality control multiplex PCR.....	42
3.5.1.2.	DNA Gel-electrophoresis .....	42
3.5.1.3.	Statistical analysis .....	43

3.5.2.	PIK3CA Exons 9 and 20 specific PCRs .....	43
3.5.3.	Cleaning of PCR products .....	44
3.5.3.1.	ExoSAP-IT® protocol.....	44
3.5.3.2.	DNA gel-extraction.....	44
3.5.4.	DNA quantification .....	44
3.5.5.	PIK3CA Exons 9 and 20 Sanger sequencing.....	45
3.5.6.	Sequencing data analysis .....	45
<b>4.</b>	<b>Results.....</b>	<b>46</b>
4.1.	Enrichment and detection of patient-matched EpCAM <sup>high</sup> and EpCAM <sup>low/negative</sup> CTCs combining CellSearch® and VyCAP™ systems .....	46
4.1.1.	Validation of immunostaining on cytopins.....	46
4.1.2.	Tumour cell recovery rates of VyCAP™ filters.....	47
4.1.3.	Validation of immunocytostaining on microsieves.....	47
4.1.4.	Processing patients' blood samples.....	48
4.1.5.	Processing patients' DLA samples.....	52
4.2.	Enrichment and isolation of patient-matched EpCAM <sup>high</sup> and EpCAM <sup>low/negative</sup> CTCs combining CellSearch®, Parsortix™ and CellCelector™ systems .....	55
4.2.1.	Validation of immunostaining on cytopins.....	55
4.2.2.	Tumour cell recovery rates of Parsortix™ system.....	56
4.2.3.	Validation of immunocytostaining inside Parsortix™ cassettes .....	56
4.2.4.	Processing patients' blood samples through 6.5 µm Parsotix™ cassettes .....	58
4.2.5.	Isolation of single tumour cells via CellCelector™ .....	60
4.3.	Molecular characterization of single patient-matched EpCAM <sup>high</sup> and EpCAM <sup>low/negative</sup> CTCs.....	62
4.3.1.	Amplification of whole genomes of single tumour cells.....	62
4.3.2.	Detection of PIK3CA exons 9 and 20 amplicons .....	64
4.3.3.	Sequencing of PIK3CA hotspot regions .....	66
<b>5.</b>	<b>Discussion.....</b>	<b>70</b>
5.1.	Enrichment and detection of patient-matched EpCAM <sup>high</sup> and EpCAM <sup>low/negative</sup> CTCs combining CellSearch® and VyCAP™ systems .....	71
5.2.	Enrichment and isolation of patient-matched EpCAM <sup>high</sup> and EpCAM <sup>low/negative</sup> CTCs combining CellSearch®, Parsortix™ and CellCelector™ systems .....	74
5.3.	Molecular characterization of single patient-matched EpCAM <sup>high</sup> and EpCAM <sup>low/negative</sup> CTCs.....	77

5.4. Conclusions and outlooks .....	79
<b>Summary .....</b>	<b>81</b>
<b>Zusammenfassung .....</b>	<b>83</b>
<b>References .....</b>	<b>85</b>
<b>Appendix .....</b>	<b>98</b>
A. <i>Statement</i> .....	98
B. <i>List of Abbreviations</i> .....	99
C. <i>List of Figures</i> .....	101
D. <i>List of Tables</i> .....	102
E. <i>Acknowledgments</i> .....	104
F. <i>Scientific Curriculum Vitae</i> .....	105

# 1. Introduction

## 1.1. Hallmarks of (breast) cancer

Cancer is a genetic disorder caused by a rapid and abnormal growth of cells beyond physiological boundaries of the related tissue [1]. The process which leads a normal cell to progressively acquire the malignant phenotype is named “carcinogenesis” and requires the accumulation of multiple genetic alterations [2]. As result of many research studies performed in the last decade, the malignant cell phenotype has been depicted by eight fundamental biological capabilities [3]. The so called “hallmarks of cancer” comprise sustaining proliferative signalling, evasion of growth inhibition, tissue invasion and spreading to distant sites (metastasis; see chapter **1.3**), replicative immortality, sustained angiogenesis, evasion of apoptosis and the “emerging hallmarks”, deregulation of energy metabolism and evasion of the immune system [3]. Last but not least, genome instability, mutations, and tumour-promoting inflammation enable the acquisition of both core and emerging cancer traits (Figure 1) [3].

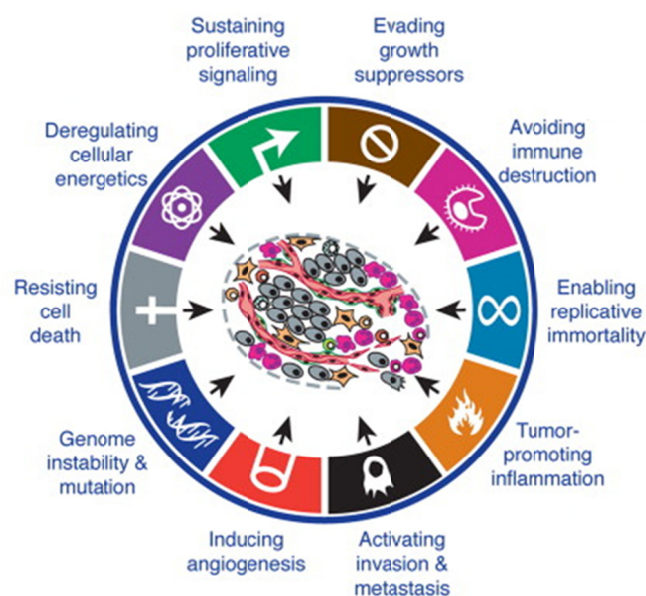


**Figure 1. The Hallmarks of Cancer, adapted from Hanahan and Weinberg, 2011 [3]**

The phenotype of a malignant tumour cell is characterized by eight properties, named hallmarks of cancer, which are all required for the tumorigenesis. Any lack within them, may block the whole invasion and metastatic process.

Over a period of time, several tumours acquire greater malignant abilities and consequently become more aggressive. This so called “tumour progression” can be explained with the genomic instability and the accumulation of multiple mutations in different cells which generate sub-clones with different phenotypes, leading to tumour heterogeneity. Moreover, during tumour progression, abnormal cells in the tumour mass are exposed to selection pressures which enrich sub-clones capable to survive, grow, invade surrounding tissues and metastasize (Figure 2) [2,4]. Both the concepts of heterogeneity and positive selection shed light on the trend for tumours to become more aggressive and resistant to therapies over the time.

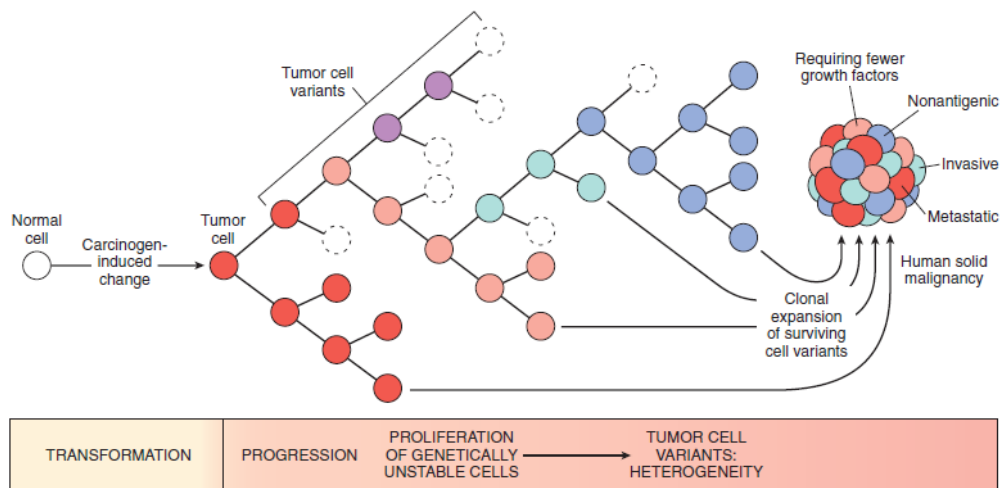


**Figure 2. Tumour progression and heterogeneity, by Kumar et al., 2014 [2]**

The tumour mass is characterized by different sub-clones originated from the same tumour cell. Each of these sub-clones has different properties in terms of growth, survival, invasion and metastatic potential. The heterogeneity of the tumour mass is involved in treatment resistance.

## 1.2. Breast cancer

### 1.2.1. Epidemiology and aetiology

Breast Cancer is a disease caused by the rapid and abnormal growth of epithelial cells from breast tissues beyond their physiological boundaries [1]. Among women worldwide, this carcinoma was reported to be the most common form of cancer as well as the main cause of death, with 1.7 million of diagnosed cases in 2012 and nearly 31% of related deceases. According to predictions, the incidence of breast cancer will reach 3.2 million new cases per year by 2050, making this disease, a major health problem worldwide [5]. In 2012,

70.000 new cases of breast cancer were registered in Germany – of which ~26% died – and it was estimated that nearly 12.5% of German women will develop this disease in their life time, at onset of 64 years on average [6]. Major risk factors for female breast cancer are obesity together with lack of physical activity, old age, heavy alcohol intake, early menarche, assumption of hormonal contraceptives and late age at first birth [1,5]. The transformation of a normal cell into a cancerous one requires the combination of multiple factors: biological intrinsic (e.g. genetic background) and extrinsic (e.g. viruses), chemical (e.g. alcohol, tobacco) and physical ones (e.g. radiations) [7]. Typically, mutations occurring on critical genes involved in regulating cell growth, proliferation, differentiation can act as triggers for pre-cancerous lesions [8]. In breast carcinoma, there are several deregulated signalling pathways, among others: hormone receptor signalling (i.e. oestrogen receptor [ER], progesterone receptor [PR] and androgen receptor [AR]), cell growth signalling (i.e. tyrosine kinase receptor [i.e. HER2/neu]), cell cycle (e.g. PI3K, see chapter **1.2.4**) and DNA damage/repair signalling (e.g. tumour protein p53, breast cancer 1 and 2 [BRCA1 and 2]) [8]. It was observed that 5-10% of all breast cancer cases are hereditary and linked to genetic mutations, comprising in about 90% of them the genes BRCA1 and BRCA2 [9,10].

## **1.2.2. Histopathology**

Breast cancer is a considerably heterogeneous disease which comprises tumours with various intrinsic features, clinical characteristics and therapeutic responses [11]. Therefore, patient stratification is required for prognostic predictions and for the identification of effective treatment strategies.

The human female breast is composed by lobes and ducts surrounded by adipose tissue. Each lobe consists of small glands named lobules, which are formed, in turn, by dozens of acini. The whole lobular architecture ends in several ducts, transferring milk provided by the acini, to the nipple. Both lobules and ducts are composed by a single layer of luminal epithelial cells, surrounded by a layer of myoepithelial cells, enclosed in turn, by the basement membrane. The basement membrane separates this epithelial bilayer from the stromal tissue, comprising the extracellular matrix, fibroblasts, immune cells, adipocytes, blood and lymphatic vessels (Figure 3) [1,11].

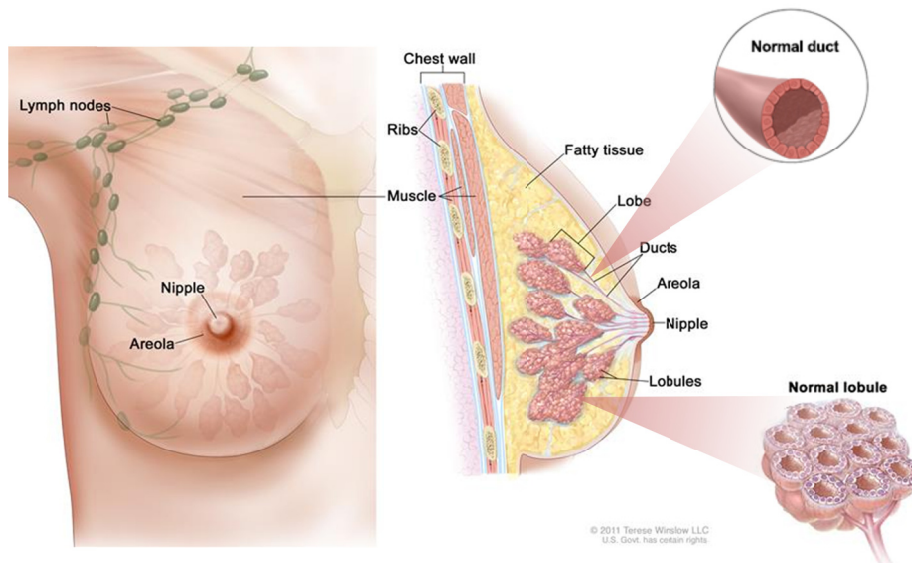


**Figure 3. The human female breast, adapted from National Cancer Institute and Afaigo.net [12,13]**

The human female breast mainly consists of ducts, lobes, and adipose tissue in proximity of the axillar lymph nodes. Tumour masses may originate either within the ducts (ductal-tumour) or within the lobes (lobular-tumour).

During the progression of the pre-cancerous lesion, the destruction of the basement membrane by the tumour cells, distinguishes between carcinoma *in situ* and invasive carcinoma (Figure 4) and contributes to define the staging of the disease. With the breach of the basement membrane, tumour cells can spread in various sites of the body through tissues, lymph and blood vessels, thus starting an invasive tumour [11].

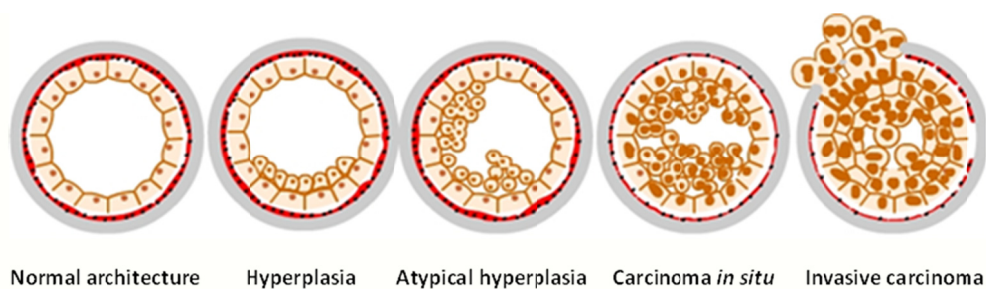


**Figure 4. The formation of an invasive carcinoma, adapted from RNCeus.com [14]**

The formation of an invasive carcinoma is a multistep process during which cells proliferate more than usual (phase named “hyperplasia), no longer lined up in two layers (phase named “atypical hyperplasia), then these cells may originate an abnormal structure and loss of differentiation (phase named “carcinoma *in situ*”). The hyperproliferation of these tumour cells over the physiological tissue boundaries defines the “invasive carcinoma”.

The stage of a tumour refers to how extended the cancer is and it is usually expressed as a number on a scale from 0 to IV, with “stage 0” describing non-invasive disease and “stage IV” invasive one which has disseminated over the breast tissues. Major factors taken in consideration for the staging are: size of the tumours, whether it has spread to lymph nodes and/or to a different site of the body, and whether it is invasive or non-invasive.

It was observed that breast cancer usually develops in cells from the lining of the ducts (*ductal carcinoma*) and of the lobules (*lobular carcinoma*). The invasive ductal and lobular carcinomas represent together the 90% of the cases of breast cancer. Remaining “special cases” of this disease comprise medullary, neuroendocrine, tubular, apocrine, metaplastic, mucinous, inflammatory, comedo, adenoid cystic, and micro papillary breast cancers [11].

### **1.2.3. Clinical subtypes and treatment approaches**

The identification of breast carcinoma subtypes is of great importance due to specific treatment approaches available and related different outcomes. The expression of the human epidermal growth factors 2 (HER2/neu) and of hormone receptors was identified to classify the three major clinical subtypes of breast cancer: HER2/neu-enriched, estrogen receptor (ER) positive and triple negative [15].

The “*HER2/neu enriched*” subtype is characterized by the overexpression of the HER2/neu oncogene and by a low/no expression of both ER and PR. This gene was found overexpressed in ~15% of the breast cancers and is currently aim of specific therapies which improved the overall survival (OS) of patients suffering of this breast cancer subtype [11,16,17]. These targeted treatments mainly comprise monoclonal antibodies interfering with signalling pathways involved in carcinogenesis, such as tyrosine kinase receptors signalling inhibitors (e.g. trastuzumab [anti-HER2/neu], lapatinib [anti-ERK], PI3K inhibitors) [18].

The expression of both hormone receptors ER and PR defines the “*luminal*” subtype which can be further sub-classified according to the proliferation rate and to the HER2/neu status (positive or negative). Hormone receptor positive subgroups represent the most common molecular types of breast cancer (~70% of the cases) and are associated with the best OS [11,16,17,19]. Treatment strategies in luminal breast cancer often comprise

hormone receptor modulators (e.g. tamoxifen), inhibitors of oestrogen synthesis (e.g. aromatase inhibitors) or ER antagonists (e.g. fulvestrant) [18].

Nearly 15% of breast cancer cases were observed to express low or no levels of the above mentioned molecular receptors and therefore they were grouped within the so called "triple negative" subtype. This breast carcinoma subgroup is commonly diagnosed among young women and associated with the worst prognosis due to the non-response to either endocrine treatment or monoclonal antibodies approaches [16,17]. Nevertheless, in the last decades, some studies have pointed out the existence of a subpopulation of triple negative breast cancer which might be sensitive to epidermal growth factor receptors inhibitors [18].

#### **1.2.4. PI3K pathway and PIK3CA mutations**

The HER2/neu receptor is one of the major triggers of the Phosphatidylinositol 3-kinases (PI3K) pathway, which is named based on the PI3Ks proteins, a family of intracellular signal transducer proteins. Upon interaction with tyrosine kinase receptors, these kinases phosphorylate the 3-position hydroxyl group of the inositol ring of the phosphatidylinositol of protein kinases AKTs [20]. PI3Ks are classified in three major classes according to their structures and roles. The class IA of PI3Ks is the most involved in the development of cancer [21]. PI3Ks IA proteins are heterodimers comprising a regulatory subunit, the p85, and a catalytic subunit, the p110 which consists of subunits  $\alpha$  and  $\beta$ , whose activity is inhibited upon binding to p85. The regulatory subunit, by interacting with HER2/neu, transduces activation signals to the p110 protein which, then, activates a cascade of signalling events involved in several vital functions such as cell survival, proliferation, differentiation, intracellular trafficking and migration (Figure 5) [8,21–23].

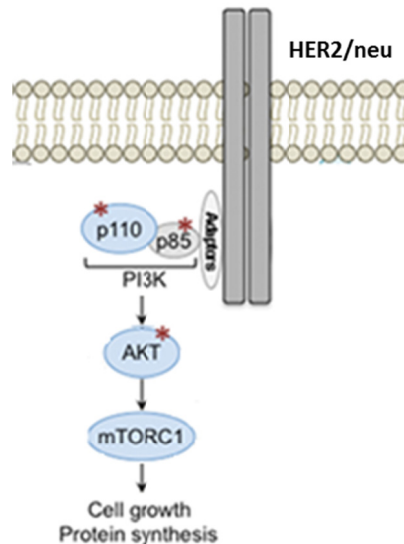


**Figure 5. The simplified PI3K pathway, adapted from Weigelt and Downward, 2012 [24]**

The PI3K signalling pathway is involved in cell growth and survival. It is mainly triggered by the HER2 receptor, transducing then the signal to PI3K proteins which phosphorylate the protein kinase AKT. AKT activates the mTOR complex 1, which can then migrate into the nucleus and promote the translation of proteins.

Abnormal activation and (epi)genetic alterations in the PI3K signalling pathway components are commonly observed in several types of cancer (gastric, ovarian, breast and lung) and are involved in tumour initiation and progression [8,21,23]. Among these involved components, the PIK3CA is the most mutated oncogene in breast cancer [8,21–23]. The PIK3CA gene is located on the long arm (q) of the Chromosome 3 and encodes for the catalytic subunit p110 $\alpha$ , ubiquitously expressed in all types of cells [25]. The p110 $\alpha$  subunit is composed by 5 domains: an N-terminal binding subunit p85 (ABD), a RAS-binding domain (RBD), a C2 domain binding to the cell membrane, a helical domain and a C-terminal kinase catalytic domain involved in regulating the catalytic activity of PI3K [8,21]. The PIK3CA gene was reported to be mutated in up to 40% of primary breast cancer cases[8], and in higher frequency in related metastasis [26]. Most common breast carcinomas harbouring PIK3CA mutations express ER at frequency of 30%-50% and HER2/neu in 15%-30% of the cases [8,22,23]. The majority of PIK3CA oncogenic mutations are “gain of function” changes occurring in exons 9 (kinase domain) and 20 (helical domain), more precisely in the “hotspots” codons E542, E545 (exon 9) and H1047 (exon 20; Figure 6) [8,21–23].



**Figure 6. The PIK3CA oncogene, adapted from Troxell, 2015 [22]**

The PIK3CA oncogene consists of following domains: p85-binding ABD, RAS-binding RBD, cell membrane-binding C2, Helical, and catalytic Kinase. Major mutations occur within the helical and the kinase domains, mainly within exons 9 and 20.

The most frequently reported amino acid substitutions are the E542K, E545K (glutamine to lysine) and H1047R (histidine to arginine) which were reported in 86% of PIK3CA-mutated breast cancer cases [27].

Even though all the mechanisms underlying the effects of the PIK3CA oncogenic mutations have not been fully clarified yet, it has been already suggested that they activate the PI3K kinase activity and therefore the PI3K pathway, in different ways [28,29]. Oncogenic mutations in the helical domain were reported to promote a gain of function by enabling the catalytic subunit p110 $\alpha$  to escape the inhibitory effect of the regulatory subunit p85 [28,29]. On the contrary, it was suggested that mutations in the kinase domain activate the PI3K signalling independently on interactions with p85 [29]. Moreover, recent results showed that the E545K mutation, unlike the H1047R, is associated with the activation of the kinase AKT1, a downstream target of PI3K [30]. The different prognostic value of exon 9 and 20 PIK3CA mutations is, to date, controversial. Preliminary data suggest better prognosis in case of mutations in the exon 20 than in exon 9, which correlate, instead, with early recurrence [31,32]. However, further investigations are surely needed to confirm these suggestions.

### **1.2.4.1. Targeting the PI3K pathway**

Initial studies reported contradictory results regarding the correlation of PIK3CA hotspot mutations and clinical outcomes [8,22]. Several research groups observed an increased resistance to HER2/neu targeted therapies caused by PI3K activating mutations, [8,25] although mechanisms of this resistance have not been clarified, yet [8]. Interestingly, it was demonstrated that the two breast cancer cell lines MDA-361 (ER+, HER2/neu+) and HCC-202 (ER-, HER2/neu+) harbouring the oncogenic mutation E545K, were resistant to the anti-HER2/neu, lapatinib. On the contrary, the breast cancer cell lines HCC-1954 (ER-, HER2/neu+) and SUM-190 (ER-/HER2/neu+) harbouring the oncogenic mutation H1047R were lapatinib

sensitive [33]. All these results combined with the reported oncogenic properties of PIK3CA hotspot mutations and with the frequent activation of the PI3K signalling observed in breast cancer, make this pathway a prime therapeutic target in patients. In the last decade, several pharmacological agents targeting PI3Ks proteins were designed. Those tested in clinical trials can be grouped into two classes: PI3K inhibitors and dual PI3K/mTOR inhibitors (Table 1).

**Table 1. PI3Ks inhibitors in clinical trials, based on Ma et al. 2015 [23]**

<b>Pan-PI3K inhibitors</b>
GDC-0941 (pictilisib)
BKM120 (buparlisib)
XL147
PX-866
BAY 80-6946
CH5132799
<b>p110<math>\alpha</math>-specific inhibitors</b>
BYL719 (alpelisib)
MLN1117
GDC-0032 (taselisib, also targets p110g and d)
<b>p110<math>\beta</math>-specific inhibitors</b>
AZD8186
SAR260301
GSK2636771
<b>Dual PI3K/mTOR inhibitors</b>
BEZ235
BGT226
XL765
GDC-0980

Promising results were observed in metastatic ER+ breast cancer patients resistant to endocrine therapy, by including an anti-PI3K drug in the therapeutic approach [23]. As well as targeting both HER2/neu and PI3K pathway in patients suffering of HER2/neu+ breast cancers has been shown to effectively overcome hormonal treatment resistance [23].

Despite all these promising results, the presence of PIK3CA mutations does not guarantee a clinical response to anti-PI3K drugs, since the downstream signalling cascade may be activated by parallel pathways. [25]. Furthermore, the pharmacological combinations able to provide best clinical results in case of PIK3CA mutations still need to be determined.

## 1.3. The invasion-metastasis cascade

The ability of a tumour cell to invade the surrounding tissue and to spread to distant organs is one of the major traits which distinguishes cancer from benign tumour [2,3]. This process involves several steps which are altogether known as “invasion-metastasis cascade” and consists of: local invasion and intravasation into blood and lymphatic vessels, transit through the haematogenous and lymphatic systems, extravasation from vessels, and formation of micro metastases which subsequently grow into macroscopic tumours (a process named “colonization”; Figure 7)[4].

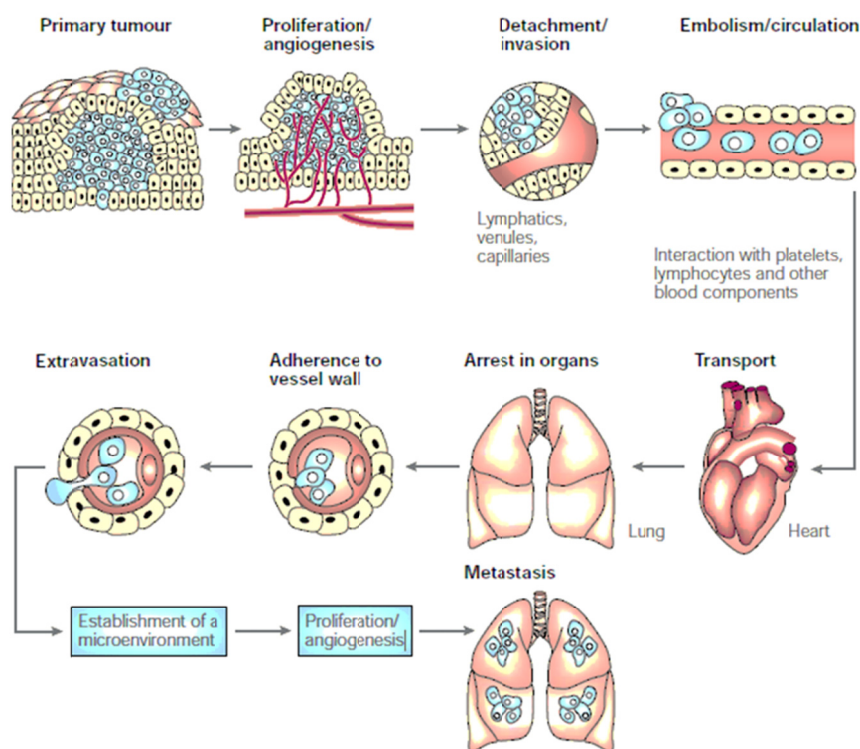


**Figure 7. The invasion-metastasis cascade, adapted from Fidler, 2003 [4]**

In order to form metastasis, tumour cells of the primary tumour need to invade blood and/or lymph vessels, circulate within the respective system and then extravasate in proximity of these organs which they possess a specific trophic to. Afterwards, tumour cells need to find an optimal niche for their growth and survival, thereby leading to the origin of a new tumour mass. *Permission to reproduce and adapt this figure has been granted by Springer Nature.*

### 1.3.1. Invasion and intravasation

In order to disseminate into blood and lymphatic vessels, a tumour cell must first disrupt the basement membrane and then cross the interstitial connective tissue. This multi-step process starts by loosening intercellular junctions between tumour cells. In fact, in human

epithelial cancers, the downregulation of the major cell-to-cell adhesion molecules was often reported [2]. The best characterized alterations involve the cell-cell interaction protein E-cadherin, frequently reported to be downregulated, mutated [34,35] and/or suppressed by other proteins (e.g. the epithelial cell adhesion molecule [EpCAM]) [36]. After the loss of intercellular connections, tumour cells actively remodel components of the basement membrane (e.g. collagen IV and laminin) either by secreting proteolytic enzymes (e.g. matrix metalloproteinases [MMPs]) or by inducing stromal cells to produce them. In parallel, MMPs-inhibitors are downregulated in order to facilitate the tissue degradation [2]. Afterwards, tumour cells downregulate their receptors for the ligands expressed by the basement membrane, to enhance their own migration into blood and lymphatic vessels. The last step involves several receptors and extracellular signalling proteins (e.g. tumour cell-derived cytokines, products of membrane degradation and growth factors with a chemotactic activity) which lead to the migration of the tumour cells [2].

It was recently suggested that the dissemination of tumour cells might occur in different ways which would however coexist: **a)** mechanical dissemination: cancer cells disseminate into the circulation by preserving their epithelial phenotype; **b)** epithelial-to-mesenchymal transition (EMT): cancer cells gradually acquire mesenchymal phenotypes which supports their extra- and intravasation (Figure 8) [3,37,38].

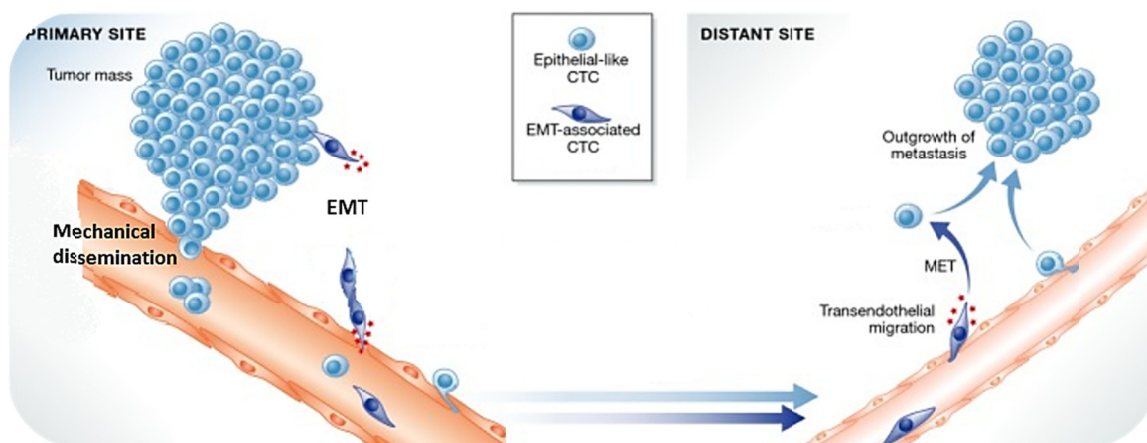


**Figure 8. The dissemination and colonization of tumour cells, adapted from Joosse et al., 2015 [39]**

The coexistence of two different processes of dissemination and colonization has been proposed. CTCs may require a change from an epithelial to a mesenchymal phenotype in order to intravasate and vice versa, from the mesenchymal to the epithelial to extravasate and colonize. Alternatively, CTCs may disseminate and colonize without any phenotypic changes.

### 1.3.1.1. The epithelial-to-mesenchymal transition

Several studies postulated that, within the first steps of the metastatic cascade, tumour cells may lose some typical epithelial traits (e.g. polygonal shape, apical-basal polarity, cell-cell junctions and cell-basement membrane connections, expression of e-cadherin, mucin1, laminin-1, EpCAM) to gain, among others, some mesenchymal properties (e.g. spindle shape, lack of both cell polarity and cell-cell junctions, expression of vimentin, fibronectin, transcriptional factors SNAI1, SNAI2, TWIST) which would facilitate both migration and invasion [40–42]. This process is named epithelial-to-mesenchymal transition (EMT) and is involved in different biological contexts such as embryo development, tissue regeneration and tumour progression (Figure 9) [43].

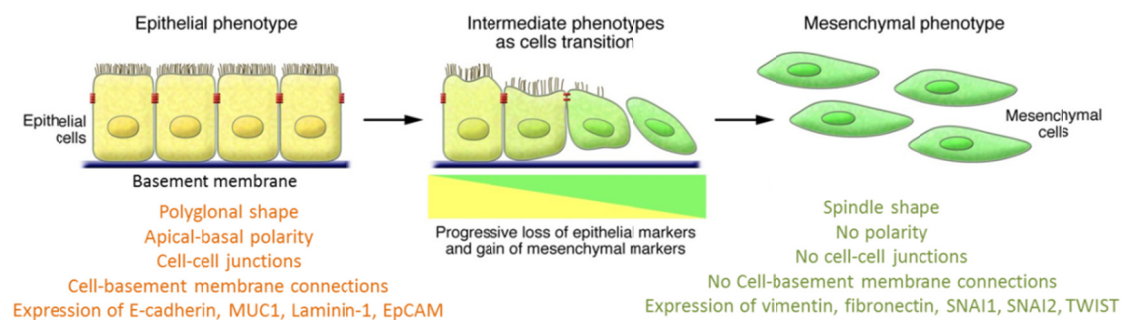


**Figure 9. The epithelial to mesenchymal transition, adapted from Kalluri and Weinberg, 2009 [43]**

During the epithelial to mesenchymal transition, epithelial cells progressively lose their phenotype in order to acquire mesenchymal traits. *Permission to reproduce and adapt this figure has been granted by the American Society for Clinical Investigation.*

However, the difficulty to live monitor such phenotypic changes in human tumours makes the involvement of EMT in tumour progression still subject of debate [40–42], although one hypothesis is that EMT supports the invasion steps within the metastatic cascade. In fact, immunohistochemical and expression analysis on diverse human tumours, including breast cancer, showed a reduction of epithelial markers (e.g. E-cadherin) and/or an increased expression of mesenchymal traits (e.g. vimentin and EMT-associated transcription factors) which are correlated with poor prognostic outcomes [44–48]. Furthermore, the existence of an intermediate CTC-phenotype (between the epithelial and the mesenchymal) was suggested as result of the progressive EMT [43,49]. In fact, independent research groups have recently postulated that a complete EMT process is not mandatory for a tumour cell to acquire invasive properties and to disseminate into the circulation. A partial EMT would already be adequate to produce cancer-initiating cells [50,51]. Moreover, tumour cells might

disseminate into the blood circulation by mechanical processes only, thus preserving their epithelial phenotype [37].

### **1.3.2. Extravasation and colonization**

Tumour cells which gain access into the bloodstream are named “circulating tumour cells” (CTCs; comprehensively described in chapter 1.4). CTCs mostly circulate as single cells, but sometimes they aggregate to platelets which provide tumour cells some protection from host immune cells [2]. Furthermore, CTCs may survive immune defense mechanisms in blood by expressing PD-L1 on their surface, thereby binding to the receptor PD-1 expressed on T-cells. In fact, the bound of PD-L1 with PD-1 anergize these lymphocytes [52,53]. CTCs in the blood stream can potentially spread to all tissues. Although molecular mechanisms of tissue colonization have not been fully understood, yet, it is known that the extravasation takes place through inverse mechanisms to those involved in the intravasation: arrest and adhesion to the vascular endothelium, and access to the tissue parenchyma via enhanced focal adhesions with the basement membrane [2]. Thus, it was hypothesized that tumour cells which underwent EMT during the initial invasion may face the reverse process, named mesenchymal-to-epithelial transition (MET) [54–56]. The location of metastatic sites is usually associated to the entity of the primary tumour. For instance, breast cancer metastases are more likely to occur into brain, bones, liver and lungs [57]. This organ tropism may be explained with the expression of certain adhesion molecules and chemokines by the tumour cells, whose receptors are most likely to be expressed in specific organs. Binding of chemokines may prime the environment at specific sites to provide better seeding conditions for the arriving tumour cells [2]. However, not all tumour cells are able to successfully colonize certain organs, as well as some micro metastases can survive without any real progression in a quiescent status named “dormancy” [2,3]. In a large pooled analysis of bone marrow micro metastases derived from breast cancer, Braun et al. observed that only half of the patients with hundreds of micro metastases at the time of diagnosis, actually developed macroscopic metastases [58].

Concluding, as Stephen Paget already theorized for the first time in 1889, the outcome of the multi-step metastatization process depends on both properties of tumour cells (“seed”) and of host cells forming the microenvironment (“soil”), a concept known as “seed

and soil theory”[4,59,60]. In fact, failure of any of the mechanisms involved in the metastatic cascade could block the whole process [2,4,60].

## 1.4. Circulating tumour cells

### 1.4.1. Definition and characteristics

CTCs are rare cells observed in the peripheral bloodstream (PB) of cancer patients and are believed to be released from primary tumours, their recurrences or from metastases [39]. CTCs were first described in 1869 by Ashworth and later in 1889 by Paget [59,61]. They may be found in PB of patients suffering of most solid epithelial tumours, with a frequency of 1-10 cells/ml PB surrounded by approximately  $4 \times 10^9$  erythrocytes (RBCs),  $2 \times 10^8$  platelets and  $6 \times 10^6$  leukocytes [62,63]. Their half-life has been estimated to be 1.0 – 2.4 h [64]. According to the only FDA (Food and Drug Administration)-approved CTCs-enrichment system, CellSearch® (Menarini Silicon Biosystems, Bologna, Italy), a CTC is phenotypically determined by a regular, round shape of mainly 4 – 30  $\mu\text{m}$  in diameter (Figure 10), with an intact, viable nucleus, expression of both cytokeratins (mainly cytokeratins 8, 18, and 19) and EpCAM and negativity for the expression of the hematopoietic marker CD45.

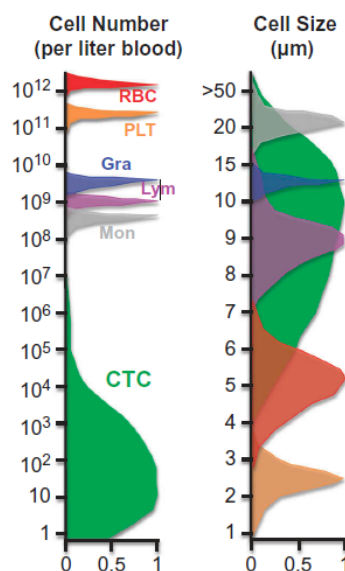


**Figure 10. Frequency and size of CTCs compared to blood cells, adapted from Stoecklein et al., 2016 [65]**

The extremely low frequency of CTCs in PB – compared to other cells in the blood (left) – together with their estimated size overlapping with the whole white blood cell population (right) make their isolation quite challenging.

However, CTCs with diverse phenotypes were described, in terms of irregular shape [66–68], lack of EpCAM expression and/or expression of mesenchymal markers [68–71], as well as clustering with other cancer cells [72–74] or leukocytes [75].

#### **1.4.2. The EpCAM<sup>low/negative</sup> subset of CTCs**

The glycosylated transmembrane protein EpCAM is located within intercellular adherent junctions and is involved in cellular migration, proliferation and differentiation [76]. Already in 1979, EpCAM was identified as one of the first tumour-associated antigens [77]. Subsequently, due to its strong expression in several cancers as well as to its absence on hematopoietic cells [78,79], EpCAM was taken in consideration as main antigen to identify CTCs. Thus, the CellSearch® system was designed to capture and detect EpCAM-expressing cells [80,81]. However, in the last decade, several research groups have shown that EpCAM expression is heterogeneous and can even be absent on several cancers and CTCs [82–84]. Therefore EpCAM-based enrichment technologies may overlook a considerable amount of CTCs (e.g. in breast [85] and lung cancer patients [68,86–88]). The existence of an EpCAM-negative subgroup of CTCs was reported in breast, lung, prostate [89], oesophageal [90] and colorectal cancers [91]. It was proposed that mesenchymal CTCs might actually represent a big portion of the total CTC population and that CTCs with a transient phenotype may also be present as a result of a partial EMT [69,88,92].

Several theories were postulated to explain the downregulation of EpCAM, such as the exposure to tumour necrosis-factor- $\alpha$  [93] or to cytokins [94], or the hypermethylation of the gene's promotor [95,96]. Among all these potential mechanisms, EMT was hypothesized to be the most important process involved in the modulation of EpCAM expression [97]. This hypothesis could be supported by further studies which reported the presence of EpCAM<sup>negative</sup> CTCs expressing EMT-related genes in metastatic breast cancer (mBC) patients [70,88]. Furthermore, EMT was theorized to play a central role in cancer dissemination and therapy resistance conferring more malignant phenotypes [37,98]. In agreement with this model, different groups observed a considerable amount of mesenchymal CTCs in cancer patients suffering of the progression of the disease [69,70,85]. Altogether, these findings suggest that only relying on EpCAM expression to enrich CTCs may lead to overlook relevant CTC-subsets.

### **1.4.3. Challenges in CTC-research: rarity and heterogeneity**

Due to their low frequency in blood, CTCs require highly specific and sensitive enrichment techniques able to capture one single tumour cell in the background of millions of white blood cells (WBCs) and RBCs in order to limit the occurrence of false positive and false negative events [99]. Furthermore, capturing methods should guarantee high purity of the enriched cell fraction as well as high reproducibility and reliability – independently on the patient [100]. As explained above, the most used technologies to enrich CTCs in blood samples rely on the expression of EpCAM protein by tumour cells. In the CellSearch® system, anti-EpCAM antibodies are coated to ferrofluidic paramagnetic nano-beads which can assure the automated enrichment of EpCAM-expressing cells. The subsequent CTC-detection is performed via immunofluorescence, focusing on the presence of nucleic signal, cytokeratin expression and lack of the hematopoietic marker CD45 [66,81,101]. However, as previously mentioned, EpCAM might be not the proper choice to collect a wide population of CTCs. Furthermore, Punnoose and colleagues demonstrated that the capturing efficiency of the CellSearch® system is approximately 75% for tumour cells expressing high levels of EpCAM and 42% for EpCAM<sup>low</sup> tumour cells [102]. Therefore, in the last decades several alternative CTC enrichment technologies were designed and they can be mainly grouped in label-dependent approaches – targeting antigens only expressed by CTCs – and label-free approaches, focusing on size, deformability, density and electrical properties of tumour cells [100,103,104]. Besides the low frequency, the second big challenge in CTC-research is the heterogeneity of tumour cells. Therefore, it is of major interest to singularize CTCs in order to perform a single-cell genomic, transcriptomic and proteomic (known as “-omic” analysis) characterization which may provide a comprehensive molecular portrait of the cancerous disease, absolutely necessary to better understand it [103,105].

#### **1.4.3.1. Label-dependent enrichment strategies**

Label-dependent CTC-capturing techniques may be categorized in positive selection and negative selection approaches, based on whether they focus on properties of tumour cells or on blood cells, respectively [88]. Positive selection aims to collect CTCs expressing certain surface proteins (e.g. EpCAM) by utilizing specific antibodies which are often conjugated to

immunomagnetic microbeads (e.g. CellSearch®) [106]. However, the choice of the target protein is challenging: it needs to be sufficiently expressed on the surface of the tumour cell and should specifically be related to cancer, in order to distinguish CTCs from WBCs and RBCs. To the end of overcoming limits related to the EpCAM expression, research groups have investigated the validity of alternative markers, such as: HER2/neu, mucin 1, EGFR, neural cadherin, the CUB domain-containing protein 1 (CDCP1, CD318), and the prostate-specific membrane antigen [69,88,100,107–110]. Moreover, the feasibility of the combination of anti-EpCAM antibodies with further antibodies was tested for the Thomsen-Friedenreich antigen (CD176), the melanoma cell adhesion molecule, the cell surface glycoprotein mucin18, and integrin alpha 6 (CD49f) [84,111,112]. An additional possibility is to perform a sequential enrichment on the EpCAM-depleted fraction of blood samples. By applying this approach, Schneck et al. managed to enrich EpCAM<sup>low/negative</sup> CTCs in mBC samples, through nano-immunomagnetic beads coated to antibodies anti-CD49f, Trop2 and CK8, involved in the invasion-metastasis cascade [113]. However, to date, no specific “tumour-associated” mesenchymal markers are known to enrich and detect CTCs with epithelial-mesenchymal plasticity in a wide spectrum of cancers [88].

Another approach is the negative selection of CTCs via depletion of blood samples of WBC and RBC, by targeting antigens exclusively expressed by blood cells (e.g. CD2, CD16, CD19, CD38, CD45, CD66b, glycophorin A, and according to the type of cancer CD36 or CD56), with specific antibodies often conjugated to magnetic beads [114–116]. The major limit of this procedure consists in finding the right balance between blood cell depletion rate and CTC loss and these strategies were reported to be not so suitable to enrich consistent pure fractions of tumour cells [88,114–116].

Due to the above reported limits, many research groups and companies focus on the development of label-free collection approaches.

### **1.4.3.2. Label-free enrichment strategies**

Label-free enrichment techniques are based on different biophysical properties of tumour cells compared to WBCs and RBCs, regardless of their protein expression. In the last decades, several CTC collection approaches were designed, such as density-based gradient

centrifugation, (micro) filtration systems, and microfluidic devices and each of them provides different capturing performances [88].

The density-based centrifugation was the first enrichment approach already investigated in 1959, since CTCs were reported to possess similar density to the mononuclear blood cells [65,117,118]. In the following years, this method was implemented and improved by independent research groups. Nevertheless, the heterogeneous densities of tumour cells and the considerable leukocyte contamination still lead to poor recovery rate which is the major limit of this approach [88,119–122]. By exploiting the similar density of CTCs and leukocytes, a novel strategy was tested by Fischer and colleagues [118] which achieved considerable CTC-enrichment rates via diagnostic leukapheresis (DLA). During the DLA sampling, patients' high blood volumes are continuously centrifuged on a density gradient to separate mononuclear cells and CTCs from the blood, which is then, immediately returned to the patients [65,118]. In 23 patients suffering from different cancers (breast, pancreatic and gastro-intestinal), the authors observed an increased CTC detection rate of 44% in comparison to standard PB volumes (7.5 Ml within the CellSearch®), by processing 2 mL DLA product for CTC detection [65,118]. However, this approach was and is still under extensive clinical validations within the European projects CTC-Trap [123] and Cancer-ID [124].

CTCs were described to be larger and stiffer than blood cells, therefore several technologies were designed to enrich them based on these physical properties [63,66,88,125–131]. The main investigated approach is the filtration of blood samples by utilizing filter membranes (e.g. VyCap®) [68,125,132–137], track-etched membranes (e.g. ISET®) [138–142], three-dimensional microfilters (e.g. Parsortix®)[87,89,143] and microfluidic devices (e.g. Vortex Chip®, Clear Cell®) [127,144–147]. Membrane-based filtration strategies were shown to be easy, quick and suitable for clinical routine in various types of cancer, although some aspects still require improvements, such as the purity of the enriched CTC fraction – essential for a proper CTC detection – and the detachment of cells retained by membranes, required for further molecular characterizations [68,88,141,148–152]. Moreover, these methods cannot enrich small CTCs whose role is still unknown. In fact, they might be either relevant in cancer dormancy or just the result of cell death[153]. Microfluidic platforms were shown to be able to capture CTCs in different types of cancer, in a fast high-

throughput fashion, assuring consistent recovery, purity rates, and cell-viability [87–89,127,143–147,154].

Data reported so far suggest that the best strategy might be a subsequent application of label-based and label-free techniques in order to collect wider subsets of CTCs.

### **1.4.3.3. Detecting and isolating CTCs**

The heterogeneity of cancer requires the single-CTC characterization which may be hampered by the leukocyte contamination affecting enrichment technologies. Therefore, it is of major interest to perform proper detection and isolation of single tumour cells, prior to molecular analysis. The field of the single cell-isolation is currently dominated by three major techniques: fluorescent activated cell sorting (FACS), dielectrophoresis (DEP) and micromanipulation [88].

The FACS-sorting is automated, fast, robust and provides details about the expression of several biomarkers, due to the possibility of utilizing several fluorophores which is the major limit of other “classical” approaches [155,156]. However, flow cytometry does not provide a visual control of the isolated cell which may predict the suitability of the CTC for further analysis (i.e. DNA degradation) [88,157]. The automated DEPArray™ system (Menarini Silicon Biosystems) isolates CTCs based on their different dielectric properties compared to blood cells, and it also provides visual controls as well as information about biomarkers expression [157–159]. However, the whole processing may take up to 3 h and may lose relevant cells due to high volumes of sample lost in the tubing system [88]. Semi-automated micromanipulators such as the CellCelector™ may be effectively utilized to detect and isolate CTCs by combining an epifluorescence inverted microscope and a robotic arm with a glass capillary which can aspirate the selected cell and deposit it in a PCR tube or onto a glass slides [160]. Among its major advantages, the system provides a visual control during the cell isolation procedure and the shear forces acting on cells are lower compared to these of the FACS-sorting. Furthermore, the risk of isolating unselected material is below  $\leq 9\%$  for a density of 25-50 cells/100 mm<sup>2</sup> [160].

Each of these approaches was reported to be appropriate for effective isolation of single tumour cells to the end of molecular analysis [155–160]. However, according to the needs, one technology might be more suitable than another.

#### **1.4.4. Clinical role of CTCs in metastatic breast cancer**

Since the phenotype of primary tumours may differ from related metastases (e.g. HER2/neu status in mBC [161]), and since the sampling of both primary and metastatic lesions is an invasive and complex procedure, both the detection and characterization of CTCs in PB may represent a powerful alternative to investigate cancerous diseases. These tumour cells are, therefore, currently considered as a “liquid biopsy” [103]. However the topic is still in its infancy and no clinical applications based on CTCs are available so far, although some of the currently running clinical trials might be approved in the near future and subsequently applied in the clinical practice [162]. The discussion about the clinical role of CTCs can be mainly grouped in two topics: **1)** the validity of CTC enumeration as a prognostic and therapy decision tool; **2)** the clinical utility of CTC characterization in the treatment selection [163].

##### **1.4.4.1. Validity of CTC enumeration**

Even though the abundance of CTCs in PB is scant, their presence correlates with poor clinical outcomes in breast, colorectal, lung and prostate cancers [81,162,164,165]. CTCs’ prognostic significance in mBC was first investigated by Cristofanilli et al. in 2004, which reported a cut-off value of  $\geq 5$  CTCs/7.5 mL PB – detected via CellSearch® – to predict poor progression free survival (PFS) and OS for patients suffering of mBC [81]. After this milestone, the scientific community gradually shifted from the detection of disseminated tumour cells (DTCs) in bone marrow samples – as markers of minimal residual disease – to the detection of CTCs in PB samples, due to the invasiveness of the former procedure [62]. On the contrary, PB sampling is easy, painless and can be repeated several times to monitor patients’ treatment responses. However, any study on CTC enumeration highly depends on the technique used for both cell-enrichment and detection, as well as on the volume of the processed PB (see chapter **1.4.4**). For this reason, most of the research groups rely on the only one FDA-approved CellSearch® system, missing though, CTCs with mesenchymal-like and intermediate phenotypes (see chapter **1.4.3**) which might play a major role in metastasis

and treatment resistance [69,70,166,167]. After Cristofanilli and colleagues' publication, the correlation between CTC enumeration and outcomes in mBC patients was further confirmed by other numerous studies [62,163]. The prognostic role of the CTC-count was investigated not only in terms of absolute quantification, but also in terms of dynamic variations. It was reported that mBC patients with a decreased CTC-count after the first line of treatment, have better PFS and OS than patients with constant high CTC numbers [81,168]. Comparable observations were described in metastatic cancers of colon, prostate and lung as well [164,165,169].

Clinical trials involving mBC patients are currently investigating the efficacy of the CTC count for the choice of therapies. Within the clinical trial SWOG S0500 – involving 120/595 mBC with >5 CTCs after the first line of therapy – it was confirmed that high CTC counts predict disease progression. However, Smerage et al. reported that patients' OS was not improved by an early switch to a second line chemotherapy [170]. In the ongoing study CirCe01 (NCT01349842) clinicians are testing a similar approach to evaluate whether CTC-variations may guide the third line of chemotherapy [171]. The STITC-CTC study (NCT01710605) aims to test the validity to treat >700 hormone receptor positive mBC patients either with hormone therapy for baseline CTC count <5 or with chemotherapy in case of  $\geq 5$  CTCs [62,162].

Although all together above reported studies suggest a valuable role of CTCs as therapy monitoring instrument, the clinical utility of CTC-enumeration still requires further elucidations in order to be implemented in the clinical routine practice.

#### **1.4.4.2. Utility of CTC characterization**

In the last years, the characterization of CTCs has acquired lots of interest, mainly due to the availability of new high resolution technologies for “-omic” analysis on single cells, thereby required to investigate the cancer heterogeneity. Currently, there are no ongoing clinical trials based on CTC-“omic” analysis yet, although several research groups are investigating CTC genotypes to better understand the systemic disease [69,155,157,172]. On the contrary, the phenotypical characterization of CTC (biomarker expression) – typically based on immunofluorescence staining combined with high-resolution imaging – is already in its evaluation phase for clinical applications. Among these studies, the trials NCT00820924[173], NCT00820924[174], DETECT III (NCT01619111)[175] and DETECT IVa/b

(NCT02035813)[176] focus on the efficacy of HER2/neu-targeted therapies in patients suffering of HER2/neu-negative mBC but with HER2/neu-positive CTCs (NCT00820924, DETECT III/IV) or EGFR-positive CTCs (NCT00820924).

However, the validity of CTC-characterization in the choice of treatments is in its very early stages and surely requires further investigations.

#### **1.4.4.3. Clinical relevance of CTCs with epithelial-mesenchymal plasticity**

As above mentioned, the detection of EpCAM<sup>positive</sup> CTCs in cancer patients generally predicts adverse prognoses. However, it was recently hypothesized that patients with undetectable CTCs might also encounter worse outcomes due to the existence of an EpCAM<sup>low/negative</sup> subpopulation of CTCs [88,177]. Still very little is known about these cells and this hypothesis is currently investigated by several research groups. Mego and colleagues observed a correlation between the scarcity of EpCAM<sup>positive</sup> CTCs and the occurrence of brain metastasis in mBC patients [85]. Subsequently, Zhang et al. reported high brain metastatic potentials for an isolated EpCAM<sup>negative</sup> subpopulation of CTCs injected in nude mice[178]. In agreement with these observations, Vishnoi and colleagues suggested that stem-cell-like EpCAM<sup>negative</sup> CTCs, expressing markers for cancer dormancy (e.g. urokinase-type plasminogen activator receptor and integrin  $\beta$ 1), might play a role in the development of brain metastases [179]. Furthermore, Lustberg et al. observed decreased OS in mBC patients presenting more than 100 EpCAM<sup>negative</sup> CTCs/mL of blood. Interestingly, in contrast with these observations, de Wit and colleagues recently reported no inferior prognoses in metastatic lung cancer patients with EpCAM<sup>low/negative</sup> CTCs [68]. Similar conclusions could be drawn for metastatic prostate cancer patients, investigated within the CTC-Trap consortium [180].

To date, only few studies addressed the question whether this subset of CTCs might be of clinical relevance and all agree on the importance of investigating the presence and molecular signatures of EpCAM<sup>low/negative</sup> CTCs, in order to acquire new insights into cancer development and progression.

## 2. Aim of the study

Despite enormous efforts for therapeutic improvements, more than 30% of mBC patients from all over the world still die of distant metastases, due to a minimal residual disease. The major obstacle for effective cures is the heterogeneity of primary tumours. They are composed by various cellular subsets with different metastatic potentials and sensitivity to treatments. Therefore, investigating the heterogenous biology of CTCs – considered surrogates of minimal residual disease – is of major importance to select the optimal treatment and shed light on eventual therapeutic failures. The field of CTC analysis is still in its infant and most of the knowledge regards the enumeration of the EpCAM<sup>positive</sup> tumour cells in relation to the patients' prognosis.

The aim of the study was to significantly contribute to the optimization of strategies to enrich, isolate and characterize two different subsets of CTCs – EpCAM<sup>high</sup> and EpCAM<sup>low/negative</sup> – within same mBC patients' blood and DLA samples. Both enrichment and molecular analysis are necessary for the real-time monitoring of the disease in the patients and to achieve personalized therapies which may help to overcome treatment failures. To this end, the European "CTC-Trap" consortium (funded through FP7 health.2012.1.2-1 #305341) was founded [123,180,181]. The main goal of this consortium consisted in the validation of a filtration technique to enrich and detect the EpCAM<sup>low/negative</sup> subpopulation of CTCs from EpCAM-depleted blood and DLA samples of mBC patients.

Within the herein described study, additional methods enabling the enrichment as well as the isolation of patient-matched EpCAM<sup>high</sup> and EpCAM<sup>low/negative</sup> CTCs were validated and subsequently, the enrichment/isolation workflow should be adapted for single cell molecular analysis. The second part of this study aimed to perform the comparative characterization of the status of the PIK3CA oncogene within patient-matched EpCAM<sup>high</sup> and EpCAM<sup>low/negative</sup> CTCs, since PIK3CA activating mutations might be involved in HER2/neu-targeted treatment resistance. To this end, a protocol for PIK3CA-specific PCRs and Sanger sequencing of single cells should be validated to achieve mutational analysis of PI3KCA hotspots mutations E542K/E545K and H1047R. The above described aims should be achieved in a translational project connected to the studies DETECT III, DETECT IV, AUGUSTA and SETTEMBRA.

In the future, the information on the presence of EpCAM<sup>low/negative</sup> CTCs and on the presence of PIK3CA hotspot mutations, in both subsets of CTCs, will be correlated to patients' follow-up data and might positively contribute to achieve more precise patients' prognosis as well as personalized treatment choices.

## 3. Materials and Methods

### 3.1. Cell lines

The MCF-7 and T47D breast cancer cell lines were purchased from the American Type Culture Collection (ATCC, Manassas, VA, USA; catalogue number: HTB-22™ and HTB-133™). The MCF-7 was generated from an adenocarcinoma of a 69-year old Caucasian woman. The T47D cell line was generated from a ductal carcinoma of a 54-year old Caucasian woman.

#### 3.1.1. Culture conditions

All cell lines were cultured in RPMI 1640 L-glutamine containing 1% Penicillin-Streptomycin and 10 % foetal calf serum (all Gibco, Karlsruhe, Germany). MCF-7 cells were further supplemented with 25 mM HEPES and the T47D cells with 10 mM HEPES, 1 mM sodium pyruvate and 0.45% D-(β) Glucose solution (Gibco). All cell lines were grown at 37°C in a humidified atmosphere with 5% CO<sub>2</sub> and were subsequently authenticated through highly-polymorphic short tandem repeat loci (STRs) analysis.

#### 3.1.2. Sub-culturing of MCF-7 and T47D cells

At a confluency of 60-80%, the culture medium was discarded and cells were washed with PBS (Gibco). After discarding the PBS, cells were incubated with 0.05% trypsin (Gibco) for 5 min at 37°C, in order to detach them from the surface of the culturing flasks. Afterwards, the proteolytic action of the trypsin was stopped by transferring the complete medium into the flasks. Cells were collected and transferred in 15 mL Falcon® tubes (Corning Incorporated, New York, USA) and then centrifuged at 1100 rpm for 5 min, in order to completely remove trypsin traces. To this end, the supernatant – consisting of medium and trypsin – was then discarded and the cell-pellet was resuspended in complete medium and sub-cultivated in new flasks with a ratio of 1:2 or 1:4, according to the density of the cells.

#### 3.1.3. Cryopreservation and re-culturing

Aliquots of cells were cryopreserved by transferring 1 mL of the resuspended pellet into 2 mL cryo tubes (Greiner, Solingen, Germany) supplemented with 5% dimethyl sulfoxide (DMSO; Sigma-Aldrich, Munich, Germany) and slowly freezed in freezing container at -80°C, for 24 h. Afterwards, cryos were transferred in liquid nitrogen for long term storage.

In order to re-culture cryopreserved cells, frozen aliquots were thawed at 37°C, transferred into 15 mL Falcon® tubes along with new complete medium. Cells in new medium were centrifuged at 1100 rpm for 5 min, to remove traces of the DMSO. The supernatant was discarded and the cell-pellet was resuspended in new complete medium and transferred in a new flask for culturing.

## 3.2. Cytospins preparation

To the end of validating different immunostainings utilized for CTC-detection, cytospins of MCF-7 cells and of leukocytes – isolated from healthy donor whole blood samples – were prepared.

### 3.2.1. MCF-7 and whole blood fixation

In order to simulate the conditions of CTCs in patients' whole blood samples processed in the clinical routine, MCF-7 cells and whole blood were fixed. At a confluency of 60-80%, MCF-7 cells were processed for sub-culturing as above described, omitting the transfer of the cell-pellet into new flasks. Cells were instead resuspended in 7.2 mL of PBS, transferred into CellSave® preservative tubes (Menarini Silicon Biosystems) and incubated for 24 h at room temperature (RT). Afterwards, cells were centrifuged at 1100 rpm for 5 min, the supernatant was discarded and the cell-pellet was resuspended in 1 mL PBS.

An amount of 7.5 mL of whole blood samples was transferred into CellSave® preservative tubes and incubated for 24 h, at RT. Afterwards, whole blood samples were processed to isolate leukocytes.

### 3.2.2. Isolation of leukocytes from whole blood

To the end of isolating leukocytes, fixed blood samples were diluted in PBS (1:2) and then slowly pipetted on 15 mL of Biocoll separating solution (Merck Millipore, Billerica, Massachusetts, USA), previously deposited into a new 50 ml Falcon® tube. Then, samples were processed for density gradient centrifugation at 1500 rpm, RT, for 30 min, without breaks (Figure 11). Afterwards, the supernatant was discarded and the interphase, comprising the majority of leukocytes, was carefully aspirated and transferred into a new 50 ml Falcon® tube.

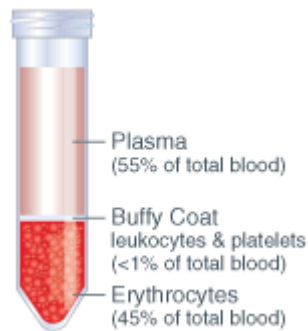


**Figure 11. Whole blood centrifuged on a density gradient, from *humanimmunologyportal.com* [182]**

As a result of density gradient centrifugation, blood components are divided in three parts according to their densities: plasma in the supernatant, most of leukocytes and platelets in the interphase (buffy coat) and red cells in the pellet.

The buffy coat was washed with 50 mL PBS and centrifuged again. Then, the supernatant was discarded and the pellet was resuspended in 1 mL PBS.

### **3.2.3. Cell counting**

The amount of cells was determined through the improved Neubauer counting chambers (Paul Marienfeld GmbH & Co. KG, Lauda-Königshofen, Germany) composed of 2 sampling areas of 4 mm<sup>2</sup>, each divided into 4 squares. All 4 squares are further divided in 16 squares. In order to determine the amount of the cells per mL of suspension, 10 µL of cells diluted in PBS were transferred into an Eppendorf tube (Eppendorf, Hamburg, Germany) and mixed with Trypan blue (Sigma-Aldrich) 1:1. Half of the suspension was pipetted into one sampling area and the chamber was examined under the microscope. The number of cells located in the 64 small squares was recorded and the total amount of cells per mL was calculated as following: Cell count x 2 x 10 000 / 4.

### **3.2.4. Spinning of cells**

Resuspended MCF-7 and leukocytes were diluted with PBS down to a concentration of 125 000 – 250 000 cells/mL. An amount of 400 µL of diluted cell suspensions were transferred onto SuperFrost glass slides (Paul Marienfeld GmbH & Co. KG) and centrifuged at 600 g for 3 min though the ROTOFIX 32 A centrifuge (Hettich GmbH & Co.KG, Tuttlingen, Germany). The supernatant containing PBS was removed and cells were spun onto glass slides and dried overnight. Afterwards, cytopins were stored at -20 °C.

### 3.3. Enrichment, detection and isolation of patient-matched EpCAM<sup>high</sup> and EpCAM<sup>low/negative</sup> CTCs combining CellSearch® and VyCAP™ systems

The first workflow is based on de Wit et al. [68] and on Fischer et al. [118] and was further improved within the CTC-Trap, as illustrated below [123,180]. First, blood and DLA samples were drawn from patients, discarding the first 2-3 mL of samples in order to dispose of possible skin contaminating cells which may be responsible of false positivity during the following CTC detection. Then, an aliquot of DLA and 7.5 mL blood samples were fixed in CellSave® preservative tubes for up to 96 h. The processed volumes of DLA aliquots which usually ranged between 2 mL and 4 mL depend on the concentration of mononuclear blood cells which has to be  $200 \times 10^6$  in total. After fixation, samples are sequentially processed through CellSearch® and then via VyCAP™ filtration, in order to enrich EpCAM<sup>high</sup> and EpCAM<sup>low/negative</sup> CTCs, respectively. The CellSearch® is composed by the CellTracks® Autoprep® system, designated to capture and stain CTCs, and by the CellTracks Analyzer II® designated to detect them (Figure 12).

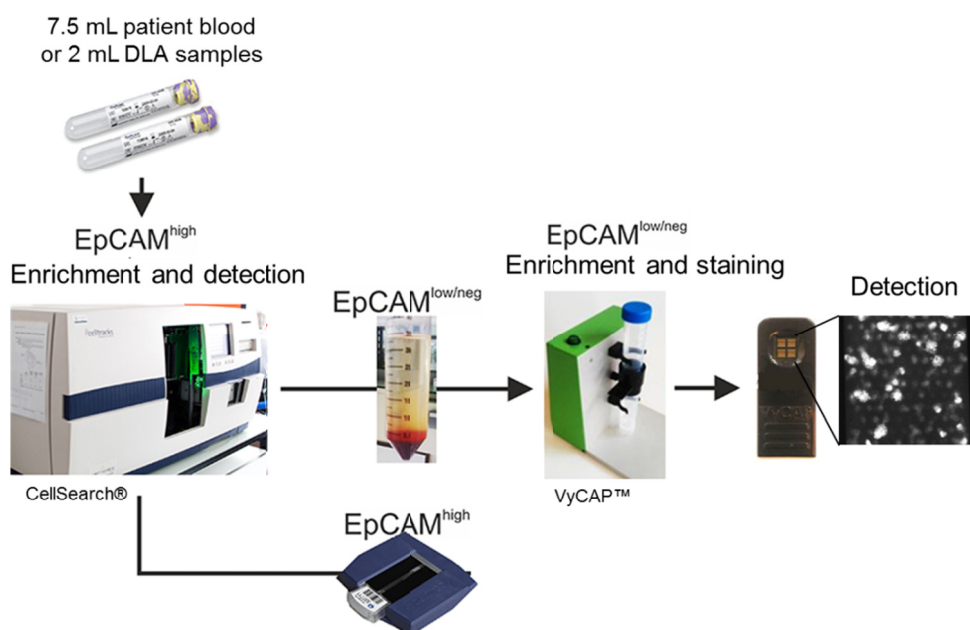


**Figure 12. Workflow #1 for CTC-enrichment and detection, adapted from Lampignano et al., 2017b [183]**

The first workflow combines CellSearch® and VyCAP™ systems to enrich respectively patient-matched EpCAM<sup>high</sup> and EpCAM<sup>low/negative</sup> CTCs, by sequentially processing blood or DLA samples.

Within the CellTracks® Autoprep® system, CTCs are captured by virtue of anti-EpCAM antibodies coated to immunomagnetic ferrofluids. Captured cells are stained with DAPI for nuclei detection, anti-cytokeratins 8, 18, 19/PE conjugated, and anti-CD45/APC conjugated and then, are collected in disposable magnetic cartridges. At last, cartridges are scanned within the CellTracks Analyzer II® and EpCAM<sup>high</sup> CTCs are identified according to positive staining signals for nuclei and cytokeratins and negative for the leukocyte marker CD45. Blood or DLA samples depleted of EpCAM<sup>high</sup> CTCs are collected and further processed within 48 h via VyCAP™ filtration device (VyCAP™, Deventer, Netherlands) which consists of a pump unit and of disposable slides with a microsieve composed of a silicon nitride filters with 5 µm pores (Figure 13).

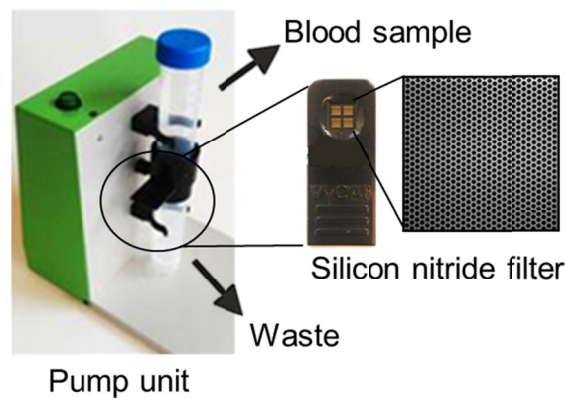


**Figure 13. The VyCAP™ filtration device**

The VyCAP™ filtration device is composed by a pump unit and two 50 ml tubes separated by a slide with a microsieve. Each microsieve is composed of thousands 5 µm pores.

Blood or DLA samples are transferred into the upper tube, then, are filtered under a constant pressure of 100 mbar. Big and stiff cells are retained by the microsieve and all cells smaller than 5 µm are collected into the lower tube. Afterwards, retained cells are stained for nuclei, cytokeratins and CD45, and then observed under an epifluorescence microscope for the detection of EpCAM<sup>low/negative</sup> CTCs.

### **3.3.1. Validation of the immunocytostaining**

Prior to the establishment of the workflow described above, the immunostaining mastermix utilized within the CTC-Trap consortium to detect CTCs was validated on cell lines.

### 3.3.1.1. Immunocyto staining of cytopins

In order to test the efficacy and specificity of the immunostaining mastermix #1 (Table 2) targeting nuclei, cytokeratins and CD45 altogether, cytopins of fixed MCF-7 (expected cytokeratin<sup>positive</sup> and CD45<sup>negative</sup>) and leukocytes (expected cytokeratin<sup>negative</sup> and CD45<sup>positive</sup>) were washed with 200 µL PBS/BSA (Gibco/Sigma-Aldrich) 1 % and then incubated with 200 µL PBS/BSA 1 %/saponin (Gibco/Sigma-Aldrich) 0.15 %, in order to permeabilize cells. During the incubation, the immunostaining mastermix solution was prepared diluting below reported antibodies in 200 µL PBS/BSA 1 %/saponin 0.05 %.

Table 2. Immunostaining mastermix #1

Antibody	Clone	Conjugation	Final concentration	Company
Anti-CD45	HI30 [68]	PerCP	1:25	Life Technologies, Carlsbad, California, USA
Anti-PanCytokeratins (1, 4, 5, 6, 8, 10, 13, 14, 15, 16, 18, 19)	C11/AE1/AE3 [68,113]	NanoParticles 575	1:50	Aczon srl, Monte San Pietro, Italy

After the permeabilization, cells were incubated with the immunostaining mastermix, for 1 h, at RT, dark. Then, cells were washed twice with 200 µL PBS/BSA 1 %, in order to remove the unbound antibodies. Afterwards, 200 µL of ProLong® mounting medium containing DAPI (Life Technologies, Carlsbad, California, USA) were pipetted on cells and a glass coverslip (Paul Marienfeld GmbH & Co. KG) was placed on cytopins.

### 3.3.1.2. Epifluorescence microscopy

Glass slides were observed under the epifluorescence microscope Nikon Eclipse E400, located in Prof. Dr. Stoecklein's research lab, and the whole area of the microsieve was automatically scanned with a 20 x objective in the following channels: DAPI for the detection of the nuclei, PE for the cytokeratins-NP575 and PerCP for the detection of the CD45 antigen. The following exposure times were used: 10 ms for DAPI, 800 ms for PE and 300 ms for PerCP.

### 3.3.2. Validation of the workflow

Prior to processing blood and DLA clinical samples, the recovery capability of the VyCAP™ filtration approach was tested on healthy donor blood samples previously processed within the CellSearch® system and then spiked with MCF-7 cells. Since the enrichment of EpCAM<sup>high</sup> CTCs within the CellSearch® system has previously been established [113,172] and is currently performed in the clinical routine, the establishment of the herein described workflow focused on the novel part of the protocol only: the enrichment of EpCAM<sup>low/negative</sup> CTCs via VyCAP™ filtration of patients' blood samples, previously depleted of EpCAM<sup>high</sup> CTCs.

#### 3.3.2.1. Immunostaining of cells in suspension

Prior to the spiking experiments, fixed MCF-7 cells were stained in suspension. To this end, the cell pellet was resuspended in 1 mL of PBS/BSA 1 %/saponin 0.15 % and incubated 15 min at RT. Afterwards, cells were centrifuged at 1100 rpm for 5 min and the supernatant was discarded to remove the reagents. The cell pellet was washed with 1 mL PBS/BSA 1 % and further centrifuged. Cells were resuspended in 400 µL of the immunostaining mastermix solution #1 and incubated for 1 h, at RT, dark.

#### 3.3.2.2. Cell line spiking experiments

In order to measure the capturing efficacy of the VyCAP™ filtration device, three independent spiking experiments were performed. Defined amounts of MCF-7 cells were pipetted into blood samples previously processed with the CellSearch® (Table 3). Then, spiked blood samples were processed with the VyCAP™ filtration device, as explained above.

**Table 3. Amount of MCF-7 cells spiked per each spiking experiment**

# Spiking experiment	# Spiked MCF-7 cells
Experiment 1	64
Experiment 2	97
Experiment 3	70

### 3.3.2.3. Immunocytostaining on microsieves

In order to verify the effective immunostaining of tumour cells retained by the VyCAP™ microsieve, fixed un-stained MCF-7 cells were spiked into blood samples of healthy donors, previously processed within the CellSearch® (see above). Afterwards, spiked blood samples were filtered through the VyCAP™ device as reported above. Then, the slide was transferred into its holder (Figure 14) and the microsieve was washed with 50 µL PBS/BSA 1 %/saponin 0.15 %.

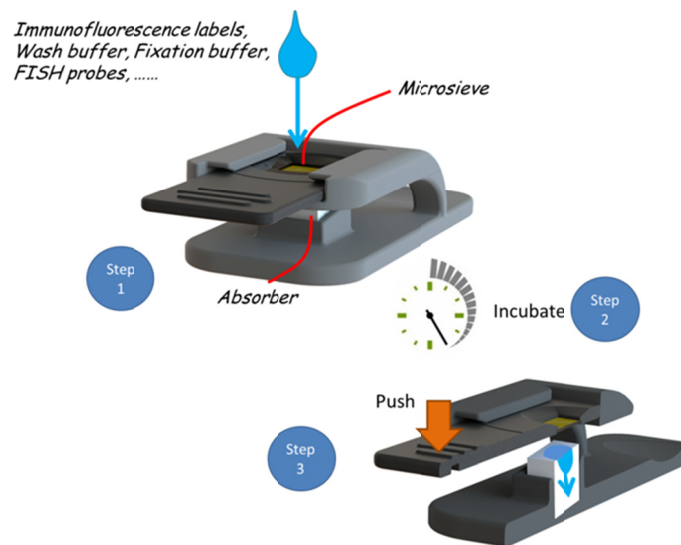


**Figure 14. VyCAP™ slide holder, by VyCAP™ [184]**

In order to proceed with the *in situ* immunostaining, VyCAP™ slides are placed into their holders, equipped with a disposable sponge to remove exceeding reagents.

Retained cells were incubated with 50 µL PBS/BSA 1 %/saponin 0.15 % for 15 min at RT to allow the transient permeabilization of the cells membrane. In order to remove the solution, the microsieve was gently pressed down on the sponge. Then, 50 µL of the staining mastermix solution #1 was prepared as above reported. Cells were incubated with the immunostaining solution for 1 h, at RT, dark. Then, reagents were removed through the sponge and the microsieve was incubated with 50 µL PBS/BSA 1 %, for 5 min to remove unbound antibodies. After the incubation, the solution was removed and the microsieve was incubated with 50 µL 1 % formaldehyde (Merck KGaA, Darmstadt, Germany), for 10 min, at RT, dark, in order to fix the cells. The formaldehyde was removed and the microsieve was washed twice with 50 µL PBS/BSA 1 %. At last, 10 µL of ProLong® mounting medium containing DAPI were pipetted on the upper side and on the lower of the microsieve. Then,

one coverslip of 0.85 cm<sup>2</sup> (0.13-0.16mm thick; Menzel-Gläser, Saarbrückener, Germany) was applied on each side. Slides were stored at -20 °C, dark, until the scanning. Afterwards, the effective immunostaining of both MCF-7 and co-captured leukocytes was checked under the epifluorescence microscope Nikon Eclipse E400 according to the parameters above reported. As negative controls, unspiked blood samples of healthy donors were processed as well.

The above described immunostaining protocol on microsieves is based on de Wit et al.[68] and was further improved within the CTC-Trap [180].

### **3.3.3. Processing mBC patients' blood samples**

Blood samples of patients suffering from mBC were collected within the German DETECT III/IV (III: NCT01619111, IV: NCT02035813; for more information: [www.detect-studien.de](http://www.detect-studien.de)) and AUGUSTA studies. Written informed consent was obtained from all participating patients and the studies were approved by the Ethical Committee of the Eberhard-Karls University Tuebingen (responsible for DETECT III: 525/2011AMG1) and the local Ethical Committee of the Heinrich-Heine University Duesseldorf (DETECT III: MC-531; DETECT IV: MC-LKP-668 AGUSTA: 3430).

### **3.3.4. Processing mBC patients' DLA samples**

DLA samples of patients suffering from mBC were collected within the German SEPTEMBRA study, in cooperation with Prof. Dr. Stoecklein's research group (Department of General, Visceral and Paediatric Surgery, University Hospital and Medical Faculty of the Heinrich-Heine University, Duesseldorf, Germany) as previously published. Written informed consent was obtained from all participating patients and the study was approved by the local Ethical Committee of the Heinrich-Heine University Duesseldorf (AUGUSTA: 3430; SEPTEMBRA: 3460).

### **3.3.5. Detecting tumour cells: image analysis**

For the detection of the cells retained by VyCAP™ filters, the open source image analysis software "ICY" was used. All the images of each sample were loaded simultaneously and separated series of time frames of images for each channel were automatically created. The

three different channels were merged and all the positive events for DAPI and cytokeratins, negative for CD45 and with a spherical shape bigger than 4  $\mu\text{m}$  were recorded.

### 3.4. Enrichment and isolation of patient-matched $\text{EpCAM}^{\text{high}}$ and $\text{EpCAM}^{\text{low/negative}}$ CTCs combining CellSearch<sup>®</sup>, Parsortix<sup>™</sup> and CellCelector<sup>™</sup> systems

The workflow #2 consists in a sequential processing of patients' blood samples via CellSearch<sup>®</sup> first and then via Parsortix<sup>™</sup>, in order to enrich  $\text{EpCAM}^{\text{high}}$  and  $\text{EpCAM}^{\text{low/negative}}$  CTCs, respectively. A fixed volume of 7.5 mL of blood were processed via CellSearch<sup>®</sup> system, as above explained. After depletion of  $\text{EpCAM}^{\text{high}}$  CTCs, blood samples were collected and further processed within the Parsortix<sup>™</sup> system (Angle plc, Guildford, UK) to enrich  $\text{EpCAM}^{\text{low/negative}}$  CTCs uncaptured by the CellSearch<sup>®</sup> (Figure 15).

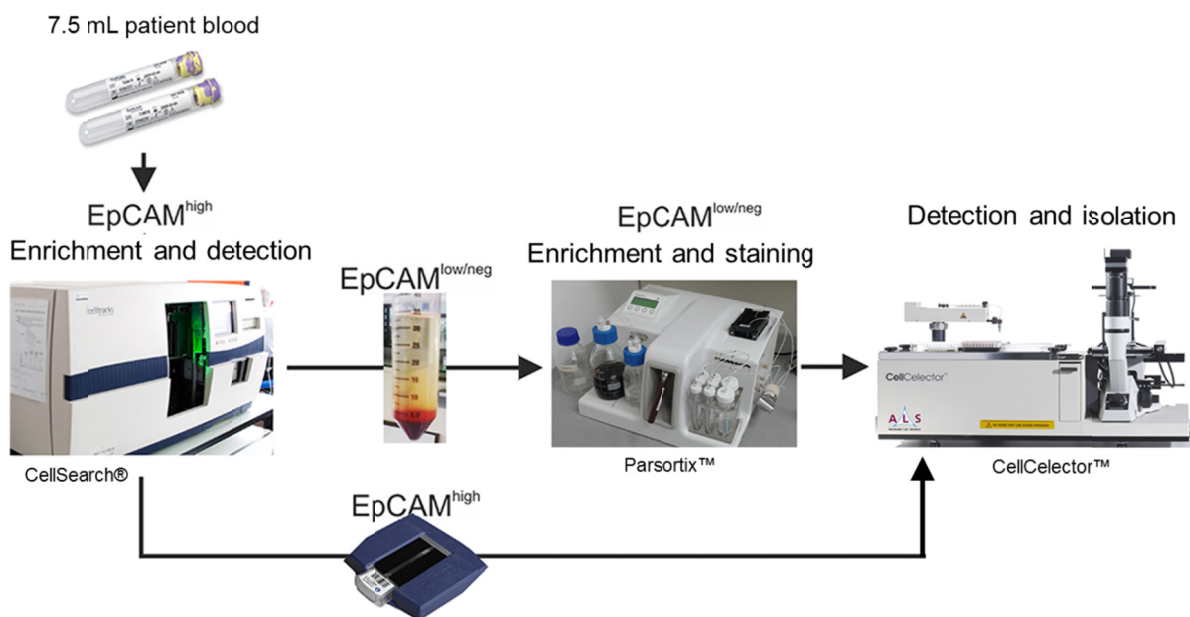


**Figure 15. Workflow #2 for CTC-enrichment, detection and isolation, adapted from Lampignano et al., 2017b [183]**

The second workflow combines the CellSearch<sup>®</sup>, the Parsortix<sup>™</sup> and the CellCelector<sup>™</sup> systems to enrich, detect and isolate patient-matched  $\text{EpCAM}^{\text{high}}$  and  $\text{EpCAM}^{\text{low/negative}}$  CTCs.

The Parsortix<sup>™</sup> system is a semi-automated microfluidic device capable to enrich cells based on their size and stiffness, in a label-free fashion. It consists of a pumping system which draws blood samples into a disposable cassette at a pressure of 99 mbar. Each cassette is composed by separation steps of 6.5  $\mu\text{m}$  (Cell Separation Cassette GEN3D6.5,

ANGLE plc) in height blocking the flow of most cells bigger than leukocytes, including CTCs. On the contrary, small cells can flow through the cassette and are discarded in the waste container (Figure 16).

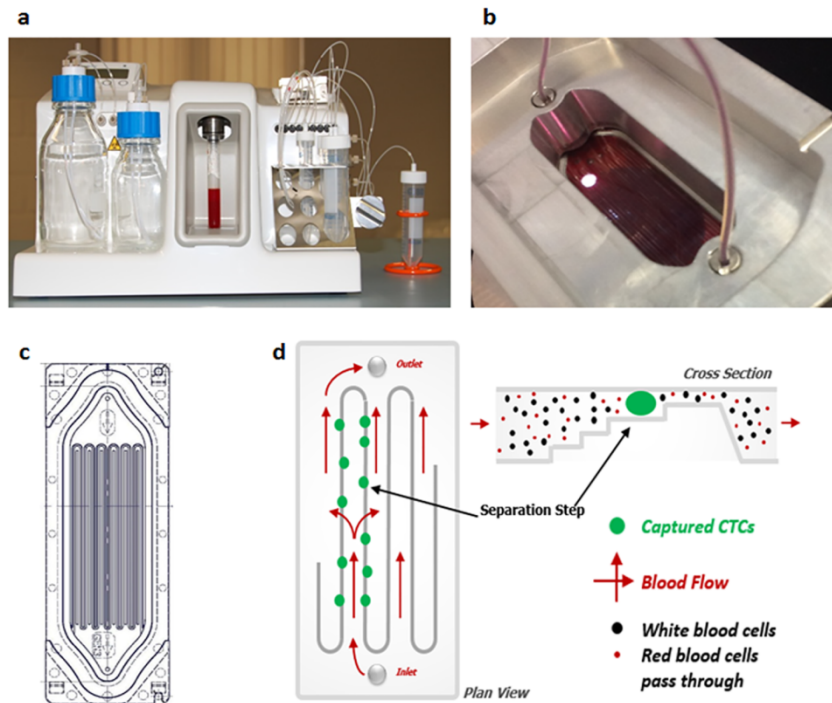


**Figure 16. The Parsortix™ system, by Xu et al., 2015 [89]**

The Parsortix™ device is composed by an inner pump tubing system, a sampling area (at the centre), waste and buffer area (left side) and reagents and harvest area (right side) (a). On the top it is located the clamp (b) holding the enrichment cassette (c). The disposable cassette consists of several lanes. Each of them is formed by numerous separation steps which retain cells bigger than 6.5  $\mu\text{m}$  (or 10  $\mu\text{m}$  in the former version) (d).

At first, the whole device was automatically primed through PBS and Ethanol 100% (Merck KGaA), in order to remove air bubbles and to sterilize both tubing systems and disposable cassettes. Then, blood samples were placed into their holder and the blood was pumped through the cassette. Afterwards, captured cells were permeabilized and stained *in situ* for nuclei, cytokeratins, EpCAM, and CD45. By inverting the flow of the buffer into cassette, stained cells are collected in a tube, outside the system. By virtue of an automated cleaning protocol based on Deconmatic reagent (Decon Laboratories Ltd, Hove, UK), clean and sterile working conditions could be guaranteed.

At last, both EpCAM<sup>high</sup> and EpCAM<sup>low/negative</sup> cells are detected and isolated in PCR tubes through the CellCelector™ (ALS, Jena, Germany), a semi-automated micromanipulator

consisting of an inverted epifluorescence microscope (CKX41, Olympus) with a CCD camera system (XM10-IR, Olympus) and a robotic arm with a vertical glass capillary (Figure 17).

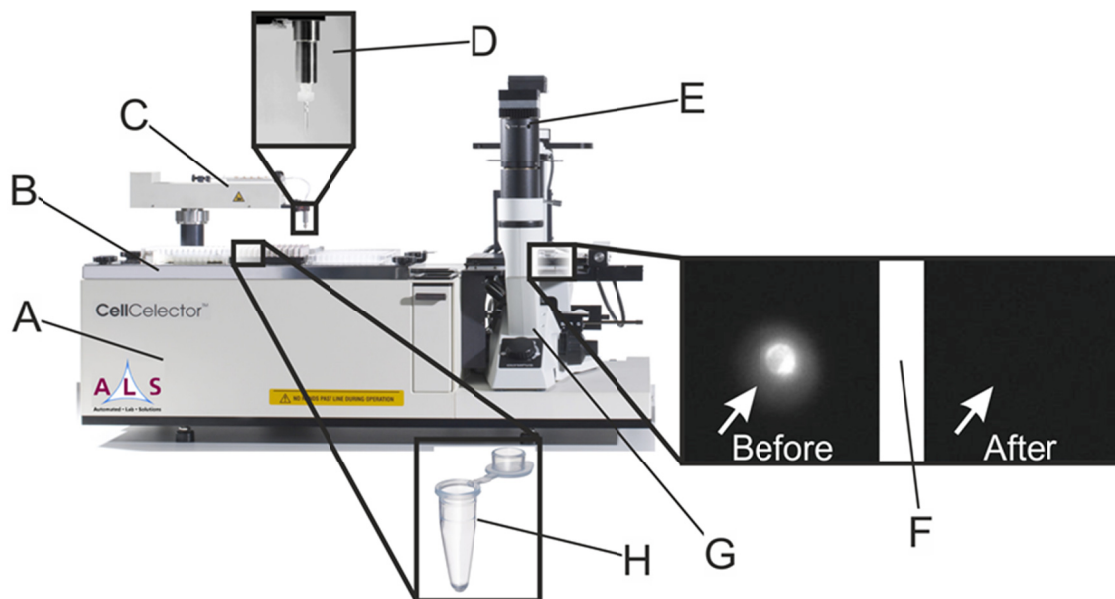


**Figure 17.** The CellCelector™ micromanipulator, *inspired by Neumann et al., 2016 [160]*

The CellCelector™ device is composed by a micromanipulator (A) with a robotic arm ending with a glass capillary (C, D), a motorized stage (G) and a deposit tubes holder (B, H). The integrated fluorescence microscope (E) enables the visual control of the single cell isolation (F).

Enriched cells were deposited onto a glass slide located on a magnetic slide holder placed in the motorized stage of the microscope. CTCs could be detected through observation under the epifluorescence microscope and subsequently isolated. The robotic arm with a glass capillary is able to aspirate selected cells from the glass slide and to deposit them into PCR tubes located into the deposit holders.

### **3.4.1. Validation of the immunocytostaining**

Prior to the establishment of the workflow described above, the staining of markers whose expression is required for the CTC-detection, was validated on cell lines. As described above, MCF-7 cells and whole blood samples were fixed in CellSave®. Then, leukocytes were isolated from whole blood and both white blood and MCF-7 cells were spun onto different glass slides.

### 3.4.1.1. Immunocytostaining of cytopins

In order to test the efficacy and specificity of the immunostaining mastermix targeting nuclei, cytokeratins, EpCAM and CD45 altogether, cytopins of fixed MCF-7 (cytokeratin<sup>pos</sup>, EpCAM<sup>pos</sup> and CD45<sup>neg</sup>) and leukocytes (cytokeratin<sup>neg</sup>, EpCAM<sup>neg</sup> and CD45<sup>pos</sup>) were washed with 200  $\mu$ L PBS and then incubated with 200  $\mu$ L Triton X-100 (Sigma-Aldrich) 0.1 % for 10 min, in order to permeabilize cells. During the incubation, the immunostaining mastermix solution #2 was prepared diluting reagents in DAKO antibody diluent, as described below (Agilent, Santa Clara, USA; Table 4).

Table 4. The immunostaining mastermix #2.

Reagent	Antibody-clone	Conjugation	Final concentration	Company
DAPI	-	-	1:20	Roche Diagnostics GmbH, Indiana, USA
Anti-CD45	3S-Z5 [113]	AlexaFluor647 <sup>®</sup>	1:25	Santa Cruz Biotechnology Inc., Dallas, Texas, USA
Anti-PanCytokeratins (1, 4, 5, 6, 8, 10, 13, 14, 15, 16, 18, 19)	C11/AE1/AE3 [68,113]	TRITC	1:50	Aczon srl, Monte San Pietro, Italy
Anti-EpCAM	VU1D9 [113]	AlexaFluor488 <sup>®</sup>	1:50	Cell Signaling Technology Inc., Danvers, Massachusetts, USA

After the permeabilization, cells were incubated with 200  $\mu$ L of the immunostaining mastermix, for 1 h, at RT, dark. Then, cells were washed twice with 200  $\mu$ L PBS, in order to remove the unbound antibodies. Afterwards, 200  $\mu$ L of DAKO mounting medium were pipetted on cells and a glass coverslip was placed on cytopins.

### 3.4.1.2. Epifluorescence microscopy

Glass slides were observed under the epifluorescence microscope integrated into the CellCelector<sup>™</sup>. The following channels were checked with a 20 x object: DAPI for the detection of nuclei, TRITC for the cytokeratins, FITC for EpCAM-AF488 and Cy5 for the detection of the CD45-AF647. The following exposure times were used: 50 ms for DAPI, 300 ms for TRITC and FITC and 500 ms for Cy5.

### 3.4.2. Validation of the workflow

Since the enrichment of EpCAM<sup>high</sup> CTCs within the CellSearch® system has previously been established [113,172] and is currently performed in the clinical routine, the establishment of the herein described workflow focused on the novel part of the protocol only: the enrichment of the EpCAM<sup>low/negative</sup> CTCs via Parsortix™ processing of patients' blood samples, previously depleted of the EpCAM<sup>high</sup> CTCs.

#### 3.4.2.1. Immunostaining of cells in suspension

Prior to the spiking experiments, fixed MCF-7 cells were stained in suspension. To this end, the cell pellet was resuspended in 1 mL of Triton X-100 0.1 % in PBS and incubated 10 min at RT. Afterwards, cells were centrifuged at 1100 rpm for 5 min and the supernatant was discarded to remove the Triton X-100. The cell pellet was washed with 1 mL PBS and further centrifuged. Cells were resuspended in 400 µL of the immunostaining mastermix solution #2 and incubated for 1 h, at RT, dark.

#### 3.4.2.2. Cell line spiking experiments

In order to measure capturing and harvesting efficacy of the 6.5 µm Parsortix™ cassette, three independent spiking experiments were performed. Blood samples of healthy donors were processed through the CellSearch® as above described, and the discarded blood was collected. Defined amounts of MCF-7 were pipetted into the CellSearch®-processed blood samples (Table 5) which were subsequently processed with the Parsortix™ system, as explained above.

**Table 5. Amount of MCF-7 cells spiked per each spiking experiment.**

# Spiking experiment	# Spiked cells
Experiment 1	41
Experiment 2	105
Experiment 3	48

Recovered cells were counted before (capturing rate) and after harvesting (harvesting rate), under the epifluorescence microscope integrated into the CellCelector™.

### 3.4.2.3. Detection and isolation of tumour cells

Recovered cells – either from Parsortix™ or from CellSearch® cartridges – were transferred onto glass slides, located on their magnetic holder on the motorized stage, and were allowed to settle for 10 min. Instead, in order to evaluate the capturing of cells within the Parsortix cassettes, these were directly placed on the holder on the motorized stage. Analysis was performed using the CellCelector™ software 3.0 (ALS, Jena, Germany).

#### Imaging

By virtue of ferrofluid coating, EpCAM<sup>high</sup> cells could firmly settle onto glass slides and samples could be automatically scanned with a cross-stage speed of 20 % and 20 x magnification in the following epifluorescence channels: DAPI (for visualization of nuclei), TRITC (for CK) and Cy5 (for CD45). The following exposure times were used: 300 ms for TRITC, 500 ms for Cy5 and 50 ms for DAPI[160]. EpCAM<sup>low/negative</sup> cells were manually scanned with a cross-stage speed of 20 % and 40 x magnification in the epifluorescence channels above listed, utilizing the same exposure times. Images of single cells in all epifluorescence channels were recorded and stored for later documentation.

#### Selection criteria

Detected cells were analysed utilizing the following scan parameters: diameter signals ranging from 5–40 µm and grey value mean (fluorescence intensity of >2000 for cytokeratins signal). DAPI<sup>positive</sup>/Cytokeratins<sup>positive</sup>/EpCAM<sup>low/negative</sup>/CD45<sup>negative</sup> events were observed in the bright field as well (BF). Only events with a round shape in BF, specific epifluorescence signals, and without any sign of DNA fragmentation in DAPI – suggesting apoptosis – were isolated.

#### Cell isolation parameters

Cell isolation was performed with glass capillaries of 30 µm in diameter, in DAPI channel to ensure no co-isolation of surrounding cells. At first, the glass capillary was calibrated 15–25 µm above the slide surface, then, selected cells were aspirated with a volume of 20–100 nL using. For optimal cell deposition 2–9 µL PBS was aspirated prior to the isolation process. After aspiration, cells were deposited into PCR tubes prefilled with 50–100 µL PBS buffer. The whole cell isolation process for 50 CTCs took approx. 1–2.5 h. Therefore, fast processing

of samples was guaranteed. At last, PCR tubes containing single cells were centrifuged for 10 min at 1300 rpm and the supernatant was removed leaving 1  $\mu$ L of PBS in each tube. The cells were stored at  $-80^{\circ}\text{C}$  until further use.

The above reported protocol to isolate CTCs is based on Neumann et al., 2016[160].

#### **3.4.2.4. Immunocytostaining in cassette**

In order to verify the effective immunostaining of tumour cells into the separation cassette, fixed un-stained MCF-7 cells (EpCAM<sup>high</sup> and cytokeratins<sup>high</sup>) were spiked into blood samples of healthy donors, previously processed within the CellSearch® (see above). Afterwards, spiked blood samples were processed within the Parsortix™ system, as above reported, and captured cells were stained *in situ* utilizing to the immunostaining mastermix #2. Afterwards, cells were harvested, transferred onto a glass slide and the effective immunostaining of both MCF-7 and co-captured leukocytes was checked under the epifluorescence microscope integrated into the CellCelector™. As negative controls, unspiked blood samples of healthy donors were processed as well.

#### **3.4.3. Processing MBC patients' blood samples**

Blood samples of patients suffering from mBC were collected within the German DETECT III/IV and AUGUSTA studies.

##### **3.4.3.1. Statistical analysis**

The dependence of the EpCAM<sup>low/negative</sup> CTC abundance on the frequency of the EpCAM<sup>high</sup> CTCs was investigated through a linear regression test for Gaussian distribution, with 95% of confidence. The significance of the MCF-7 recovery rate comparison between the VyCAP™ and the Parsortix™ approaches was investigated through the unpaired t-test.

### 3.5. Molecular characterization of single patient-matched EpCAM<sup>high</sup> and EpCAM<sup>low/negative</sup> CTCs

The PIK3CA mutational status was investigated on single isolated EpCAM<sup>low/negative</sup> CTCs in comparison with patient-matched EpCAM<sup>high</sup> CTCs. To this end, isolated cells were lysed and their genomes amplified. Then, PIK3CA hotspot regions were Sanger sequenced through an amplicon-based approach. Prior processing patients' CTCs, the characterization workflow was tested on single isolated MCF-7 and T47D cells, known to harbour the PIK3CA hotspot mutations in exon 9 (amino acid change at position E542 and E545) and in exon 20 (amino acid change at position 1047) respectively [185,186].

#### 3.5.1. Whole genome amplification

In order to obtain optimal genomic DNA concentration for sequencing analysis, isolated cells were processed for whole genome amplification (WGA) through Ampli1 WGA™ kit (Figure 18; Menarini Silicon Biosystems), according to the manufacturer's protocol which is based on Klein and colleagues' protocol [187].

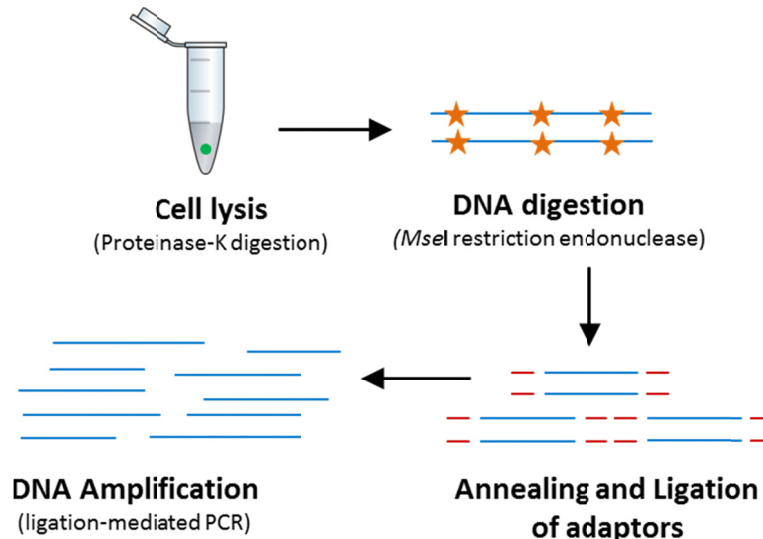


Figure 18. Ampli1™ WGA steps

Within the Ampli1™ WGA protocol, single cells are lysed and their genomes digested through MseI restriction endonucleases. Afterwards, DNA fragments are ligated to adaptors and subsequently amplified through adaptor-specific primers.

At first, cells isolated in 1 µL of PBS were incubated overnight at 65°C with Proteinase-K and co-adjuvant reagents in order to lyse cell membranes. Proteinase-K is an enzyme that

cleaves the peptide bond in proteins next to the carboxyl group of hydrophobic amino acid residues. It is often used at 50-65°C because most nucleases that would digest DNA are inactivated at these temperatures [187].

Then, the released genome was incubated for 3 h, at 37°C with a reagents mix based on *MseI* restriction endonuclease, in order to digest DNA. *MseI* is a unique restriction endonuclease which recognizes the palindromic sequence 5'-TTAA-3' and cleaves between the two T residues to produce the following 2 base 5' extension: 
$$\begin{array}{l} 5' \text{ T} \downarrow \text{TAA} 3' \\ 3' \text{ AAT} \uparrow \text{T} 5' \end{array}$$
 [187]. Afterwards, digested DNA was ligated to two DNA adaptors designed according to the previously generated *MseI*-base extensions. A primer-specific PCR was performed afterwards, in order to amplify the genome of the single processed cell. At last, WGA products were stored at -20 °C.

The WGA protocol is estimated to produce equally amplified DNA fragments of 0.2-2 kb, ~2 µg dsDNA/~5 µg ssDNA, starting from ~ 6pg of dsDNA of a single cell. As positive and negative controls, 100 ng/µL of genomic DNA of MCF-7 cells and water (Menarini Silicon Biosystems) were respectively used.

### **3.5.1.1. Quality control multiplex PCR**

The efficacy of the WGA was verified processing 1 µL of WGA products for a multiplex PCR of 4 markers located on the chromosomes 12p, 5p, 17p, 6p, by utilizing the Ampli1 WGA-QC™ kit (Menarini Silicon Biosystems), according to manufacturer's protocol. As positive and negative controls, 100 ng/µL of genomic DNA of MCF-7 cells and water were used, respectively.

### **3.5.1.2. DNA Gel-electrophoresis**

In order to assess the multiplex PCR, a DNA gel-electrophoresis was performed. At first, a mixture of 2 % agarose/ 1 % TAE/0.01 % gel red (Sigma-Aldrich/Biotium Inc., Fremont, USA) was prepared and let it polymerize for 45 min, at RT. Then, 5 µL of PCR product together with 1 µL of Loading dye "LD 6x" (Thermo Fischer Scientific) were loaded into a gel well. As a marker, 6 µL of DNA Ladder "Mass ruler LR" (Thermo Fischer Scientific) were additionally loaded into a gel well. The gel run was performed in DNA electrophoresis

chambers, for 30 min at 100 V. Afterwards, gels were observed under UV lights, in a transilluminator.

### 3.5.1.3. Statistical analysis

The difference between high integrity WGA rates of EpCAM<sup>high</sup> and EpCAM<sup>low/negative</sup> CTCs was investigated through a two-tailed t-test.

### 3.5.2. PIK3CA Exons 9 and 20 specific PCRs

WGA products were further processed for two separated PCRs amplifying PIK3CA exons 9 and 20, through the primers reported in Table 6.

**Table 6. PIK3CA exons 9 and 20 PCR primers, adapted from Lampignano et al., 2017b [183]**

PIK3CA exon	Primer name	Sequence (5' → 3')	Primer size (bp)
9	forward	CATCCGATGTACCTGATTGAACTGCATGCAGACAAAGAACAGCTCAAAGCAA	52
	reverse	CATTCCTTAGATAGCTCGGAAGTCCATTGCATTTTAGCACTTACCTGTGAC	52
20	forward	CATCCGATGTACCTGATTGAACTGCATGCATTGATGACATTGCATACATTTCG	52
	reverse	CATTCCTTAGATAGCTCGGAAGTCCATTGCGTGGAAGATCCAATCCATT	50

Per each PCR reaction, 1 µL of WGA products was added in 9 µL PCR mix consisting of: 0.2 µM forward primer, 0.2 µM reverse primer (both Exiqon, Vedbaek, Denmark), 1 U DreamTaq (Thermo Fischer Scientific) polymerase and nuclease-free water. Then, samples were incubated according to the thermal cycler program reported in Table 7.

**Table 7. Thermal cycler program of PIK3CA exons 9 and 20 PCRs.**

Cycles	Temperature °C	Hold
	95	5 min
35	95	45 sec
	58	45 sec
	72	45 sec
	72	10 min
4		∞

Afterwards, PCR products were checked through a DNA-gel electrophoresis, according to the protocol described above. Amplified DNA was stored at -20 °C.

### 3.5.3. Cleaning of PCR products

In order to remove unused primers and dNTPs, PCR products displaying amplicons of PIK3CA exons 9 and/or 20 were subsequently processed according to the ExoSAP-IT® (Affymetrix, Santa Clara, USA) protocol. In case of PCR products showing PIK3CA amplicons as well as primer dimers, a DNA-gel extraction procedure was preferred over the ExoSAP-IT®.

#### 3.5.3.1. ExoSAP-IT® protocol

The ExoSAP-IT® PCR Product Cleanup is a reagents mix mainly based on Exonuclease I activity, consisting in the removal of nucleotides from ssDNA in the 3' to 5' direction. Two  $\mu\text{L}$  of this reagent were added to 5  $\mu\text{L}$  of the amplified DNA and incubated according to the thermal program reported in the Table 8.

**Table 8. Thermal cycler program of ExoSAP-IT® cleaning protocol.**

Temperature °C	Hold
37	15 min
80	15 min

Afterwards, cleaned PCR products were stored at  $-20\text{ }^{\circ}\text{C}$ .

#### 3.5.3.2. DNA gel-extraction

In order to extract DNA from the agarose gel, the DNA band was excised with a scalpel and further processed within the QIAEX II Gel Extraction Kit (Qiagen, Hilden, Germany), according to the manufacturer's protocol.

Afterwards, cleaned PCR products were stored at  $-20\text{ }^{\circ}\text{C}$ .

### 3.5.4. DNA quantification

At last, 1  $\mu\text{L}$  of cleaned amplified DNA was quantified through the NanoDrop™ Spectrophotometer (Thermo Fischer Scientific) and if necessary, it was subsequently diluted in water, down to the optimal concentration for the Sanger sequencing (between 5  $\text{ng}/\mu\text{L}$  and 15  $\text{ng}/\mu\text{L}$ ).

### 3.5.5. PIK3CA Exons 9 and 20 Sanger sequencing

Sanger sequencing of PIK3CA exons 9 and 20 was performed by the Genomics & Transcriptomics Laboratory (GTL) of the Biological and Medical Research Centre of Düsseldorf (BMFZ) utilizing 1 µL of diluted cleaned PCR products and specific primers (Exiqon; Table 9), thought an Ion Torrent platform.

**Table 9. PIK3CA exons 9 and 20 sequencing primers, adapted from Lampignano et al., 2017b [183]**

Primer name	Sequence (5' → 3')	Product size (bp)
forward	TCCGATGTACCTGATTGAAC	20
reverse	TTCCTTAGATAGCTCGGAAG	20

### 3.5.6. Sequencing data analysis

Sequencing data analysis was performed through the software “Chromas”. Sequencing profiles of CTCs were compared to these of MCF-7, T47D cells in order to detect hotspot base exchanges.

## 4. Results

### 4.1. Enrichment and detection of patient-matched EpCAM<sup>high</sup> and EpCAM<sup>low/negative</sup> CTCs combining CellSearch® and VyCAP™ systems

#### 4.1.1. Validation of immunostaining on cytopins

Prior proceeding with the establishment of the workflow, the immunostaining mastermix #1 necessary to identify CTCs was validated on cell lines, in order to verify potential interferences between fluorophores directly conjugated to the antibodies. The breast cancer cell line MCF-7 was utilized as positive control for cytokeratins expression (clones C11/AE1/AE3) and as negative control for CD45 expression (clone HI30). On the contrary, leukocytes were utilized as positive control for CD45 and as negative control for cytokeratins. MCF-7 cells and leukocytes were effectively stained for the expected markers (Figure 19).

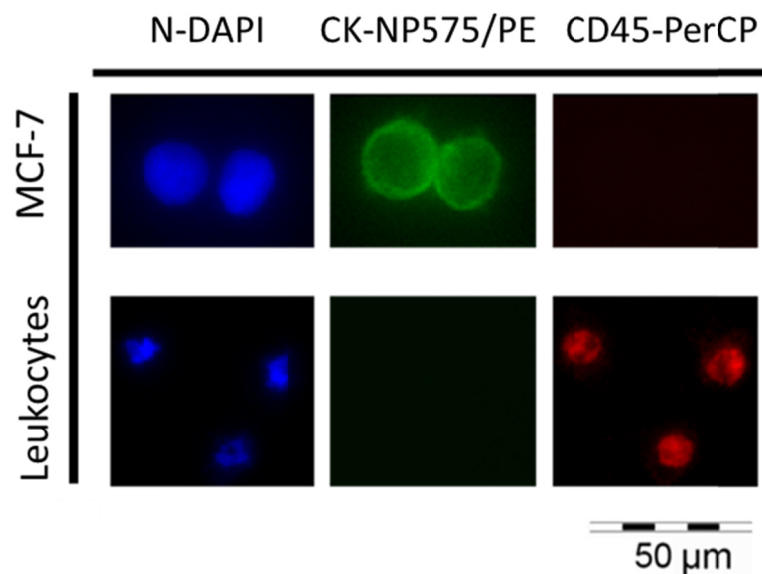


**Figure 19. Validation of the immunostaining #1 on cytopins**

In epifluorescence microscopy, MCF-7 cells exhibit positivity for nuclear (DAPI) and cytokeratins (PE) staining and negativity for CD45 (PerCP). Leukocytes shows positive staining of the nucleus (DAPI) and of CD45 (PerCP) and no expression of cytokeratins (TRITC). Magnification: 40 x.

No interferences among utilized fluorophores could be detected.

### 4.1.2. Tumour cell recovery rates of VyCAP™ filters

Prior processing patients' blood and DLA samples, the enrichment of tumour cells via VyCAP™ filtration device was validated with 3 independent spiking experiments of pre-stained MCF-7 cells into healthy donor blood samples, discarded after CellSearch® processing. The diameter of MCF-7 cells – measured via microscopy – was in average  $18 \pm 1$   $\mu\text{m}$ . After filtration, filters were inspected in epifluorescence microscopy, in order to determine the recovery rate of tumour cells. Cells positive for nuclear (DAPI) and cytokeratins (PE) staining, negative for CD45 (PerCP) expression and with a round shape, were defined as tumour cells. In Table 10 amounts of pre-stained tumour cells spiked and subsequently enriched are reported.

**Table 10. Amount of MCF-7 cells spiked and enriched per each spiking experiment.**

# Spiking experiment	# Spiked MCF-7 cells	# Enriched MCF-7 cells
Experiment 1	64	3
Experiment 2	97	7
Experiment 3	70	25

The average recovery rate for MCF-7 cells was  $16 \pm 14$  %.

### 4.1.3. Validation of immunocytostaining on microsieves

The effective immunostaining of tumour cells retained by VyCAP™ microsieves was validated through further spiking experiments. After spiked blood samples were processed with the VyCAP™ filtration device, cells retained by the filter were immunostained *in situ* and then inspected in epifluorescence microscopy. Captured tumour cells and co-enriched leukocytes were effectively stained for the expected markers (Figure 20).

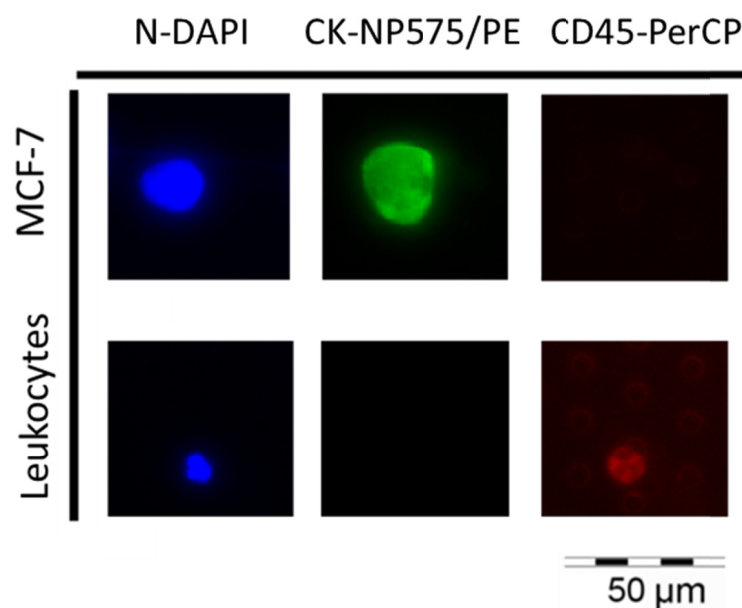


**Figure 20. Validation of the immunostaining #1 on the microsieve**

In epifluorescence microscopy, MCF-7 cells exhibit positivity for nuclear (DAPI) and cytokeratins (PE) staining and negativity for CD45 (PerCP). Leukocytes shows positive staining of the nucleus (DAPI) and of CD45 (PerCP) and no expression of cytokeratins (PE). Magnification: 40 x.

Within unspiked blood samples, only leukocytes could be detected.

#### **4.1.4. Processing patients' blood samples**

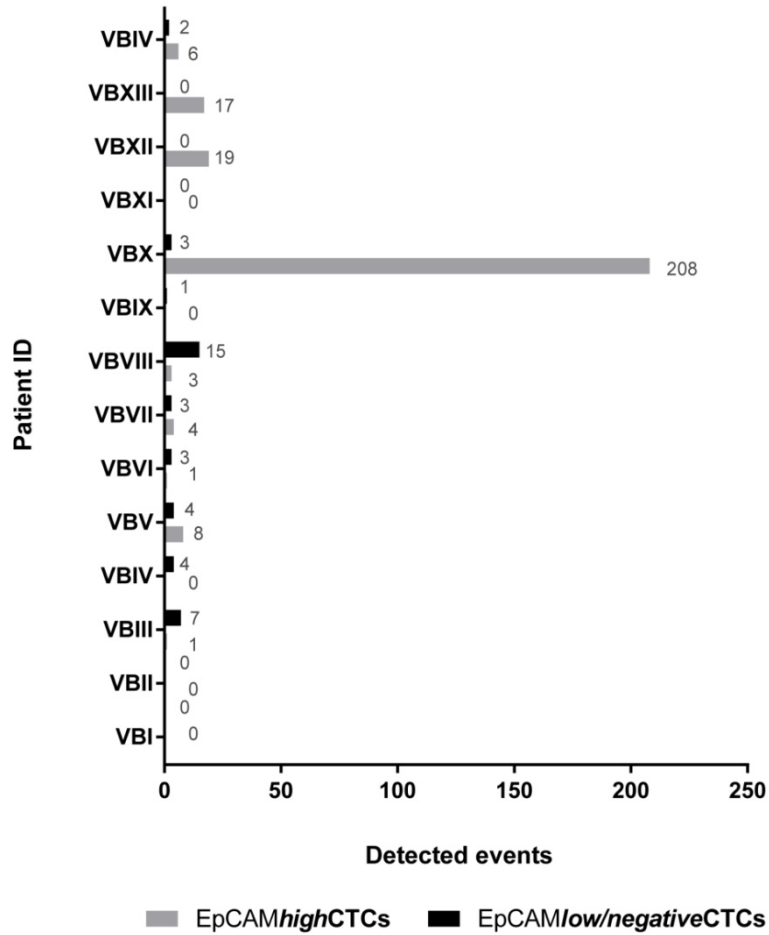
From 09/2015 to 06/2016, 14 blood samples of 14 mBC patients were sequentially processed as described above (see chapter 3.3). Patients' primary tumours characteristics are reported in the Table 11.

Table 11. Clinical features of patients' primary tumours.

	# Patients with EpCAM <sup>high</sup> and EpCAM <sup>low/negative</sup> CTCs (%)	# Patients with only EpCAM <sup>high</sup> CTCs (%)	# Patients with only EpCAM <sup>low/negative</sup> CTCs (%)	# Patients with no CTCs
<b>Total patients</b>	7 (50)	2 (14)	2 (14)	3 (22)
<b>Tumour size</b>				
T1	1 (25)	1 (50)	1 (50)	0
T2	2 (50)	1 (50)	0	1 (33)
T3	0	0	0	2 (67)
T4	1 (25)	0	1 (50)	0
<i>Missing data</i>	3	0	0	0
<b>Lymph nodes involved</b>				
N-	2 (50)	0	0	1 (33)
N+	2 (50)	2 (100)	2 (100)	2 (67)
<i>Missing data</i>	3	0	0	0
<b>Metastases status*</b>				
M0	2 (50)	1 (50)	1 (50)	3 (100)
M1	2 (50)	1 (50)	1 (50)	0
<i>Missing data</i>	3	0	0	0
<b>Histological grade</b>				
I	0	0	0	0
II	2 (50)	1 (50)	0	1 (33)
III	2 (50)	1 (50)	2 (100)	2 (67)
<i>Missing data</i>	3	0	0	0
<b>Her2 positive</b>				
	1 (25)	0	0	0
<i>Missing data</i>	3	0	0	0
<b>ER positive</b>				
	4 (80)	2 (100)	2 (100)	2 (67)
<i>Missing data</i>	2	0	0	0
<b>Triple negative</b>				
	0	0	0	1 (33)

\*: at the time of blood draw all patients were metastasized

In 64% (n=9) of processed blood samples, the EpCAM<sup>high</sup> fraction of CTCs could be observed. In 78% (n=7) of these, the EpCAM<sup>low/negative</sup> CTC subpopulation could be detected as well. The EpCAM<sup>low/negative</sup> CTC-fraction was observed in ~14% (n=2) of samples (Figure 21).



**Figure 21. Patient-matched EpCAM<sup>high</sup> and EpCAM<sup>low/negative</sup> CTCs collected from blood samples with CellSearch® and VyCAP™**

Five blood samples out of 14 (~36 %) showed no CTCs. Within CTC-positive samples, 78 % (n=7) had both fractions of tumour cells. VB: VyCAP™ blood.

In Figure 22, CTCs detected in patients' blood samples are depicted.

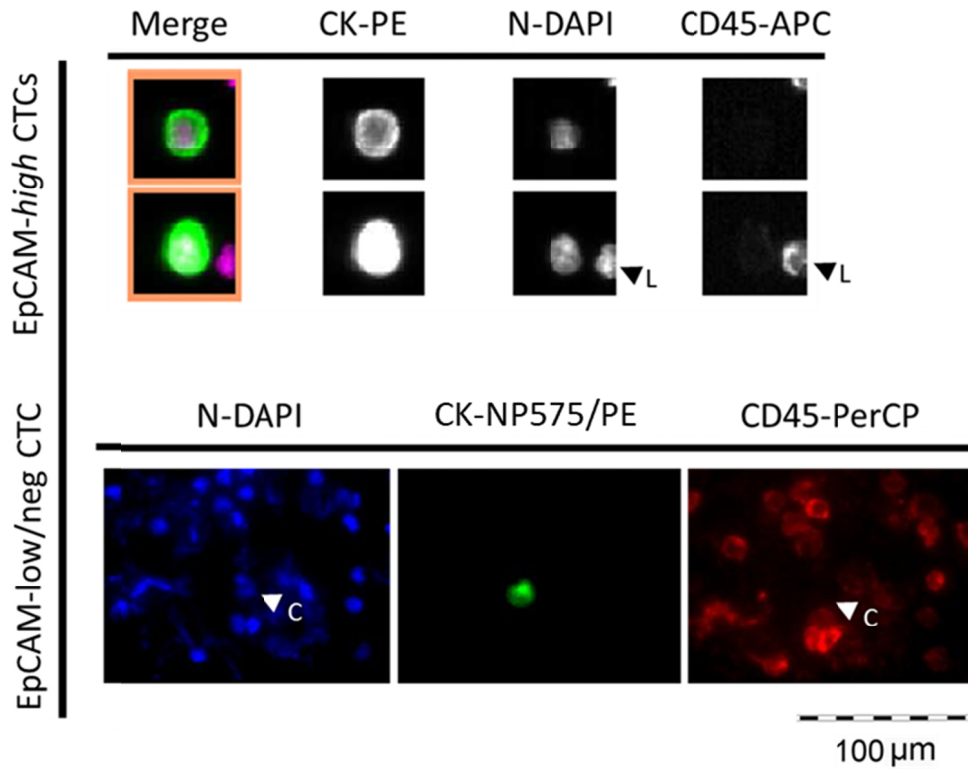


**Figure 22. Two EpCAM<sup>high</sup> and one EpCAM<sup>low/negative</sup> CTC collected from blood samples via CellSearch® and via VyCAP™, respectively**

Enriched CTCs could be detected through their positivity for nuclear (DAPI) and cytokeratins staining (PE) and negativity for the expression of the leukocyte marker CD45 (APC or PerCP). Cells surrounding CTCs are identified as co-captured leukocytes by virtue of positive nuclear and CD45 staining and of negativity for cytokeratins expression. C: CTC; L: leukocytes.

*Results reported in the paragraph above were generated within the CTC-Trap and included in de Wit et al., 2017, submitted [180]*

### 4.1.5. Processing patients' DLA samples

From 10/2015 to 09/2016, 8 DLA samples of 8 mBC patients were sequentially processed, starting from 2 ml of DLA product, as previously described (see chapter 3.3). Patients' primary tumours characteristics are reported in Table 12.

**Table 12. Clinical features of patients' primary tumours.**

	# Patients with EpCAM <sup>high</sup> and EpCAM <sup>low/negative</sup> CTCs (%)	# Patients with only EpCAM <sup>high</sup> CTCs (%)	# Patients with no CTCs
<b>Total patients</b>	3 (37.5)	3 (37.5)	2 (25)
<b>Tumour size</b>			
T1	1 (33)	1 (33)	0
T2	1 (33)	1 (33)	2 (100)
T3	0	1 (33)	0
T4	0	0	0
<i>Missing data</i>	1	0	0
<b>Lymph nodes involved</b>			
N-	2 (66)	0	1 (50)
N+	0	3 (100)	1 (50)
<i>Missing data</i>	1	0	0
<b>Metastases status*</b>			
M0	0	0	2 (100)
M1	2 (66)	3 (100)	0
<i>Missing data</i>	1	0	0
<b>Histological grade</b>			
I	0	0	0
II	0	2 (66)	2 (100)
III	1 (33)	1 (33)	0
<i>Missing data</i>	2	0	0
<b>Her2 positive</b>	0	1 (33)	2 (100)
<i>Missing data</i>	1	1	0
<b>ER positive</b>	2 (66)	3 (100)	1 (50)
<i>Missing data</i>	1	0	
<b>Triple negative</b>	0	0	0

\*: at the time of blood draw all patients were metastasized

The EpCAM<sup>high</sup> fraction of CTCs could be observed in 75% (n=6) of processed DLA samples. In 50% of these (n=3), the EpCAM<sup>low/negative</sup> CTC subpopulation could be detected as well (Figure 23) [123]. No patient exhibited EpCAM<sup>low/negative</sup> CTCs only [180].

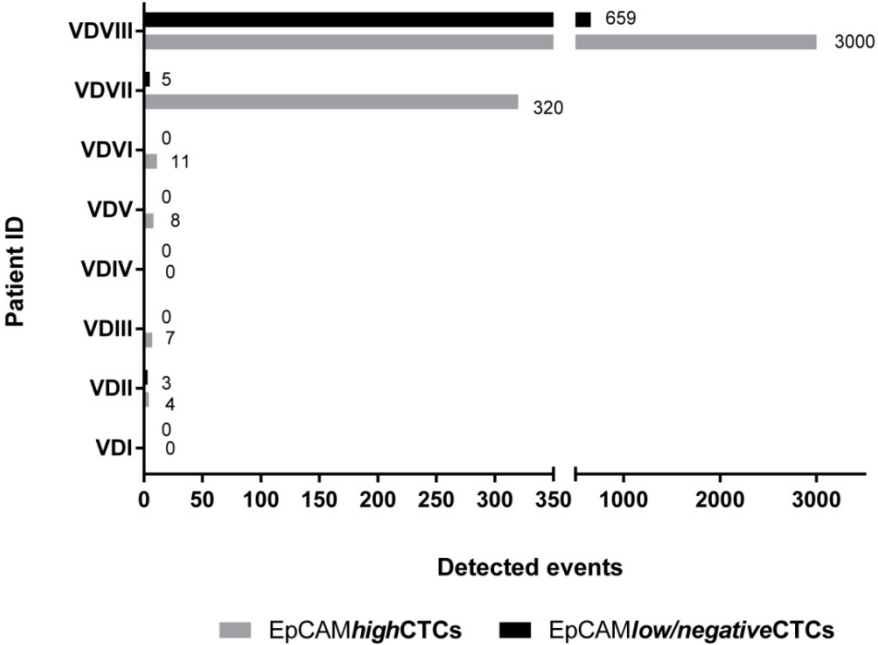


**Figure 23. Patient-matched EpCAM<sup>high</sup> and EpCAM<sup>low/negative</sup> CTCs collected from DLA samples with CellSearch® and VyCAP™**

Two DLA samples out of 8 (25 %) contained no CTCs. Within CTC-positive samples, the 50 % (n=3) had both fractions of tumour cells.

In Figure 24, CTCs detected in patients' DLA samples are depicted.

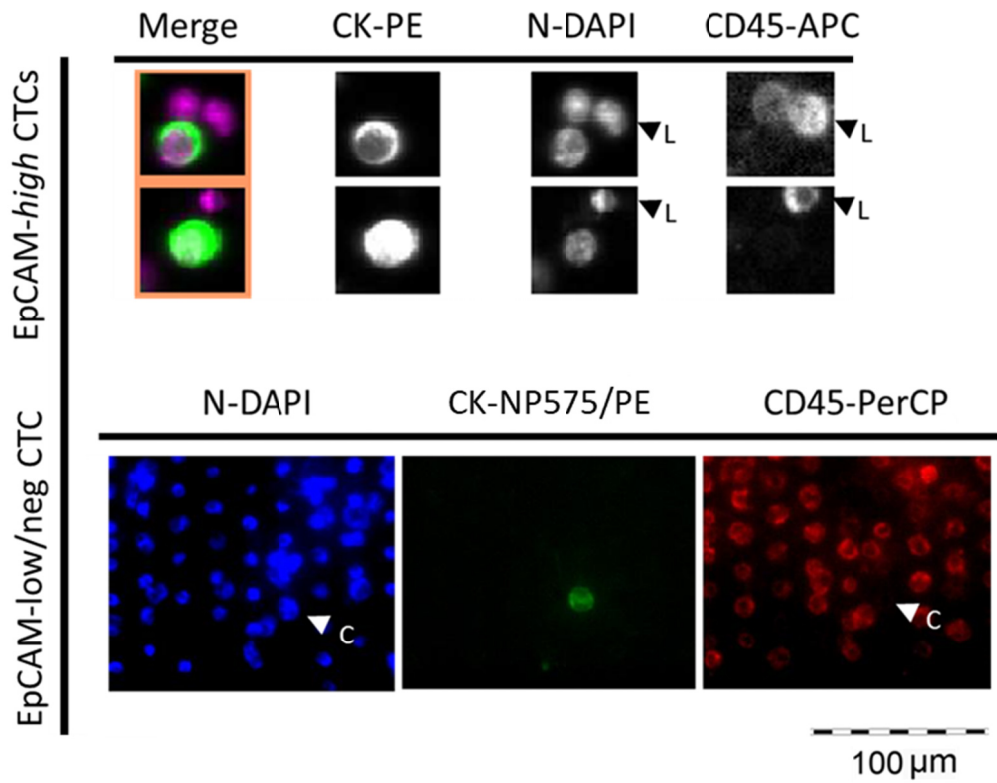


**Figure 24.** Two EpCAM<sup>high</sup> and one EpCAM<sup>low/negative</sup> CTC collected from DLA samples via CellSearch® and via VyCAP™, respectively

Enriched CTCs could be detected through their positivity for nuclear (DAPI) and cytokeratins staining (PE) and negativity for the leukocyte marker CD45 expression (APC or PerCP). Cells surrounding the CTC are identified as co-captured leukocytes by virtue of positive nuclear and CD45 staining and of negativity for cytokeratins expression.

*Results reported in the paragraph above were generated within the CTC-Trap and included in Andree et al., AACR annual meeting 2017 [123]*

## 4.2. Enrichment and isolation of patient-matched EpCAM<sup>high</sup> and EpCAM<sup>low/negative</sup> CTCs combining CellSearch®, Parsortix™ and CellCelector™ systems

### 4.2.1. Validation of immunostaining on cytopspins

Prior proceeding with the establishment of the workflow, the immunostaining mastermix #2 necessary to identify CTCs was validated with cell lines, in order to analyse potential interferences between fluorophores directly conjugated to each antibody. The breast cancer cell line MCF-7 was utilized as positive control for cytokeratins (clones C11/AE1/AE3) and EpCAM (clone vu14D9) expression and as negative control for CD45 (clone 3Z5S) expression. On the contrary, leukocytes were utilized as positive control for CD45 and as negative control for cytokeratins and EpCAM immunostaining. Each cell line was effectively stained for the expected markers (Figure 25).

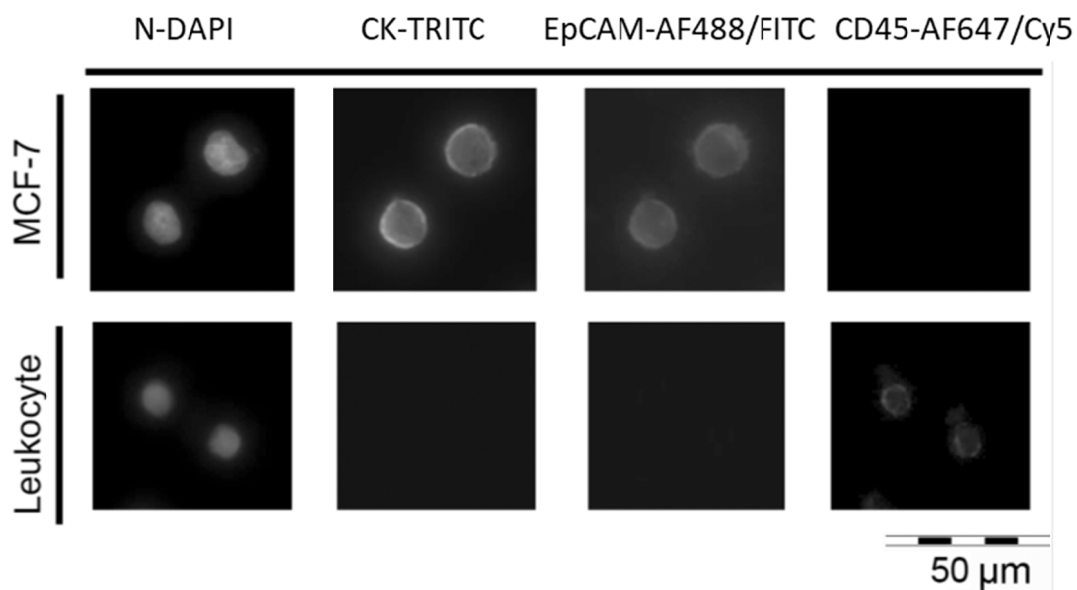


Figure 25. Validation of immunostaining #2 on cytopspins, *adapted from Lampignano et al., 2017b [183]*

In epifluorescence microscopy, MCF-7 cells exhibit positivity for nuclear (DAPI), cytokeratins (TRITC) and EpCAM (FITC) staining and negativity for CD45 (Cy5). Leukocytes shows positive staining of the nucleus (DAPI) and of CD45 (Cy5) and no expression of cytokeratins (TRITC) and EpCAM (FITC). Magnification: 40 x.

No interferences among utilized fluorophores could be detected.

## 4.2.2. Tumour cell recovery rates of Parsortix™ system

Prior processing patients' blood samples, the enrichment of tumour cells via Parsortix™ system was validated through 3 independent spiking experiments of pre-labelled MCF-7 cells in healthy donor blood samples (Table 13), previously processed within the CellSearch® system.

**Table 13. Amount of MCF-7 cells spiked, captured and harvested per each spiking experiment.**

# Spiking experiment	# Spiked MCF-7 cells	# Captured MCF-7 cells	# Harvested MCF-7 cells
Experiment 1	41	20	15
Experiment 2	105	85	35
Experiment 3	48	48	14

The diameter of MCF-7 cells – measured via microscopy – was in average  $18 \pm 1 \mu\text{m}$ . After processing via Parsortix™, in order to determine the recovery rates of tumour cells, the suspension of enriched MCF-7 was placed onto a glass slide and observed in epifluorescence microscopy. Cells positive for nuclear (DAPI), cytokeratins (TRITC), and EpCAM (FITC) staining, negative for CD45 (Cy5) expression and with a round shape, were defined as tumour cells.

The average capturing rate of MCF-7 cells was  $78 \pm 25 \%$ . Out of it,  $48 \pm 24 \%$  tumour cells could be harvested. The global recovery rate was  $33 \pm 4 \%$ .

## 4.2.3. Validation of immunocytostaining inside Parsortix™ cassettes

The effective immunostaining of tumour cells captured within Parsortix™ cassettes was validated through further spiking experiments. Fixed MCF-7 cells were spiked into healthy donor blood samples, previously processed within the CellSearch™ system, and were further processed through the Parsortix™ device. After capturing, enriched cells were immunostained inside the cassette and then collected outside the system. The suspension of the enriched cells was placed onto a glass slide and observed in epifluorescence microscopy. Captured tumour cells and co-enriched leukocytes showed to be effectively stained for the expected markers (Figure 26).

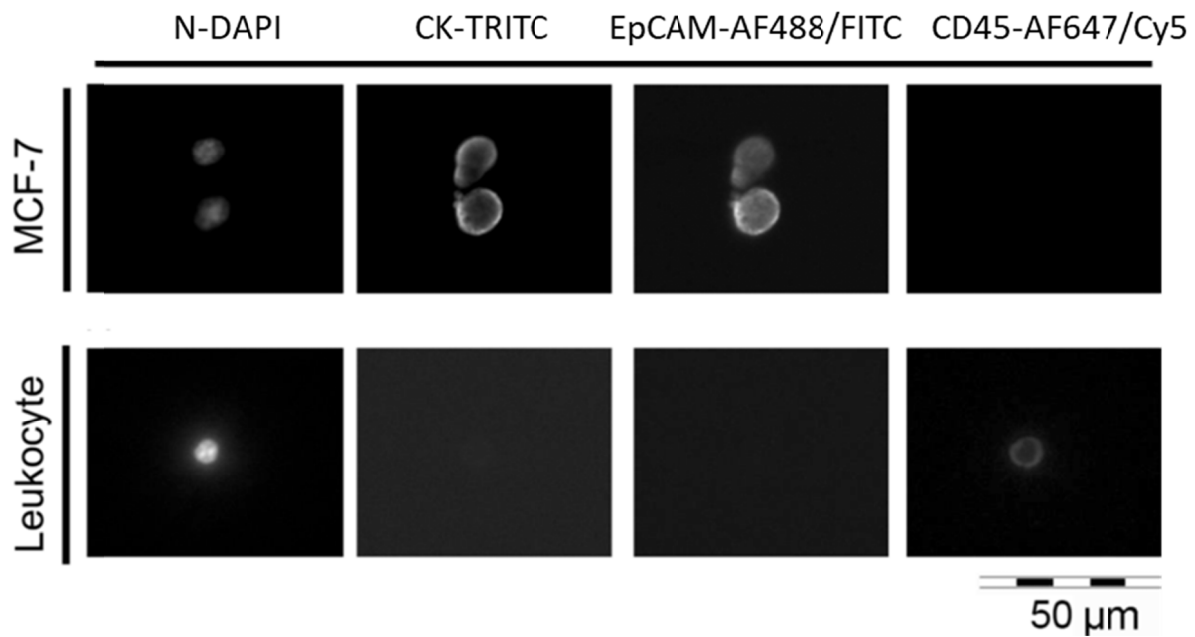


**Figure 26. Validation of immunostaining #2 inside Parsortix™ cassette, adapted from Lampignano et al., 2017b [183]**

In epifluorescence microscopy, MCF-7 cells exhibit positivity for nuclear (DAPI), cyokeratins (TRITC) and EpCAM (FITC) staining and negativity for CD45 expression (Cy5). A representative leukocyte shows positive staining of the nucleus (DAPI) and of CD45 (Cy5) and no expression of cyokeratins (TRITC) and EpCAM (FITC). Magnification: 40 x.

Within the unspiked blood samples, only leukocytes were detected.

#### 4.2.4. Processing patients' blood samples through 6.5 µm Parsotix™ cassettes

From 07/2015 to 11/2016, 52 blood samples of 47 mBC patients – diagnosed with HER2/neu-negative primary tumours and positive for EpCAM<sup>high</sup> CTCs – were sequentially processed. Patients' primary tumours characteristics are reported in the Table 14.

**Table 14. Clinical features of patients' primary tumours**

	# Patients with EpCAM <sup>high</sup> and EpCAM <sup>low/negative</sup> CTCs (%)	# Patients with only EpCAM <sup>high</sup> CTCs (%)
<b>Total patients</b>	27 (57)	20 (43)
<b>Tumour size</b>		
T1	12 (46)	7 (37)
T2	13 (50)	8 (42)
T3	0	1 (5)
T4	1 (4)	3 (16)
<i>Missing data</i>	1	1
<b>Lymph nodes involved</b>		
N-	12 (48)	10 (50)
N+	13 (52)	10 (50)
<i>Missing data</i>	2	0
<b>Metastases status*</b>		
M0	19 (73)	14 (78)
M1	7 (27)	4 (22)
<i>Missing data</i>	1	2
<b>Histological grade</b>		
I	1 (4)	0
II	13 (52)	17 (94)
III	11 (44)	1 (6)
<i>Missing data</i>	2	2
<b>ER positive</b>	23 (85)	13 (68)
<i>Missing data</i>	0	1
<b>Triple negative</b>	0	1 (5)

\*: at the time of blood draw all patients were metastasized

In 56 % (n=29) of processed blood samples, both EpCAM<sup>high</sup> and EpCAM<sup>low/negative</sup> cell subpopulations could be detected (Figure 27).

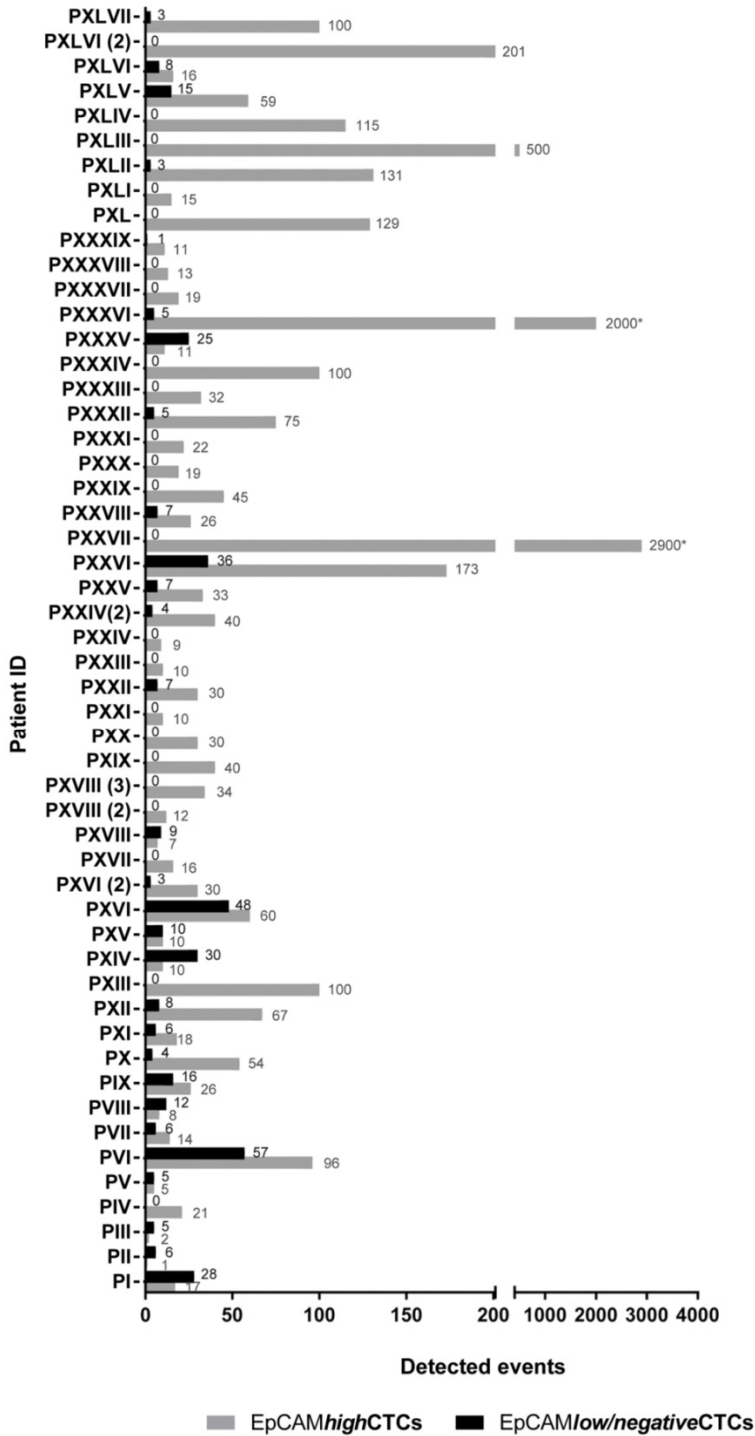
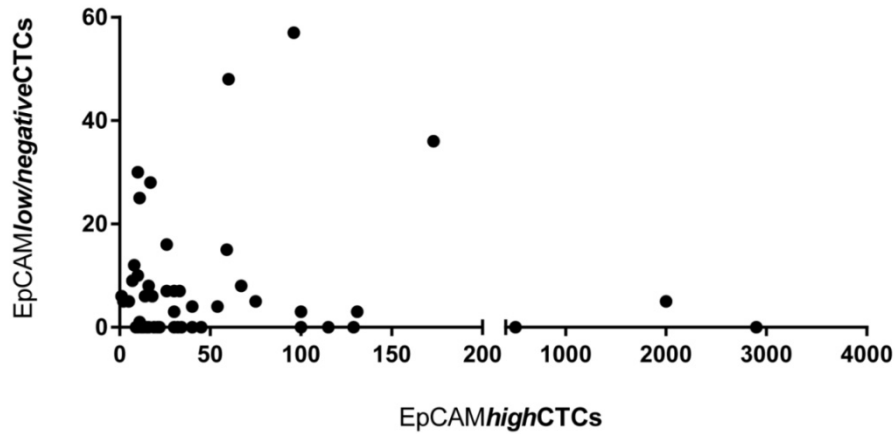


Figure 27. Patient-matched EpCAM<sup>high</sup> and EpCAM<sup>low/negative</sup> CTCs enriched in blood samples with CellSearch® and Parsortix™, adapted from Lampignano et al., 2017b [183]

Out of 52 blood samples, 56 % (n=29) exhibited both fractions of tumour cells. Remaining 44 % (n=23) had only EpCAM<sup>high</sup> CTCs. P: parsortix.

No linearity could be observed between the positivity rates of the two subpopulations of CTCs ( $R^2 = 0.007$ ;  $P = 0.57$ ; Figure 28).



**Figure 28. Counts of EpCAM<sup>high</sup> and EpCAM<sup>low/neg</sup> CTCs compared with a linear regression test**

At an increased abundance of EpCAM<sup>high</sup> CTCs does not correspond an increased frequency of EpCAM<sup>low/negative</sup> CTCs ( $R^2 = 0.007$ ;  $P = 0.57$ ; Gaussian distribution with 95% of confidence).

#### **4.2.5. Isolation of single tumour cells via CellCelector™**

Tumour cells suitable for downstream applications were sorted according to their morphology and expression of proper markers, as previously described by Polzer and colleagues [157]. From 13 patients, 107 EpCAM<sup>high</sup> and 145 matched-EpCAM<sup>low/negative</sup> cells were selected and successfully isolated via CellCelector™ micromanipulator (Figure 29).

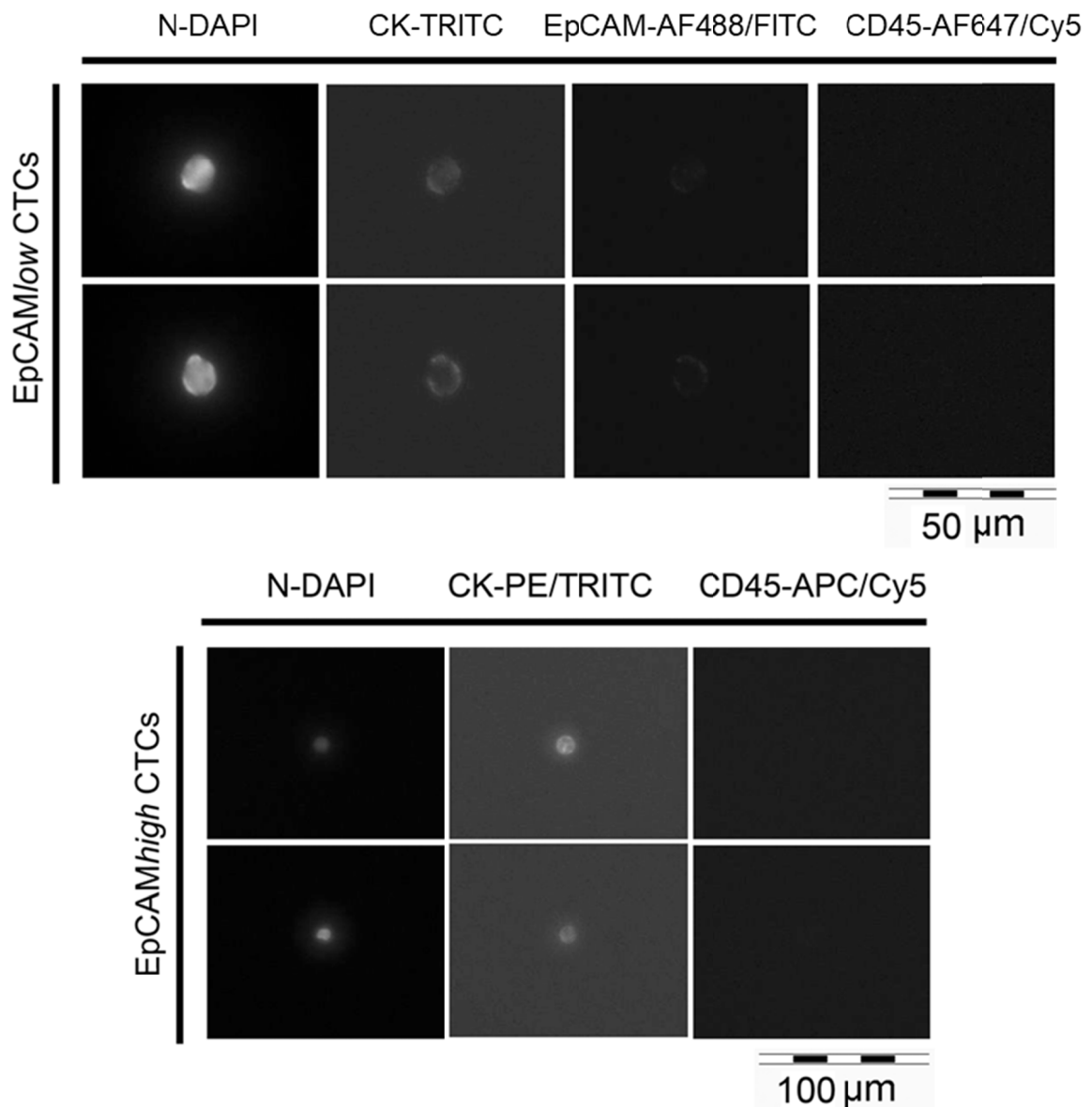


**Figure 29. Isolated EpCAM<sup>low/negative</sup> cells and EpCAM<sup>high</sup> cells, by Lampignano et al., 2017b [183]**

During the detection of EpCAM<sup>low/negative</sup> cells, glass slides were scanned at a magnification of 40 x in the following channels: DAPI for nucleic DNA, TRITC for cytokeratins, FITC for EpCAM, Cy5 for CD45. EpCAM<sup>low/negative</sup> cells show positivity for nuclear and cytokeratins staining, very weak or no expression of EpCAM, and no expression of CD45. EpCAM<sup>high</sup> cells enriched in CellSearch® cartridges were automatically scanned at a magnification of 20 x in same epifluorescence channels. They show positivity for nuclear and cytokeratins staining, and no expression of CD45. After scanning, single cells were isolated in DAPI to guarantee the purity of the isolation.

Results reported in the section above (except for the paragraph 4.2.2.) were included in Lampignano et al., 2017b [183]

### 4.3. Molecular characterization of single patient-matched EpCAM<sup>high</sup> and EpCAM<sup>low/negative</sup> CTCs

At first, the characterization workflow was tested on single isolated MCF-7 and T47D cells and then applied to patients' CTCs. MCF-7 and T47D cells were chosen due to the harbouring of PIK3CA hotspot mutations respectively in exon 9 (amino acid change at position E542 and E545) and in exon 20 (amino acid change at position 1047) [185,186].

#### 4.3.1. Amplification of whole genomes of single tumour cells

In order to obtain sufficient quantity of DNA for sequencing analysis, genomes of single isolated tumour cells were amplified. At first, the technique was validated on single fixed and stained MCF-7 cells. Along with single MCF-7, no cell control buffer (NC) were processed for WGA, to verify the absence of contaminations of genomic DNA or circulating DNA of cells eventually destroyed during the workflow. The NC samples exhibited no DNA contaminations (Figure 30).

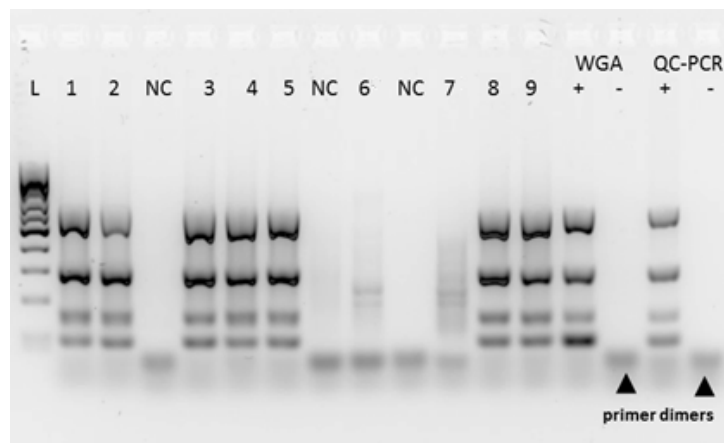


Figure 30. Representative Gel-Electrophoresis of WGA-QC PCR products

The presence of 4 amplicons indicates high genomic integrity. L: ladder; NC: no cell control. Primer dimers have been confirmed by Sanger sequencing.

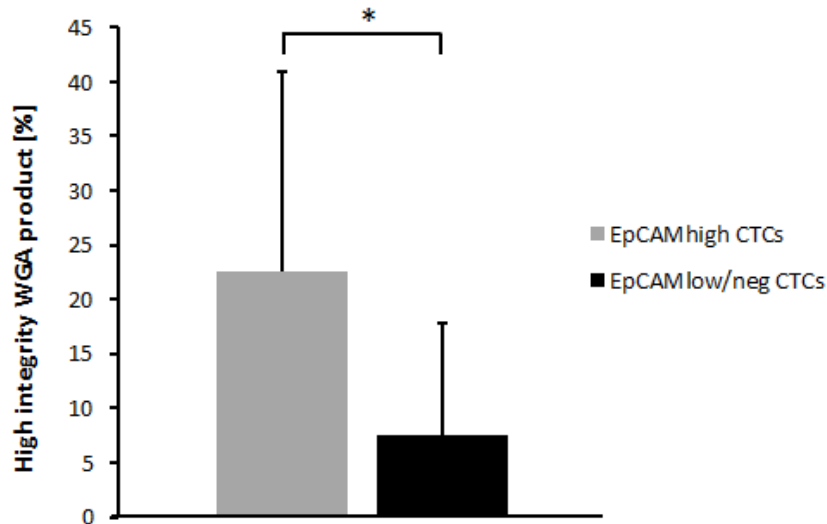
Then, the protocol was applied to single CTCs isolated according to the workflow previously described (see chapter 3.5.1). Considering the total amount of processed CTCs, high genomic integrity was observed in ~28 % WGA libraries of EpCAM<sup>high</sup> CTCs vs. ~8 % WGA libraries of EpCAM<sup>low/negative</sup> CTCs (Table 15).

Table 15. CTCs processed for WGA show different integrity of their amplified genomes, *adapted from Lampignano et al., 2017b [183]*

Sample number	Patient ID	EpCAM <sup>high</sup> CTCs			EpCAM <sup>low/negative</sup> CTCs		
		Sorted CTCs	High integrity WGA products	Low Integrity WGA products	Sorted CTCs	High integrity WGA products	Low Integrity WGA products
1	PI	5	0	5	19	0	19
2	PV	1	0	1	2	0	2
3	PVI	11	5	6	24	3	21
4	PVIII	8	0	8	12	0	12
5	PIX	26	11	15	16	2	14
6	PX	13	4	9	5	0	5
7	PXI	7	3	4	6	0	6
8	PXVI	9	1	8	27	1	26
9	PXXIV (2)	6	1	5	4	0	4
10	PXXXV	8	2	6	18	3	15
11	PXXXVI	2	1	1	5	1	4
12	PXLVI	7	2	5	4	0	4
13	PXLVII	4	0	4	3	1	2
		<b>107</b>	<b>30</b>	<b>77</b>	<b>145</b>	<b>11</b>	<b>134</b>

P: parsortix.

The difference between mean values of high integrity WGA products of the two CTC subgroups showed to be statistically significant ( $p < 0.02$  for  $22.5 \pm 18.4$  % EpCAM<sup>high</sup> CTCs vs.  $7.6 \pm 10.2$  % EpCAM<sup>low/negative</sup> CTCs; Figure 31).



**Figure 31. Comparison of high integrity WGA products of EpCAM<sup>high</sup> and EpCAM<sup>low/negative</sup> CTCs sorted from 13 patients**

Mean values of high integrity WGA products within EpCAM<sup>high</sup> and EpCAM<sup>low/negative</sup> CTCs were respectively 22.5 ± 18.4 and 7.6 ± 10.2 % and in a comparison through a two-tailed t-test, they showed to differ significantly (\*: p < 0.02).

In all performed WGA reactions, no DNA contaminations could be detected within NC samples.

### 4.3.2. Detection of PIK3CA exons 9 and 20 amplicons

Prior sequencing, WGA libraries of CTCs were amplified for PIK3CA hotspot regions located on exons 9 and 20, using two exon-specific PCRs. At first, the protocol was assessed through cells of MCF-7 and T47D cell lines. Then, WGA libraries of 92 EpCAM<sup>high</sup> CTCs and of 126 matched-EpCAM<sup>low/negative</sup> CTCs from 10 patients were sorted and processed as described above (see chapter 3.5.2). In Figure 32, representative images of gel electrophoresis of PIK3CA exons 9 and 20 PCRs are depicted.

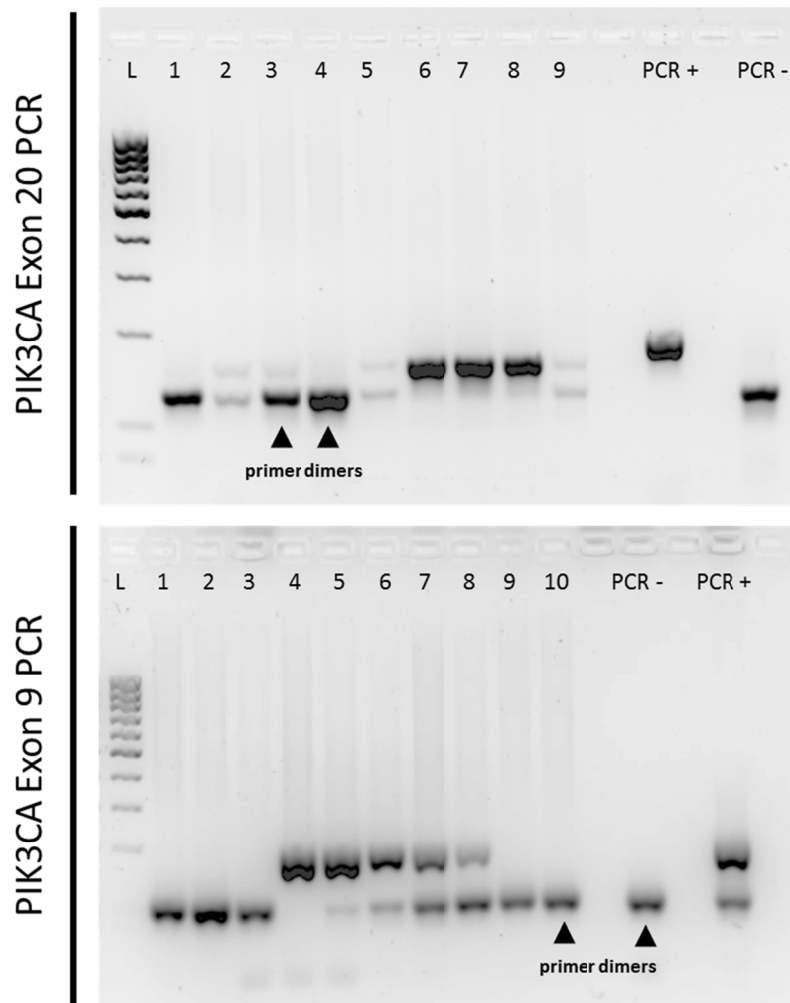


**Figure 32. Representative pictures of gel-electrophoresis of PIK3CA exons 9 and 20 PCR products of amplified genomes of CTCs**

The detection of a band at the same height of the positive control (PCR+) indicates the success of the amplification protocol. Sometimes, an excess of unutilized primers could be observed as primer dimers. All the detected bands, including primer dimers, were confirmed by sequencing. Pseudogenes have not been amplified.

Within the EpCAM<sup>high</sup> subpopulation of CTCs, 41 cells exhibited the exon 9 amplicon and 34 cells exhibited the exon 20 amplicon. Within patient-matched EpCAM<sup>low/negative</sup> CTCs, 49 CTCs exhibited the exon 9 amplicon and 38 CTCs exhibited the exon 20 amplicon (Table 16).

**Table 16. Amplified genomes of CTCs processed for PIK3CA exons 9 and 20 PCRs may not exhibit the presence of the respective amplicon**

Sample number	Patient ID	EpCAM <sup>high</sup> CTCs			EpCAM <sup>low/negative</sup> CTCs		
		Sorted CTCs	CTCs exhibiting exon 9 amplicon	CTCs exhibiting exon 20 amplicon	Sorted CTCs	CTCs exhibiting exon 9 amplicon	CTCs exhibiting exon 20 amplicon
1	PI	5	2	1	19	13	10
2	PVI	11	5	2	24	7	7
3	PIX	26	14	11	15	6	3
4	PX	13	9	5	5	5	1
5	PXI	7	1	3	6	1	1
6	PXVI	9	3	3	27	3	2
7	PXXXV	8	1	3	18	8	8
8	PXXXVI	2	1	1	5	3	3
9	PXLVI	7	3	3	4	1	1
10	PXLVII	4	2	2	3	2	2
		<b>92</b>	<b>41</b>	<b>34</b>	<b>126</b>	<b>49</b>	<b>38</b>

P: Parsortix.

### 4.3.3. Sequencing of PIK3CA hotspot regions

Within the EpCAM<sup>high</sup> subpopulation of CTCs, 38 cells could be successfully sequenced for PIK3CA exon 9 and 32 cells for exon 20. Within the patient-matched EpCAM<sup>low/negative</sup> CTCs, 39 cells could be successfully sequenced for PIK3CA exon 9 and 35 cells for exon 20. In order to detect the hotspot mutations E542K, E545K, H1047R known to induce the constitutive activity of the PI3K kinase, involved in tumorigenesis [185,186], CTCs sequencing profiles were compared to these of MCF-7 and T47D cells.

In six patients out of ten, both fractions of CTCs were classified as wild-type (WT) for the investigated PIK3CA hotspot sequences. In CTCs of four patients (PI, PIX, PX, PXLVII), PIK3CA hotspots mutations were observed along with the WT form of the oncogene (Table 17 and Figure 33).

**Table 17. Mutational analysis of PIK3CA hotspot regions in exons 9 and 20 within patient-matched EpCAM<sup>high</sup> and EpCAM<sup>low/negative</sup> CTCs, adapted from Lampignano et al., 2017b [183]**

EpCAM <sup>high</sup> CTCs					
PIK3CA Exon 9 mutational analysis				PIK3CA Exon 20 mutational analysis	
Sample number	Patient ID	Sequenced CTCs	Mutational status	Sequenced CTCs	Mutational status
1	PI	2	WT	1	WT
2	PVI	5	WT	2	WT
3	PIX	13	WT	11	2: p.H1047L (c.CAT > CTT); 9: WT
4	PX	7	WT	5	2: p.H1047R (c.CAT > CGT); 3: WT
5	PXI	1	WT	3	WT
6	PXVI	3	WT	3	WT
7	PXXXV	1	WT	3	WT
8	PXXXVI	1	WT	1	WT
9	PXLVI	3	WT	3	WT
10	PXLVII	2	WT	2	1: p.H1047L (c.CAT > CTT); 1: WT
			<b>38</b>	<b>34</b>	
EpCAM <sup>low/negative</sup> CTCs					
PIK3CA Exon 9 mutational analysis				PIK3CA Exon 20 mutational analysis	
Sample number	Patient ID	Sequenced CTCs	Mutational status	Sequenced CTCs	Mutational status
1	PI	10	1: p.E545K (c.CAG > AAG); 9: WT	7	WT
2	PVI	7	WT	7	WT
3	PIX	5	1: p.E545K (c.CAG > AAG); 4: WT	3	WT
4	PX	2	WT	1	WT
5	PXI	1	WT	1	WT
6	PXVI	0	n.d.	2	WT
7	PXXXV	8	WT	8	WT
8	PXXXVI	3	WT	3	WT
9	PXLVI	1	WT	1	WT
10	PXLVII	2	WT	2	WT
			<b>39</b>	<b>35</b>	

P: parsortix.

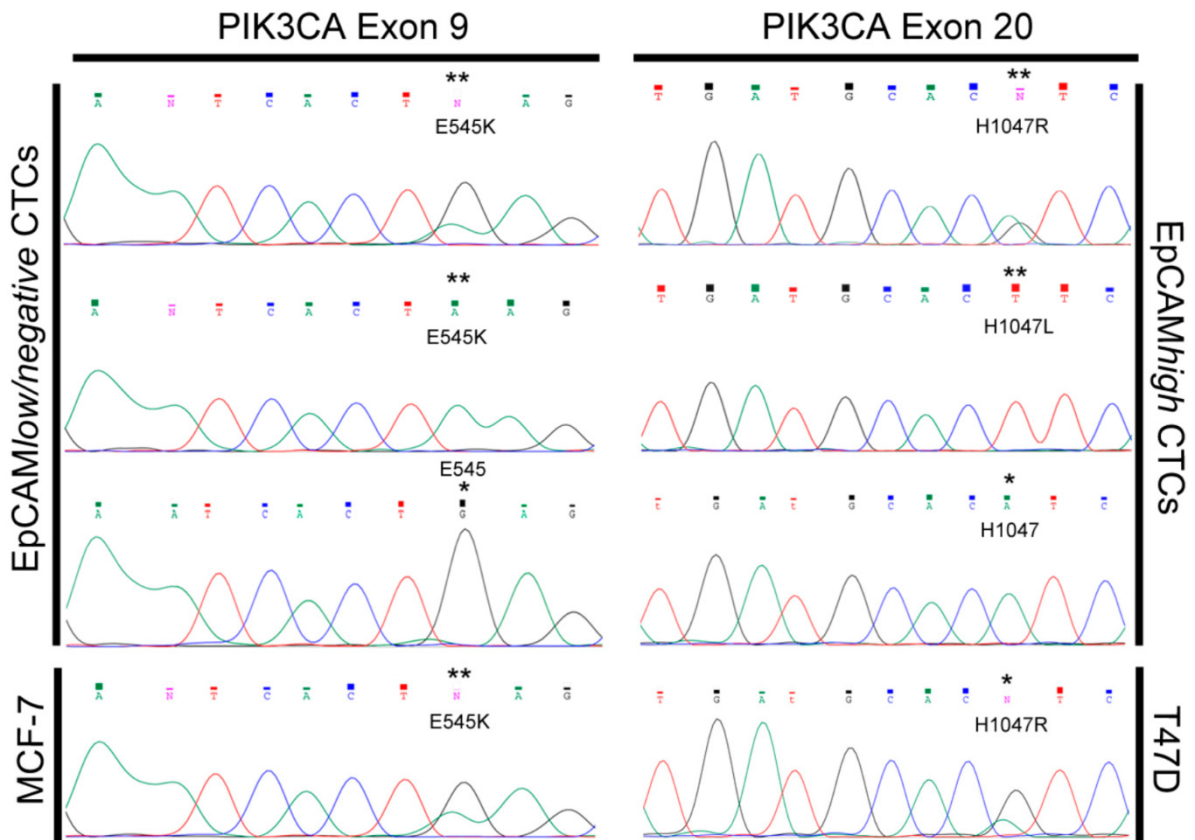


**Figure 33. Representative PIK3CA Exons 9 and 20 sequencing profiles within CTCs and cell lines, by Lampignano et al., 2017b [183]**

In two EpCAM<sup>low/negative</sup> CTCs from 2 different patients the mutation 9/E545K (\*\*) could be observed when compared to the sequencing profile of a single MCF-7 cell (\*\*). Two representative sequencing profiles of EpCAM<sup>high</sup> CTCs from different patients exhibit the mutations 20/H1047R and the 20/H1047L (\*\*) in comparison to the sequencing profile of a single T47D cell (\*\*). CTCs registered as PIK3CA wild-type show no mutations (\*). \*\*: base exchange; \* wild-type base.

Patient PI exhibited the PIK3CA mutation E545K (codon 545 of the exon 9, glutamine to lysine) within the EpCAM<sup>low/negative</sup> CTC subpopulation only, in 1/10 sequenced cells; 9/10 sequenced cells were, instead, WT. The two patient-matched EpCAM<sup>high</sup> CTCs were determined as PIK3CA-WT.

Patients PX and PXLVII carried the mutated PIK3CA in EpCAM<sup>high</sup> CTCs only. In the patient PX, the mutation H1047R (codon 1047 of the exon 20, histidine to arginine) was recorded in 2/5 sequenced cells; 3/5 sequenced cells were, instead, WT. The one patient-matched EpCAM<sup>low/negative</sup> CTC exhibited the PIK3CA WT. In patient PXLVII the rare mutation H1047L (codon 1047 of exon 20, histidine to leucine) was observed in 1/2 sequenced cells;

1/2 sequenced cells were, instead, WT. The 2 patient-matched EpCAM<sup>low/negative</sup> CTCs were recorded as PIK3CA WT.

Patient PIX exhibited different PIK3CA hotspot mutations within both subpopulations of CTCs. In 1/5 EpCAM<sup>low/negative</sup> CTCs, the mutation E545K was observed. Four residual EpCAM<sup>low/negative</sup> CTCs were PIK3CA WT. Two out of eleven EpCAM<sup>high</sup> CTCs exhibited the rare mutation H1047L (codon 1047 of exon 20, histidine to leucine). Nine residual EpCAM<sup>high</sup> CTCs were classified as PIK3CA WT.

No further base exchanges were observed within the amplicon sequences of both exons 9 and 20 of PIK3CA.

## 5. Discussion

The prognostic value of CTCs was investigated and verified in different tumour entities – including mBC – by numerous studies [81,162,164,165]. Subsequently, several research groups started to evaluate the possibility to determine the optimal treatment for cancer patients based either on the enumeration of CTCs or on the characterization of these tumour cells (e.g. DETECT studies [62,162,170,171,173–176]). However, to date, studies on CTCs as prognostic and therapy decision tools mainly focused on the EpCAM<sup>high</sup> subpopulation, thereby overlooking EpCAM<sup>low/negative</sup> CTCs with potential highly malignant phenotypes [167,177,179]. Very little is known about this transient/mesenchymal fraction of CTCs and intensive research is surely necessary to acquire further insights into their biology and potential role in tumor metastasis.

Major obstacles in investigating CTCs are represented by: **a)** their low concentration in the PB, thereby requiring highly sensitive enrichment technologies; **b)** the absence of cancer-specific markers which hampers both enrichment and detection of CTCs; **c)** the heterogeneity of tumour cells, which requires highly specific methods for both single cell isolation, and phenotypical/molecular characterization. Subsequently, intensive research to optimize workflows to enrich, isolate and characterise CTCs is of utmost importance. Furthermore, these workflows need to fit to the specific tumour entity at the core of the study.

**a-b)** As it regards the enrichment and detection of EpCAM<sup>high</sup> CTCs within mBC patients, a gold standard technique (CellSearch® system) is already available and has been comprehensively validated [62,81]. On the contrary, the enrichment and detection of the remaining EpCAM<sup>low/negative</sup> CTCs are still in their infant stages and definitely require further optimizations to shed light on this subpopulation of tumour cells. So far, these CTCs have mainly been collected either by focusing on specific mesenchymal markers [70,167], either on cancer-stemness traits [167], or on markers alternative to EpCAM [113]. As a consequence, there is the chance that CTCs with epithelial-mesenchymal plasticity have been overlooked. **c)** Research on CTCs is further hampered by the absence of a gold-standard technique for tumour cell-isolation, which is required to investigate the CTC-heterogeneity on “omic” levels in order to better understand metastatic mechanisms of

cancerous lesions. Furthermore, of major importance is the identification of biomarkers to predict the resistance to treatments and to achieve personalised and more efficient CTC-driven therapies. In this scenario, the identification of PIK3CA hotspot mutations, within primary tumours as well as within CTCs, has attracted the interest of the scientific community. The rationale behind this raising concern is that the detection of this mutated oncogene in ~40 % mBC cases – in higher rates in distant metastases – and that the increased resistance to anti-HER2/neu therapies often observed in mBC patients with PIK3CA activating mutations [8,25].

The present work has been conceived to investigate the whole population of CTCs (epithelial, transient and mesenchymal) within mBC patients, with particular attention to an efficient recovery of CTCs and subsequent molecular characterization: three workflows were validated and successfully applied to patients' samples. The first two workflows allow to enriching the EpCAM<sup>low/negative</sup> fraction of CTCs along with the collection of patient-matched EpCAM<sup>high</sup> CTCs, thus overcoming the major limit of the CellSearch® enrichment system, which is the dependence on the EpCAM expression on the surface of tumor cells. Furthermore, of these two workflows, the latter enables further single-cell molecular characterisation on the whole CTC-population. At last, the third workflow allows the analysis of genomic DNA in single CTCs which could support the identification of potential biomarkers of therapy resistance.

## 5.1. Enrichment and detection of patient-matched EpCAM<sup>high</sup> and EpCAM<sup>low/negative</sup> CTCs combining CellSearch® and VyCAP™ systems

As previously comprehensively explained (see chapter 1.4), the FDA-approved CellSearch® system enables the EpCAM-dependent enrichment of CTCs in various tumour entities. Their enumeration holds prognostic power when exceeding defined threshold levels (e.g.  $\geq 5$  CTCs/7.5 mL PB in mBC) [81,162,164,165]. The possibility to collect blood or DLA samples after CellSearch®-mediated EpCAM-depletion enabled to investigate the whole population of CTCs without any phenotypical restrictions, thus overcoming the major limit of the CellSearch®. Within the CTC-Trap consortium, a double CTC enrichment approach on

both blood and DLA was validated, by sequentially processing clinical samples via CellSearch® and VyCAP™ filters. The VyCAP™ microsieves are designed to retain all cells bigger than 5 µm, under a constant flow pressure of 100 mbar[68]. In order to apply VyCAP™ filtration to patients' blood or DLA samples previously processed within the CellSearch®, this workflow was initially established via spiking experiments using a breast cancer cell line. First and foremost, the immunofluorescence staining required for the detection of tumour cells, was successfully validated on cytopins of fixed cells of MCF-7 breast cancer cell line and of leukocytes of healthy donors. Then, MCF-7 cells fixed and stained in suspension were spiked into healthy donors' CellSearch®-processed blood samples and further filtered, to measure the collection rates of the VyCAP™ approach. A successful enrichment of  $16 \pm 14$  % MCF-7 cells could be registered. This data fits to the range of capturing rates reported by de Wit and colleagues, who tested the same method with cell lines of different tumour entities (T24:  $59 \pm 9$  %; SKBr3:  $2 \pm 1$  %; Colo-320:  $18 \pm 6$  %; SW480:  $6 \pm 7$  %; NCI-H1650:  $\pm 7$  %) [68]. The same spiking experiments were omitted for the CellSearch® system, since it already underwent a detailed establishment and it is currently utilized in the clinical routine within the German studies DETECT III/IV, AUGUSTA and SEPTEMBRA [113,172]. Afterwards, by applying this procedure to clinical samples, patient-matched EpCAM<sup>high</sup> and EpCAM<sup>low/negative</sup> CTCs could be detected in 78 % (7/9) of processed blood samples without any correlation in positivity rates, while only EpCAM<sup>low/negative</sup> CTCs could be observed in ~14 % of samples. Within patients' samples, the recorded CTC enrichment rate via filtration was higher than that reported by de Wit et al., which, by utilizing the same approach on metastatic lung cancer blood samples, observed both EpCAM<sup>high</sup> and EpCAM<sup>low/negative</sup> cells in 19 % (5/27) of the patients [68]. The higher frequency of the EpCAM<sup>low/negative</sup> CTC-subgroup in mBC blood samples could be either due to the different size of the patient-cohort and/or to the different tumour entity investigated. However, in agreement to the herein presented results, de Wit et al. reported a lack of correlation between abundance of patient-matched EpCAM<sup>high</sup> and EpCAM<sup>low/negative</sup> CTCs [68]. A possible, speculative explanation could be found in the postulation of two different, but coexistent, processes of dissemination and colonization of tumour cells (see chapter 1.3.1), which might be independent on each other [37]. However, further investigations are utmost needed to shed light on this difference of frequencies and to understand the role of EpCAM<sup>low/negative</sup> CTCs in cancer dissemination.

The Workflow #1 was also applied to DLA samples of mBC patients, to the end of increasing the yield of enriched CTCs and of implementing the DLA processing in the clinical routine [123]. In DLA products of 6 out of 8 patients, both subgroups of CTCs were found and 50 % of them presented EpCAM<sup>low/negative</sup> CTCs as well. However, this cohort of patients is still too restricted to draw any significant conclusions. In fact, even though the collection of DLA samples is relatively easy and painless, only 8 patients agreed to be enrolled into the study, due to the long collection time required (90 min to obtain 40 mL of DLA product [123]). Nevertheless, within DLA samples, similar tendencies to previously examined blood samples could be observed: lack of linearity between frequencies of epithelial and transient/mesenchymal CTCs and presence of EpCAM<sup>low/negative</sup> tumour cells in at least half of the clinical samples.

Even though this filtration approach was easy to integrate in the clinical routine and relatively inexpensive to perform, it showed some drawbacks requiring further optimizations. The major disadvantage is the high leukocyte contamination which in many cases hampers the clear detection of CTCs. Due to the same reason, the clogging of microsieves was often observed - especially when processing DLA samples- which then required further filtrations through more filters. Furthermore, it was observed a correlation between low phenotypical quality of retained cells and the time delay between CellSearch® processing and VyCAP™ filtration. Last but not least, some EpCAM<sup>high</sup> CTCs might be not captured by the CellSearch® system, thus, EpCAM-depleted blood and DLA samples might still contain some of these cells which could not be detected due to the lack of an EpCAM immunostaining, which could be, however, integrated in future experiments. Despite these limits, the double processing of both blood and DLA samples via CellSearch® and VyCAP™ systems, enabled the effective enrichment for different subgroups of CTCs. In order to investigate the molecular heterogeneity of EpCAM<sup>low/negative</sup> CTCs compared to the EpCAM<sup>high</sup>, another label-free approach was chosen over VyCAP™ filtration, due to the impossibility to singularise stained and fixed CTCs enriched on microsieves.

## 5.2. Enrichment and isolation of patient-matched EpCAM<sup>high</sup> and EpCAM<sup>low/negative</sup> CTCs combining CellSearch®, Parsortix™ and CellCelector™ systems

The Parsortix™ system enables the size-dependent enrichment of cells regardless of their protein expression and allows their further collection in small buffer suspensions. In order to optimize the CTC detection for further single cell isolation via CellCelector™, a new immunofluorescence staining had to be established on fixed MCF-7 and leukocytes cytopins, since the micromanipulator integrates a different epifluorescence microscope than the one utilized for previous imaging. Within this second immunostaining mastermix, an anti-EpCAM antibody was included, to exclude potential EpCAM<sup>high</sup> events not captured by the CellSearch® system. After the successful establishment of the second immunostaining, fixed MCF-7 cells were labelled in suspension and further utilized for spiking experiments to assess the effective capturing and harvesting rates of the Parsortix™ system, utilizing disposable cassettes with narrow passages of 6.5µm. Average capturing and harvesting rates of  $78 \pm 25 \%$  and  $48 \pm 24 \%$ , respectively, were achieved for tumour cells of  $18 \mu\text{m} \pm 1$  in diameter. As expected, the capturing rate was slightly higher than that reported by Xu et al. and by Hvichia et al. who utilized cassettes with bigger narrow passages (10 µm) to capture MCF-7 cells ( $54.7 \pm 6.1 \%$  [89]) and cell lines of different tumour entities and cell size (PANC1: 23 µm, 70 %; A375: ~17 µm, 67 %; PC3: 30 µm, 68 %; A549: 15 µm, 60 %; T24: 18 µm, 42 % [143]), spiked into blood samples. These data also confirm that the ~5-fold dilution of the CellSearch®-discarded blood occurring during its collection, does not seem to have a negative impact on the enrichment of tumour cells within the Parsortix™, as previously observed for VyCAP™ filtration [68]. Interestingly, both Xu et al. and Hvichia et al. reported higher harvesting rates than these herein described (MCF-7:  $58.7 \pm 13.3 \%$  [89]; PANC1: 60 %; A375: 69 %; PC3: 68 %; A549: 67%; T24: 54 %) [89,143], suggesting that perhaps, smaller narrow passages may hamper the collection of the cells captured and immunostained *in situ*. However, in preliminary experiments on 14 mBC blood samples processed through 10 µm, the CTC recovery rate was quite scarce (4 cells within 3 blood samples; data not shown), indicating that the dimension of CTCs in mBC might be smaller than these of cell lines tested by Xu et al. and by Hvichia et al. Altogether, these data also

highlight that the dimension of cells is not the only parameter influencing their enrichment, but an important role may also be played by their deformability, as previously already postulated [87,89,143]. The global recovery rate of MCF-7 cells achieved via Parsortix™ was  $33 \pm 4 \%$ , hence higher than the  $16 \pm 14 \%$  achieved via VyCAP™ filtration, although this difference was not significant, probably due to the high standard deviation registered with VyCAP™ ( $p = 0.17$ ; Figure 34). In fact, the high variability of this latter approach is one of its major limits.

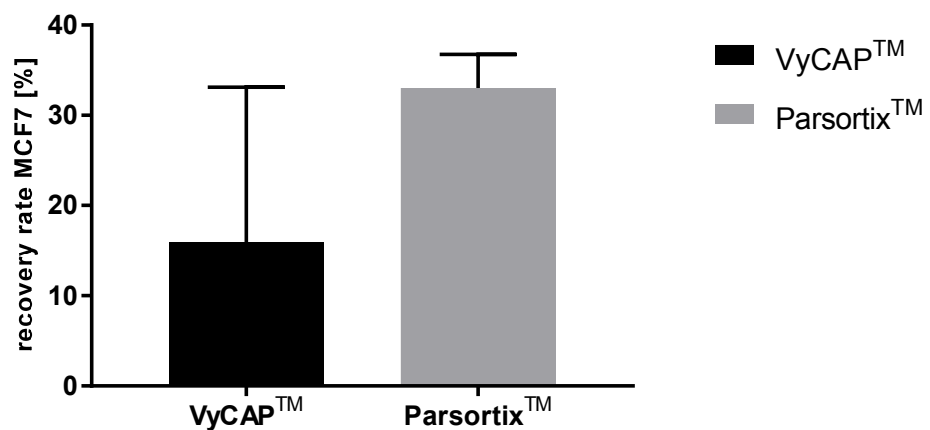


**Figure 34. Comparison of recovery rates of MCF-7 cells achieved via VyCAP™ and via Parsortix™ systems**

In a statistical comparison between Parsortix™ and VyCAP™ recovery rates of MCF-7 cells, the former approach shows higher performances. However the comparison was non-significant ( $p = 0.17$ ).

At the same time, greater cell purity could be achieved via Parsortix™ (Figure 35) which facilitated the CTC detection and made this approach sensitive and suitable enough for single cell downstream analysis.

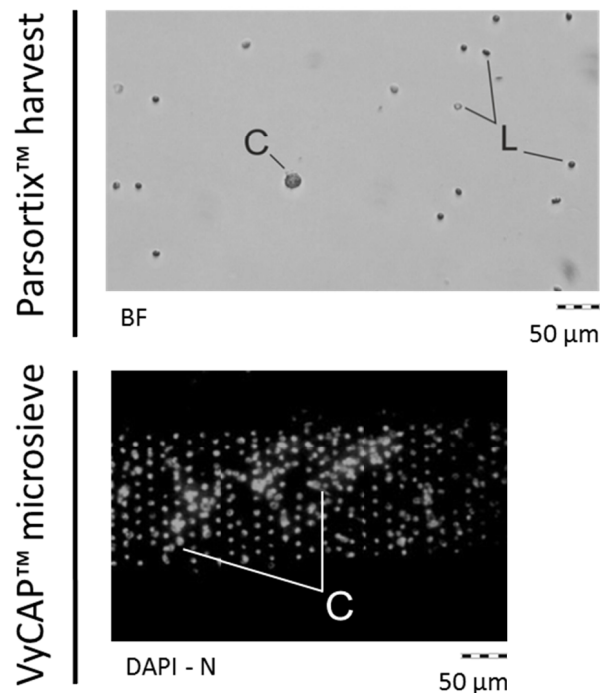


**Figure 35. Tumour cell/leukocyte ratio in blood samples processed via VyCAP™ and Parsortix™ devices.**

In a qualitative comparison between the Parsortix™ harvest and the VyCAP™ microsieve, the former approach shows higher enrichment purity. In fact, on microsieves, tumour cells (C) are totally surrounded by co-enriched leukocytes (L). Image magnification 20 x.

High tumour cell recoveries and low leukocyte contaminations within the Parsortix™ system are the basis for the effective CTC analysis since Neumann et al. already showed that the following single cell isolation via CellCelector™ micromanipulator can be performed with 97 % of efficacy [160]. Therefore, the optimization of the *in situ* immunostaining of captured cells is of high importance in order to minimize the cell loss, otherwise occurring during in suspension staining procedures (own observations and [87,89,143]). In this project, the immunostaining of enriched tumour cells in the parsortix cassettes was performed for the first time. After a first immunocytostaining validation, the whole workflow consisting of double enrichment and isolation was successfully applied to a cohort of 52 blood samples of 47 mBC patients. In 56 % of them, both EpCAM<sup>high</sup> and EpCAM<sup>low/negative</sup> CTCs could be detected without any significant linearity ( $p = 0.57$ ), confirming previous observations made with VyCAP™ filtration.

In the future, as a conclusion of the studies DETECT III/IV, AUGUSTA and SEPTEMBRA, which this project is connected to, patients' follow-up data will be collected and related to

the presence of EpCAM<sup>low/negative</sup> CTCs, in order to further investigate their potential predictive and prognostic role in mBC.

As briefly mentioned before, major advantages of the Parsortix™ system are the simplicity of use, considerable recovery rates, purity of cellular harvests, suitability for *in situ* immunostaining and the collection of the enriched cellular suspension which is useful for further downstream applications. As it regards the CellCelector™ micromanipulator, major merits are its versatility for different applications and the live monitoring of the CTC isolation, which may assure the cellular purity required for molecular analysis. However, some limits need to be taken in considerations for both systems and as a consequence, for the whole workflow. The processing through the Parsortix™ system is time consuming (4 h – 4.5 h for one blood sample previously processed within the CellSearch®) and its integration into the clinical routine may, therefore, be tough. However, most available CTC-enrichment techniques which operate in a label-free fashion and which ensure high recoveries and purity, require long processing time [88]. Last but not least, since the positivity to anti-EpCAM as well as to anti-cytokeratins immunostaining (together with the positive nuclear staining) are the only accepted proof for the CTC detection (see chapter 1.4.1), there is the possibility that tumour cells which underwent a complete EMT, might have been overlooked. As it regards the CTC-isolation approach via CellCelector™ micromanipulator, it requires an experienced user and the effective deposit of the selected cell cannot be assured due to the lack of a visual control. However, these disadvantages are also shared by the FACS-sorting, one of the other main CTC-isolation techniques [88]. Despite the described limits, the above illustrated novel approach allowed the molecular characterization of single CTCs.

### 5.3. Molecular characterization of single patient-matched EpCAM<sup>high</sup> and EpCAM<sup>low/negative</sup> CTCs

Immediately after the detection of CTCs, cells suitable for genomic analysis – identified according to Polzer and colleagues' criteria [157]– were selected for isolation and were further processed for WGA and PIK3CA Sanger sequencing through an amplicon-based approach. At first, these protocols were successfully tested with MCF-7 cells and were then applied to patients' CTCs.

In total, amplified genomes exhibited high integrity in 28% EpCAM<sup>high</sup> CTCs, in agreement with Polzer et al [157]. In contrast to their findings, only 8% WGA products of EpCAM<sup>low/negative</sup> CTCs showed high integrity ( $p < 0.02$  for mean values). This unexpected observation may suggest early apoptosis undetectable by the phenotypical analysis of CTCs' nuclei. Several studies have already described the high frequency of apoptotic EpCAM<sup>positive</sup> CTCs, which might play a role in patients' outcomes [72,188–191]. Therefore, in future experiments, the different apoptosis rates between both CTC subgroups will be investigated by implementing the immunostaining protocol with early apoptosis indicators.

After WGA, PIK3CA exons 9 and 20 were further amplified within both CTC-fractions and cells displaying the presence of the specific amplicons were processed for point mutation analysis. The hotspot mutation E545K was recorded in EpCAM<sup>low/negative</sup> CTCs from 2 patients (patients PI and PIX) and the mutation H1047R was observed in EpCAM<sup>high</sup> CTCs from another patient (patient PX). These are the two most frequently described PIK3CA hotspot mutations in breast cancer tissues ([www.mycancergenome.org](http://www.mycancergenome.org)) as well as in EpCAM<sup>positive</sup> CTCs [157,172,173,192,193]. Interestingly, in EpCAM<sup>high</sup> CTCs from two different patients (patient PIX and PXLVII), also the rare mutation H1047L could be detected, which was already reported by Gasch et al. [194].

Due to the genomic DNA amplification required for the mutational analysis, there is the possibility that artificial base exchanges may be introduced by DNA polymerases. However, considering sequencing results, this was excluded, since only specific PIK3CA hotspot mutations could be observed within sequencing profiles of both exons 9 and 20. The successful collection and isolation of different subpopulations of CTCs allowed to perform single cell mutational analysis and to assess for the first time, the heterogeneity of the PIK3CA status within single EpCAM<sup>low/negative</sup> CTCs, besides patient-matched EpCAM<sup>high</sup> tumour cells. Even though based on a small cohort of patients, the detection of PIK3CA hotspot mutations in only EpCAM<sup>low/negative</sup> CTCs in one patient (PI) and in both EpCAM<sup>low/negative</sup> and EpCAM<sup>high</sup> CTCs in another one (PIX) is of high interest. These results suggest that implementing the PIK3CA mutational analysis with EpCAM<sup>low/negative</sup> CTCs may be relevant for future CTC-based therapies targeting HER2/neu-positive CTCs, as envisioned in the DETECT III study. Furthermore, an increased resistance to anti-HER2/neu treatments could be induced by PI3K activating mutations [8,25] and in some studies on EpCAM<sup>positive</sup> CTCs, PIK3CA hotspot

mutations were already presented [157,172,173,192,193] and related to patients' overall survival and prognosis free survival [192]. Hence, numerous research groups are currently investigating the PIK3CA oncogene in both mBC primary tumours and CTCs, as a potential biomarker of therapy resistance, in order to achieve more precise personalized treatments in the near future.

## 5.4. Conclusions and outlooks

CTCs are postulated to be precursors of distant metastatic lesions. In addition, their presence in PB is related to poor clinical outcomes in patients suffering of different cancers, including breast. Therefore, investigating the biology of these tumour cells is of utmost importance to better understand this systemic disease and to improve treatment options for patients. The optimization of approaches to enrich, detect and characterize CTCs is subsequently, a central topic in the field of the "liquid biopsy". To this end, in the present work, three workflows were established and successfully validated on patients' clinical samples. The first workflow allows the detection of a wide population of CTCs (EpCAM<sup>high</sup> and EpCAM<sup>low/negative</sup>) within blood and DLA samples, by combining the sequential enrichment via CellSearch® and VyCAP™. The second workflow enables, besides the enrichment and the detection, also the isolation of these patient-matched tumour cells, by sequentially utilizing CellSearch®, Parsortix™ and CellCelector™ devices. The genomic characterization of isolated CTCs with a potential aggressive phenotype can be achieved within the third workflow. The final aim of the latest is to identify a potential treatment resistance mechanism (e.g. activating PIK3CA hotspot mutations) within patient-matched epithelial and transient/mesenchymal CTCs. Although the herein reported data are based on a small cohort of patients, they further confirm the frequent presence of the EpCAM<sup>low/negative</sup> subpopulation of CTCs, undetectable via the only FDA-approved enrichment system (CellSearch®) and additionally highlight that the combination of two sequential CTC-enrichment approaches, may be the optimal way to investigate the whole population of these tumour cells. Last but not least, the presented data point out that the investigation of the PIK3CA mutational status within patient-matched EpCAM<sup>high</sup> and EpCAM<sup>low/negative</sup> CTCs may provide further knowledge about resistance to anti-HER2/neu therapies (e.g. lapatinib) and may help to identify optimal treatment strategies for patients. In future works, the patient cohort will be expanded and longitudinal follow-up studies will be performed to

investigate the evolution of both EpCAM<sup>low/negative</sup> CTC abundance and PIK3CA mutational status during treatments as well as their potential correlation with clinical outcomes. Furthermore, apoptosis mechanisms and copy number alteration profiles will be investigated within the EpCAM<sup>low/negative</sup> sub-group of CTCs with respect to the EpCAM<sup>high</sup> cells, in order to confirm and better understand the malignant origin of the former subgroup of tumour cells.

## Summary

Circulating tumour cells (CTCs) have been observed in the peripheral blood of cancer patients and their abundance has been correlated to poor clinical outcomes in metastatic breast cancer (mBC). CTCs are mostly enriched by EpCAM-based systems (e.g. CellSearch®) which overlook EpCAM<sup>low/negative</sup> tumour cells with an epithelial/mesenchymal plasticity, postulated to be highly aggressive. Main goal of this project was to establish robust workflows to enrich, detect, isolate and characterize patient-matched EpCAM<sup>high</sup> and EpCAM<sup>low/negative</sup> CTCs in blood as well as in leukapheresis (DLA) samples of metastatic breast cancer patients.

The first enrichment-detection workflow combines the CellSearch® and VyCAP™ filtration systems and it was applied to a cohort of 14 blood samples and 8 DLA samples. In the second workflow, single CTC isolation was incorporated by combining the CellSearch®, the Parsortix™ and the CellCelector™ micromanipulation systems. This workflow was applied to a cohort of 52 mBC blood samples. Afterwards, isolated cells were characterized according to the third workflow: CTCs were processed for whole genome amplification (WGA) and sequenced for PIK3CA hotspot mutations through an amplicon-based approach.

By virtue of the first workflow, both EpCAM<sup>high</sup> and EpCAM<sup>low/negative</sup> CTCs could be observed in 78 % of blood samples and in 50 % of DLA samples, without any correlation in positivity rates. With the second workflow, both CTC-subpopulations could be detected in 56 % of processed blood samples, confirming the lack of linearity in frequencies. High integrity WGA products were observed in 7% of isolated EpCAM<sup>low/negative</sup> cells vs. 28% of patient-matched EpCAM<sup>high</sup> cells, suggesting increased apoptosis within the first CTC-fraction. CTCs harbouring PIK3CA hotspot mutations were detected in 4/10 patients' blood samples. One patient carried the E545K mutation in EpCAM<sup>low/negative</sup> CTCs only and two patients showed H1047L and H1047R mutations within EpCAM<sup>high</sup> CTCs only. The fourth patient showed hotspot mutations in both CTC-subgroups: the E545K mutation in one EpCAM<sup>low/negative</sup> CTC and the H1047L mutation in two EpCAM<sup>high</sup> CTCs.

In summary, three robust workflows were successfully established and they respectively allow to enrich, isolate, and analyse patient-matched EpCAM<sup>high</sup> and EpCAM<sup>low/negative</sup> CTCs in metastatic breast cancer. For the first time, the heterogeneous PIK3CA mutational status has

been observed within EpCAM<sup>low/negative</sup> CTCs with regards to patient-matched EpCAM<sup>high</sup> cells. In future experiments, patient cohorts will be increased and follow up data will be related to the frequency of EpCAM<sup>low/negative</sup> CTCs as well as to the presence of PIK3CA hotspot mutations to shed light on this subgroup of CTCs and to better investigate the potential role of the PIK3CA oncogene as treatment resistance biomarker.

# Zusammenfassung

Zirkulierende Tumorzellen (CTCs) können im peripheren Blut von Krebspatienten identifiziert werden und in verschiedenen Tumor-Entitäten korreliert ein erhöhtes Vorkommen von CTCs mit schlechterer Prognose. Die meisten Technologien zur Anreicherung von CTCs basieren auf dem epithelialen Marker EpCAM (CellSearch®), was jedoch zur Folge hat, dass Zellen, die sich in der epithelialen/mesenchymalen Transition befinden und potenziell sehr aggressiv sind, übersehen werden können. Ziel dieser Arbeit war daher die Etablierung eines stabilen Arbeitsablaufs für die gleichzeitige Anreicherung, Detektion, Isolierung und Charakterisierung von sowohl EpCAM<sup>positiven</sup> als auch „EpCAM<sup>niedrig/negativen</sup>“ CTCs aus Blut- und Apheresat-Proben (DLA) von Patientinnen mit einem metastasierten Mammakarzinom.

Die erste in dieser Arbeit etablierte Anreicherungs- und Detektionsmethode kombiniert die Systeme CellSearch® und VyCAP™. Sie wurde zur Anreicherung von CTCs aus 14 Blut- und 8 Apheresat-Proben von Mammakarzinom Patientinnen angewendet. Die zweite etablierte Methode zur Isolierung von CTCs umfasst die Systeme CellSearch®, Parsortix™ und CellCelector™. Mittels dieses Arbeitsablaufs wurden Blutproben von 52 Patientinnen analysiert. Die isolierten Zellen wurden im Anschluss mit einer dritten in dieser Arbeit etablierten Methode charakterisiert: zu diesem Zweck wurde die DNA der Zellen extrahiert, amplifiziert und mittels einer amplicon-basierten Methode sequenziert, um „Hot-spot“ Mutationen des Onkogens PIK3CA zu detektieren.

Mit Hilfe der ersten Anreicherungs- und Detektionsmethode konnten sowohl EpCAM<sup>hohe</sup> als auch EpCAM<sup>niedrig/negative</sup> CTCs in 78 % der Blutproben und in 50 % der Apheresat-Proben identifiziert werden, jedoch konnte keine positive Korrelation zwischen den CTC-Subtypen ermittelt werden. Mittels der zweiten Anreicherungs- und Detektionsmethode konnten beide CTC-Subpopulationen in 56 % der Blutproben detektiert und die fehlende Korrelation der Positivitätsrate bestätigt werden. In 7 % der EpCAM<sup>niedrig/negativen</sup> Zellen konnte das Genom mit hoher Integrität amplifiziert werden, die DNA von EpCAM<sup>hohen</sup> Zellen, welche jeweils aus denselben Proben isoliert wurden, konnte dagegen in 28 % mit hoher Integrität amplifiziert werden. Diese Ergebnisse suggerieren erhöhte Apoptoseraten innerhalb der ersten CTC-Gruppe, die weitere Nachforschungen erfordern. CTCs mit PIK3CA-Mutationen wurden in

4/10 der Patientenproben identifiziert. Eine Patientin wies dabei nur in EpCAM<sup>niedrig/negativen</sup> CTCs die Mutation E545K auf und zwei Patientinnen wiesen die Mutationen H1047L und H1047R nur innerhalb der EpCAM<sup>hohen</sup> CTCs auf. Die vierte Patientin wies Mutationen in beiden CTC-Gruppe auf: die Mutation E545K in einer EpCAM<sup>niedrig/negativen</sup> CTC und die H1047L Mutation in zwei EpCAM<sup>hohen</sup> CTCs.

In der vorliegenden Arbeit konnten drei stabile Arbeitsläufe erfolgreich etabliert werden. Sie ermöglichen die gleichzeitige Anreicherung, Isolation und Analyse von EpCAM<sup>hohen</sup> und EpCAM<sup>niedrig/negativen</sup> CTCs aus dem Blut metastatischer Mammakarzinom Patientinnen. Zum ersten Mal wurde ein heterogener PIK3CA-Mutationsstatus innerhalb EpCAM<sup>niedrig/negativer</sup> CTCs festgestellt. In zukünftigen Experimenten soll die Patientenkohorte erhöht werden. Außerdem werden die Follow-up-Daten der Patientinnen mit der Anzahl der EpCAM<sup>niedrig/negativen</sup> CTCs und der Anwesenheit von PIK3CA Mutationen korreliert, um diese CTC-Gruppe besser zu verstehen und die Rolle des PIK3CA Onkogens als Biomarker für Therapie-Resistenz zu erforschen.

## References

1. Breast Cancer Treatment Available online: <https://www.cancer.gov/types/breast/patient/breast-treatment-pdq#section/all> (accessed on Jan 12, 2017).
2. Kumar, V.; Abbas, A. K.; Aster, J. C. *Robbins & Cotran Pathologic Basis of Disease*; Elsevier Health Sciences, 2014; ISBN 978-0-323-29635-9.
3. Hanahan, D.; Weinberg, R. A. Hallmarks of Cancer: The Next Generation. *Cell* **2011**, *144*, 646–674, doi:10.1016/j.cell.2011.02.013.
4. Fidler, I. J. The pathogenesis of cancer metastasis: the “seed and soil” hypothesis revisited. *Nat. Rev. Cancer* **2003**, *3*, 453–458, doi:10.1038/nrc1098.
5. Jemal, A.; Bray, F.; Center, M. M.; Ferlay, J.; Ward, E.; Forman, D. Global cancer statistics. *CA. Cancer J. Clin.* **2011**, *61*, 69–90, doi:10.3322/caac.20107.
6. Krebs - Breast cancer Available online: [http://www.krebsdaten.de/Krebs/EN/Content/Cancer\\_sites/Breast\\_cancer/breast\\_cancer\\_no\\_de.html](http://www.krebsdaten.de/Krebs/EN/Content/Cancer_sites/Breast_cancer/breast_cancer_no_de.html) (accessed on Jan 11, 2017).
7. WHO | Cancer Available online: <http://www.who.int/mediacentre/factsheets/fs297/en/> (accessed on Jan 12, 2017).
8. Dirican, E.; Akkiprik, M.; Özer, A. Mutation distributions and clinical correlations of PIK3CA gene mutations in breast cancer. *Tumor Biol.* **2016**, *37*, 7033–7045, doi:10.1007/s13277-016-4924-2.
9. Gage, M.; Wattendorf, D.; Henry, L. r. Translational advances regarding hereditary breast cancer syndromes. *J. Surg. Oncol.* **2012**, *105*, 444–451, doi:10.1002/jso.21856.
10. Nelson, H. D.; Zakher, B.; Cantor, A.; Fu, R.; Griffin, J.; O’Meara, E. S.; Buist, D. S. M.; Kerlikowske, K.; van Ravesteyn, N. T.; Trentham-Dietz, A.; Mandelblatt, J.; Miglioretti, D. Risk Factors for Breast Cancer for Women Age 40 to 49: A Systematic Review and Meta-analysis. *Ann. Intern. Med.* **2012**, *156*, 635–648, doi:10.1059/0003-4819-156-9-201205010-00006.
11. Bertos, N. R.; Park, M. Breast cancer — one term, many entities? *J. Clin. Invest.* **2011**, *121*, 3789–3796, doi:10.1172/JCI57100.
12. Tumor Grade Available online: <https://www.cancer.gov/about-cancer/diagnosis-staging/prognosis/tumor-grade-fact-sheet> (accessed on Feb 2, 2017).
13. Ectasia – Dilated Milk Ducts – A Fair Go.
14. RNCeUS Available online: <http://www.rnceus.com/dcis/sub.html> (accessed on Jan 12, 2017).
15. Goldhirsch, A.; Wood, W. C.; Coates, A. S.; Gelber, R. D.; Thürlimann, B.; Senn, H.-J. Strategies for subtypes—dealing with the diversity of breast cancer: highlights of the St Gallen International Expert Consensus on the Primary Therapy of Early Breast Cancer 2011. *Ann. Oncol.* **2011**, *22*, 1736–1747, doi:10.1093/annonc/mdr304.
16. Tao, Z.; Shi, A.; Lu, C.; Song, T.; Zhang, Z.; Zhao, J. Breast Cancer: Epidemiology and Etiology. *Cell Biochem. Biophys.* **2015**, *72*, 333–338, doi:10.1007/s12013-014-0459-6.
17. Schnitt, S. J. Classification and prognosis of invasive breast cancer: from morphology to molecular taxonomy. *Mod Pathol* **2010**, *23*, doi:10.1038/modpathol.2010.33.
18. Higgins, M. J.; Baselga, J. Targeted therapies for breast cancer. *J. Clin. Invest.* **2011**, *121*, 3797–3803, doi:10.1172/JCI57152.
19. Vici, P.; Pizzuti, L.; Natoli, C.; Gamucci, T.; Di Lauro, L.; Barba, M.; Sergi, D.; Botti, C.; Michelotti, A.; Moscetti, L.; Mariani, L.; Izzo, F.; D’Onofrio, L.; Sperduti, I.; Conti, F.; Rossi, V.; Cassano, A.; Maugeri-Saccà, M.; Mottolese, M.; Marchetti, P. Triple positive breast cancer: A distinct subtype? *Cancer Treat. Rev.* **2015**, *41*, 69–76, doi:10.1016/j.ctrv.2014.12.005.
20. myo-inositol Available online: <http://www.chem.qmul.ac.uk/iupac/cyclitol/myo.html> (accessed on Feb 10, 2017).

21. Wang, W.; Lv, J.; Wang, L.; Wang, X.; Ye, L. The impact of heterogeneity in phosphoinositide 3-kinase pathway in human cancer and possible therapeutic treatments. *Semin. Cell Dev. Biol.* **2016**, doi:10.1016/j.semcdb.2016.08.024.
22. Troxell, L. M. PIK3CA/AKT1 Mutations in Breast Carcinoma: a Comprehensive Review of Experimental and Clinical Studies. *J. Clin. Exp. Pathol.* **2012**, *2*, doi:10.4172/2161-0681.S1-002.
23. Ma, C. X. The PI3K Pathway as a Therapeutic Target in Breast Cancer. *Am. J. Hematol. Oncol.* **2015**, *11*.
24. Weigelt, B.; Downward, J. Genomic Determinants of PI3K Pathway Inhibitor Response in Cancer. *Front. Oncol.* **2012**, *2*, doi:10.3389/fonc.2012.00109.
25. Mukohara, T. PI3K mutations in breast cancer: prognostic and therapeutic implications. *Breast Cancer Targets Ther.* **2015**, *7*, 111–123, doi:10.2147/BCTT.S60696.
26. Jensen, J. D.; Laenkholm, A.-V.; Knoop, A.; Ewertz, M.; Bandaru, R.; Liu, W.; Hackl, W.; Barrett, J. C.; Gardner, H. PIK3CA Mutations May Be Discordant between Primary and Corresponding Metastatic Disease in Breast Cancer. *Clin. Cancer Res.* **2011**, *17*, 667–677, doi:10.1158/1078-0432.CCR-10-1133.
27. PIK3CA in Breast Cancer - My Cancer Genome Available online: <https://www.mycancergenome.org/content/disease/breast-cancer/pik3ca/> (accessed on Feb 3, 2017).
28. Miled, N.; Yan, Y.; Hon, W.-C.; Perisic, O.; Zvelebil, M.; Inbar, Y.; Schneidman-Duhovny, D.; Wolfson, H. J.; Backer, J. M.; Williams, R. L. Mechanism of Two Classes of Cancer Mutations in the Phosphoinositide 3-Kinase Catalytic Subunit. *Science* **2007**, *317*, 239–242, doi:10.1126/science.1135394.
29. Zhao, L.; Vogt, P. K. Helical domain and kinase domain mutations in p110 $\alpha$  of phosphatidylinositol 3-kinase induce gain of function by different mechanisms. *Proc. Natl. Acad. Sci. U. S. A.* **2008**, *105*, 2652–2657, doi:10.1073/pnas.0712169105.
30. Bhat-Nakshatri, P.; Goswami, C. P.; Badve, S.; Magnani, L.; Lupien, M.; Nakshatri, H. Molecular Insights of Pathways Resulting from Two Common PIK3CA Mutations in Breast Cancer. *Cancer Res.* **2016**, *76*, 3989–4001, doi:10.1158/0008-5472.CAN-15-3174.
31. Barbareschi, M.; Buttitta, F.; Felicioni, L.; Cotrupi, S.; Barassi, F.; Grammastro, M. D.; Ferro, A.; Palma, P. D.; Galligioni, E.; Marchetti, A. Different Prognostic Roles of Mutations in the Helical and Kinase Domains of the PIK3CA Gene in Breast Carcinomas. *Clin. Cancer Res.* **2007**, *13*, 6064–6069, doi:10.1158/1078-0432.CCR-07-0266.
32. Kalinsky, K.; Jacks, L. M.; Heguy, A.; Patil, S.; Drobnjak, M.; Bhanot, U. K.; Hedvat, C. V.; Traina, T. A.; Solit, D.; Gerald, W.; Moynahan, M. E. PIK3CA Mutation Associates with Improved Outcome in Breast Cancer. *Clin. Cancer Res.* **2009**, *15*, 5049–5059, doi:10.1158/1078-0432.CCR-09-0632.
33. O'Brien, C.; Wallin, J. J.; Sampath, D.; GuhaThakurta, D.; Savage, H.; Punnoose, E. A.; Guan, J.; Berry, L.; Prior, W. W.; Amler, L. C.; Belvin, M.; Friedman, L. S.; Lackner, M. R. Predictive Biomarkers of Sensitivity to the Phosphatidylinositol 3' Kinase Inhibitor GDC-0941 in Breast Cancer Preclinical Models. *Am. Assoc. Cancer Res.* **2010**, *16*, 3670–3683, doi:10.1158/1078-0432.CCR-09-2828.
34. Berx, G.; Roy, F. van Involvement of Members of the Cadherin Superfamily in Cancer. *Cold Spring Harb. Perspect. Biol.* **2009**, *1*, a003129, doi:10.1101/cshperspect.a003129.
35. Cavallaro, U.; Christofori, G. Cell adhesion and signalling by cadherins and Ig-CAMs in cancer. *Nat. Rev. Cancer* **2004**, *4*, 118–132, doi:10.1038/nrc1276.
36. Gun, V. D.; T.f, B.; Melchers, L. J.; Ruiters, M. H. J.; Leij, D.; F.m.h, L.; McLaughlin, P. M. J.; Rots, M. G. EpCAM in carcinogenesis: the good, the bad or the ugly. *Carcinogenesis* **2010**, *31*, 1913–1921, doi:10.1093/carcin/bgq187.
37. Bednarz-Knoll, N.; Alix-Panabières, C.; Pantel, K. Plasticity of disseminating cancer cells in patients with epithelial malignancies. *Cancer Metastasis Rev.* **2012**, *31*, 673–687, doi:10.1007/s10555-012-9370-z.

38. Bonnomet, A.; Brysse, A.; Tachsidis, A.; Waltham, M.; Thompson, E. W.; Polette, M.; Gilles, C. Epithelial-to-Mesenchymal Transitions and Circulating Tumor Cells. *J. Mammary Gland Biol. Neoplasia* **2010**, *15*, 261–273, doi:10.1007/s10911-010-9174-0.
39. Joosse, S. A.; Gorges, T. M.; Pantel, K. Biology, detection, and clinical implications of circulating tumor cells. *EMBO Mol. Med.* **2015**, *7*, 1–11, doi:10.15252/emmm.201303698.
40. Craene, B. D.; Berx, G. Regulatory networks defining EMT during cancer initiation and progression. *Nat. Rev. Cancer* **2013**, *13*, 97–110, doi:10.1038/nrc3447.
41. Tsai, J. H.; Yang, J. Epithelial-mesenchymal plasticity in carcinoma metastasis. *Genes Dev* **2013**, *27*, 2192–2206.
42. Nieto, M. A.; Huang, R. Y.-J.; Jackson, R. A.; Thiery, J. P. EMT: 2016. *Cell* **2016**, *166*, 21–45, doi:10.1016/j.cell.2016.06.028.
43. Kalluri, R.; Weinberg, R. A. The basics of epithelial-mesenchymal transition. *J. Clin. Invest.* **2009**, *119*, 1420–1428, doi:10.1172/JCI39104.
44. De Wever, O.; Pauwels, P.; De Craene, B.; Sabbah, M.; Emami, S.; Redeuilh, G.; Gespach, C.; Bracke, M.; Berx, G. Molecular and pathological signatures of epithelial–mesenchymal transitions at the cancer invasion front. *Histochem. Cell Biol.* **2008**, *130*, 481–494, doi:10.1007/s00418-008-0464-1.
45. Sabbah, M.; Emami, S.; Redeuilh, G.; Julien, S.; Prévost, G.; Zimber, A.; Ouelaa, R.; Bracke, M.; De Wever, O.; Gespach, C. Molecular signature and therapeutic perspective of the epithelial-to-mesenchymal transitions in epithelial cancers. *Drug Resist. Updat.* **2008**, *11*, 123–151, doi:10.1016/j.drug.2008.07.001.
46. Guarino, M.; Rubino, B.; Ballabio, G. The role of epithelial-mesenchymal transition in cancer pathology. *Pathology (Phila.)* **2007**, *39*, 305–318, doi:10.1080/00313020701329914.
47. Sarrió, D.; Rodríguez-Pinilla, S. M.; Hardisson, D.; Cano, A.; Moreno-Bueno, G.; Palacios, J. Epithelial-Mesenchymal Transition in Breast Cancer Relates to the Basal-like Phenotype. *Cancer Res.* **2008**, *68*, 989–997, doi:10.1158/0008-5472.CAN-07-2017.
48. Lien, H. C.; Hsiao, Y. H.; Lin, Y. S.; Yao, Y. T.; Juan, H. F.; Kuo, W. H.; Hung, M.-C.; Chang, K. J.; Hsieh, F. J. Molecular signatures of metaplastic carcinoma of the breast by large-scale transcriptional profiling: identification of genes potentially related to epithelial–mesenchymal transition. *Oncogene* **2007**, *26*, 7859–7871, doi:10.1038/sj.onc.1210593.
49. Klymkowsky, M. W.; Savagner, P. Epithelial-Mesenchymal Transition. *Am. J. Pathol.* **2009**, *174*, 1588–1593, doi:10.2353/ajpath.2009.080545.
50. Cayrefourcq, L.; Mazard, T.; Joosse, S.; Solassol, J.; Ramos, J.; Assenat, E.; Schumacher, U.; Costes, V.; Maudelonde, T.; Pantel, K.; Alix-Panabières, C. Establishment and Characterization of a Cell Line from Human Circulating Colon Cancer Cells. *Cancer Res.* **2015**, *75*, 892–901, doi:10.1158/0008-5472.CAN-14-2613.
51. Barriere, G.; Fici, P.; Gallerani, G.; Fabbri, F.; Zoli, W.; Rigaud, M. Circulating tumor cells and epithelial, mesenchymal and stemness markers: characterization of cell subpopulations. *Ann Transl Med* **2014**, *2*.
52. Anantharaman, A.; Friedlander, T.; Lu, D.; Krupa, R.; Premasekharan, G.; Hough, J.; Edwards, M.; Paz, R.; Lindquist, K.; Graf, R.; Jendrisak, A.; Louw, J.; Dugan, L.; Baird, S.; Wang, Y.; Dittamore, R.; Paris, P. L. Programmed death-ligand 1 (PD-L1) characterization of circulating tumor cells (CTCs) in muscle invasive and metastatic bladder cancer patients. *BMC Cancer* **2016**, *16*, doi:10.1186/s12885-016-2758-3.
53. Mazel, M.; Jacot, W.; Pantel, K.; Bartkowiak, K.; Topart, D.; Cayrefourcq, L.; Rossille, D.; Maudelonde, T.; Fest, T.; Alix-Panabières, C. Frequent expression of PD-L1 on circulating breast cancer cells. *Mol. Oncol.* **2015**, *9*, 1773–1782, doi:10.1016/j.molonc.2015.05.009.
54. Hugo, H.; Ackland, M. L.; Blick, T.; Lawrence, M. G.; Clements, J. A.; Williams, E. D.; Thompson, E. W. Epithelial–mesenchymal and mesenchymal–epithelial transitions in carcinoma progression. *J. Cell. Physiol.* **2007**, *213*, 374–383, doi:10.1002/jcp.21223.

55. Ocaña, O. H.; Córcoles, R.; Fabra, A.; Moreno-Bueno, G.; Acloque, H.; Vega, S.; Barrallo-Gimeno, A.; Cano, A.; Nieto, M. A. Metastatic colonization requires the repression of the epithelial-mesenchymal transition inducer Prrx1. *Cancer Cell* **2012**, *22*, 709–724, doi:10.1016/j.ccr.2012.10.012.
56. Tsai, J. H.; Donaher, J. L.; Murphy, D. A.; Chau, S.; Yang, J. Spatiotemporal Regulation of Epithelial-Mesenchymal Transition Is Essential for Squamous Cell Carcinoma Metastasis. *Cancer Cell* **2012**, *22*, 725–736, doi:10.1016/j.ccr.2012.09.022.
57. Nguyen, D. X.; Bos, P. D.; Massagué, J. Metastasis: from dissemination to organ-specific colonization. *Nat. Rev. Cancer* **2009**, *9*, 274–284, doi:10.1038/nrc2622.
58. Braun, S.; Vogl, F. D.; Naume, B.; Janni, W.; Osborne, M. P.; Coombes, R. C.; Schlimok, G.; Diel, I. J.; Gerber, B.; Gebauer, G.; Pierga, J.-Y.; Marth, C.; Oruzio, D.; Wiedswang, G.; Solomayer, E.-F.; Kundt, G.; Strobl, B.; Fehm, T.; Wong, G. Y. C.; Bliss, J.; Vincent-Salomon, A.; Pantel, K. A Pooled Analysis of Bone Marrow Micrometastasis in Breast Cancer. *N. Engl. J. Med.* **2005**, *353*, 793–802, doi:10.1056/NEJMoa050434.
59. Paget, S. The distribution of secondary growths in cancer of the breast. *Cancer Metastasis Rev.* **1889**, *8*, 98–101.
60. Langley, R. R.; Fidler, I. J. The seed and soil hypothesis revisited - the role of tumor-stroma interactions in metastasis to different organs. *Int. J. Cancer J. Int. Cancer* **2011**, *128*, 2527–2535, doi:10.1002/ijc.26031.
61. Ashworth, T. A case of cancer in which cells similar to those in the tumours were seen in the blood after death. *Aust Med J* **1869**, *14*, 146–149.
62. Banys-Paluchowski, M.; Krawczyk, N.; Meier-Stiegen, F.; Fehm, T. Circulating tumor cells in breast cancer—current status and perspectives. *Crit. Rev. Oncol. Hematol.* **2016**, *97*, 22–29, doi:10.1016/j.critrevonc.2015.10.010.
63. Coumans, F. A. W.; van Dalum, G.; Beck, M.; Terstappen, L. W. M. M. Filter Characteristics Influencing Circulating Tumor Cell Enrichment from Whole Blood. *PLoS ONE* **2013**, *8*, doi:10.1371/journal.pone.0061770.
64. Meng, S.; Tripathy, D.; Frenkel, E. P.; Shete, S.; Naftalis, E. Z.; Huth, J. F.; Beitsch, P. D.; Leitch, M.; Hoover, S.; Euhus, D.; Haley, B.; Morrison, L.; Fleming, T. P.; Herlyn, D.; Terstappen, L. W. M. M.; Fehm, T.; Tucker, T. F.; Lane, N.; Wang, J.; Uhr, J. W. Circulating Tumor Cells in Patients with Breast Cancer Dormancy. *Clin. Cancer Res.* **2004**, *10*, 8152–8162, doi:10.1158/1078-0432.CCR-04-1110.
65. Stoecklein, N. H.; Fischer, J. C.; Niederacher, D.; Terstappen, L. W. M. M. Challenges for CTC-based liquid biopsies: low CTC frequency and diagnostic leukapheresis as a potential solution. *Expert Rev. Mol. Diagn.* **2016**, *16*, 147–164, doi:10.1586/14737159.2016.1123095.
66. Allard, W. J.; Matera, J.; Miller, M. C.; Repollet, M.; Connelly, M. C.; Rao, C.; Tibbe, A. G. J.; Uhr, J. W.; Terstappen, L. W. M. M. Tumor Cells Circulate in the Peripheral Blood of All Major Carcinomas but not in Healthy Subjects or Patients With Nonmalignant Diseases. *Clin. Cancer Res.* **2004**, *10*, 6897–6904, doi:10.1158/1078-0432.CCR-04-0378.
67. Riethdorf, S.; Fritsche, H.; Muller, V.; Rau, T.; Schindlbeck, C.; Rack, B. Detection of circulating tumor cells in peripheral blood of patients with metastatic breast cancer: a validation study of the Cell Search system. *Clin Cancer Res* **2007**, *13*, doi:10.1158/1078-0432.ccr-06-1695.
68. de Wit, S.; Dalum, G. van; Lenferink, A. T. M.; Tibbe, A. G. J.; Hiltermann, T. J. N.; Groen, H. J. M.; van Rijn, C. J. M.; Terstappen, L. W. M. M. The detection of EpCAM+ and EpCAM–circulating tumor cells. *Sci. Rep.* **2015**, *5*, doi:10.1038/srep12270.
69. Yu, M.; Bardia, A.; Wittner, B. S.; Stott, S. L.; Smas, M. E.; Ting, D. T. Circulating breast tumor cells exhibit dynamic changes in epithelial and mesenchymal composition. *Science* **2013**, *339*, doi:10.1126/science.1228522.
70. Gorges, T. M.; Tinhofer, I.; Drosch, M.; Röse, L.; Zollner, T. M.; Krahn, T. Circulating tumour cells escape from EpCAM-based detection due to epithelial-to-mesenchymal transition. *BMC Cancer* **2012**, *12*, 178, doi:10.1186/1471-2407-12-178.

71. Kallergi, G.; Papadaki, M. A.; Politaki, E.; Mavroudis, D.; Georgoulas, V.; Agelaki, S. Epithelial to mesenchymal transition markers expressed in circulating tumour cells of early and metastatic breast cancer patients. *Breast Cancer Res. BCR* **2011**, *13*, R59, doi:10.1186/bcr2896.
72. Jansson, S.; Bendahl, P.-O.; Larsson, A.-M.; Aaltonen, K. E.; Rydén, L. Prognostic impact of circulating tumor cell apoptosis and clusters in serial blood samples from patients with metastatic breast cancer in a prospective observational cohort. *BMC Cancer* **2016**, *16*, 433, doi:10.1186/s12885-016-2406-y.
73. Aceto, N. Circulating tumor cell clusters are oligoclonal precursors of breast cancer metastasis. *Cell* **2014**, *158*, 1110–1122.
74. Becker, T. M.; Caixeiro, N. J.; Lim, S. H.; Tognela, A.; Kienzle, N.; Scott, K. F.; Spring, K. J.; de Souza, P. New frontiers in circulating tumor cell analysis: A reference guide for biomolecular profiling toward translational clinical use. *Int. J. Cancer* **2014**, *134*, 2523–2533, doi:10.1002/ijc.28516.
75. Pantel, K.; Speicher, M. R. The biology of circulating tumor cells. *Oncogene* **2016**, *35*, 1216–1224, doi:10.1038/onc.2015.192.
76. Maetzel, D.; Denzel, S.; Mack, B.; Canis, M.; Went, P.; Benk, M.; Kieu, C.; Papior, P.; Baeuerle, P. A.; Munz, M.; Gires, O. Nuclear signalling by tumour-associated antigen EpCAM. *Nat. Cell Biol.* **2009**, *11*, 162–171, doi:10.1038/ncb1824.
77. Herlyn, D.; Herlyn, M.; Stepkowski, Z.; Koprowski, H. Monoclonal antibodies in cell-mediated cytotoxicity against human melanoma and colorectal carcinoma. *Eur. J. Immunol.* **1979**, *9*, 657–659, doi:10.1002/eji.1830090817.
78. Balzar, M.; Winter, M. J.; de Boer, C. J.; Litvinov, S. V. The biology of the 17-1A antigen (EpCAM). *J. Mol. Med. Berl. Ger.* **1999**, *77*, 699–712.
79. Patriarca, C.; Macchi, R. M.; Marschner, A. K.; Mellstedt, H. Epithelial cell adhesion molecule expression (CD326) in cancer: a short review. *Cancer Treat. Rev.* **2012**, *38*, 68–75, doi:10.1016/j.ctrv.2011.04.002.
80. Terstappen, L. W.; Rao, C.; Gross, S.; Kotelnikov, V.; Racilla, E.; Uhr, J.; Weiss, A. Flow cytometry--principles and feasibility in transfusion medicine. Enumeration of epithelial derived tumor cells in peripheral blood. *Vox Sang.* **1998**, *74 Suppl 2*, 269–274.
81. Cristofanilli, M.; Budd, G. T.; Ellis, M. J.; Stopeck, A.; Matera, J.; Miller, M. C. Circulating tumor cells, disease progression, and survival in metastatic breast cancer. *N Engl J Med* **2004**, *351*, doi:10.1056/NEJMoa040766.
82. Rao, C. G.; Chianese, D.; Doyle, G. V.; Miller, M. C.; Russell, T.; Sanders, R. A.; Terstappen, L. W. M. M. Expression of epithelial cell adhesion molecule in carcinoma cells present in blood and primary and metastatic tumors. *Int. J. Oncol.* **2005**, *27*, 49–57.
83. Konigsberg, R.; Obermayr, E.; Bises, G.; Pfeiler, G.; Gneist, M.; Wrba, F. Detection of EpCAM positive and negative circulating tumor cells in metastatic breast cancer patients. *Acta Oncol* **2011**, *50*, doi:10.3109/0284186x.2010.549151.
84. Mostert, B.; Kraan, J.; Bolt-de Vries, J.; Spoel, P.; Sieuwerts, A. M.; Schutte, M. Detection of circulating tumor cells in breast cancer may improve through enrichment with anti-CD146. *Breast Cancer Res Treat* **2011**, *127*, doi:10.1007/s10549-010-0879-y.
85. Mego, M.; De Giorgi, U.; Dawood, S.; Wang, X.; Valero, V.; Andreopoulou, E.; Handy, B.; Ueno, N. T.; Reuben, J. M.; Cristofanilli, M. Characterization of metastatic breast cancer patients with nondetectable circulating tumor cells. *Int. J. Cancer* **2011**, *129*, 417–423, doi:10.1002/ijc.25690.
86. Bozzetti, C.; Quaini, F.; Squadrilli, A.; Tiseo, M.; Frati, C.; Lagrasta, C.; Azzoni, C.; Bottarelli, L.; Galetti, M.; Alama, A.; Belletti, S.; Gatti, R.; Passaro, A.; Gradilone, A.; Cavazzoni, A.; Alfieri, R.; Petronini, P. G.; Bonelli, M.; Falco, A.; Carubbi, C.; Pedrazzi, G.; Nizzoli, R.; Naldi, N.; Pinto, C.; Ardizzoni, A. Isolation and Characterization of Circulating Tumor Cells in Squamous Cell

- Carcinoma of the Lung Using a Non-EpCAM-Based Capture Method. *PLoS ONE* **2015**, *10*, e0142891, doi:10.1371/journal.pone.0142891.
87. Chudziak, J.; Burt, D. J.; Mohan, S.; Rothwell, D. G.; Mesquita, B.; Antonello, J.; Dalby, S.; Ayub, M.; Priest, L.; Carter, L.; Krebs, M. G.; Blackhall, F.; Dive, C.; Brady, G. Clinical evaluation of a novel microfluidic device for epitope-independent enrichment of circulating tumour cells in patients with small cell lung cancer. *Analyst* **2016**, *141*, 669–678, doi:10.1039/C5AN02156A.
  88. Lampignano, R.; Schneck, H.; Neumann, M.; Fehm, T.; Neubauer, H. Enrichment, Isolation and Molecular Characterization of EpCAM-Negative Circulating Tumor Cells. *Adv. Exp. Med. Biol.* **2017a**, *994*, 181–203, doi:10.1007/978-3-319-55947-6\_10.
  89. Xu, L. Optimization and Evaluation of a Novel Size Based Circulating Tumor Cell Isolation System. *P Lo One* **2015**, *10*, e0138032.
  90. Driemel, C.; Kremling, H.; Schumacher, S.; Will, D.; Wolters, J.; Lindenlauf, N.; Mack, B.; Baldus, S. A.; Hoya, V.; Pietsch, J. M.; Panagiotidou, P.; Raba, K.; Vay, C.; Vallböhmer, D.; Harréus, U.; Knoefel, W. T.; Stoecklein, N. H.; Gires, O. Context-dependent adaption of EpCAM expression in early systemic esophageal cancer. *Oncogene* **2014**, *33*, 4904–4915, doi:10.1038/onc.2013.441.
  91. Yokobori, T. Plastin3 is a novel marker for circulating tumor cells undergoing the epithelial-mesenchymal transition and is associated with colorectal cancer prognosis. *Cancer Res* **2013**, *73*, 2059–2069.
  92. Poruk, K. E. Circulating Tumor Cell Phenotype Predicts Recurrence and Survival in Pancreatic Adenocarcinoma. *Ann Surg* **2016**.
  93. Gires, O.; Kieu, C.; Fix, P.; Schmitt, B.; Münz, M.; Wollenberg, B.; Zeidler, R. Tumor necrosis factor alpha negatively regulates the expression of the carcinoma-associated antigen epithelial cell adhesion molecule. *Cancer* **2001**, *92*, 620–628.
  94. Fliieger, D.; Hoff, A. S.; Sauerbruch, T.; Schmidt-Wolf, I. G. Influence of cytokines, monoclonal antibodies and chemotherapeutic drugs on epithelial cell adhesion molecule (EpCAM) and LewisY antigen expression. *Clin. Exp. Immunol.* **2001**, *123*, 9–14.
  95. Spizzo, G.; Gastl, G.; Obrist, P.; Fong, D.; Haun, M.; Grünewald, K.; Parson, W.; Eichmann, C.; Millinger, S.; Fiegl, H.; Margreiter, R.; Amberger, A. Methylation status of the Ep-CAM promoter region in human breast cancer cell lines and breast cancer tissue. *Cancer Lett.* **2007**, *246*, 253–261, doi:10.1016/j.canlet.2006.03.002.
  96. Tai, K.-Y.; Shiah, S.-G.; Shieh, Y.-S.; Kao, Y.-R.; Chi, C.-Y.; Huang, E.; Lee, H.-S.; Chang, L.-C.; Yang, P.-C.; Wu, C.-W. DNA methylation and histone modification regulate silencing of epithelial cell adhesion molecule for tumor invasion and progression. *Oncogene* **2007**, *26*, 3989–3997, doi:10.1038/sj.onc.1210176.
  97. Gires, O.; Stoecklein, N. H. Dynamic EpCAM expression on circulating and disseminating tumor cells: causes and consequences. *Cell. Mol. Life Sci. CMLS* **2014**, *71*, 4393–4402, doi:10.1007/s00018-014-1693-1.
  98. Thiery, J.-P. [Epithelial-mesenchymal transitions in cancer onset and progression]. *Bull. Académie Natl. Médecine* **2009**, *193*, 1969–1978–1979.
  99. Allan, A. L.; Keeney, M. Circulating tumor cell analysis: technical and statistical considerations for application to the clinic. *J. Oncol.* **2010**, *2010*, 426218, doi:10.1155/2010/426218.
  100. Gabriel, M. T.; Calleja, L. R.; Chalopin, A.; Ory, B.; Heymann, D. Circulating Tumor Cells: A Review of Non–EpCAM-Based Approaches for Cell Enrichment and Isolation. *Clin. Chem.* **2016**, *62*, 571–581, doi:10.1373/clinchem.2015.249706.
  101. Kagan, M.; Howard, D.; Bendele, T.; Mayes, J.; Silvia, J.; Repollet, M.; Doyle, J.; Allard, J.; Tu, N.; Bui, T.; Russell, T.; Rao, C.; Hermann, M.; Rutner, H.; Terstappen, L. A sample preparation and analysis system for identification of circulating tumor cells. *J. Clin. Ligand Assay* **2002**, *25*, 104–110.

102. Punnoose, E. A.; Atwal, S. K.; Spoerke, J. M.; Savage, H.; Pandita, A.; Yeh, R.-F.; Pirzkall, A.; Fine, B. M.; Amler, L. C.; Chen, D. S.; Lackner, M. R. Molecular Biomarker Analyses Using Circulating Tumor Cells. *PLoS ONE* **2010**, *5*, doi:10.1371/journal.pone.0012517.
103. Alix-Panabières, C.; Pantel, K. Technologies for detection of circulating tumor cells: facts and vision. *Lab. Chip* **2013**, *14*, 57–62, doi:10.1039/C3LC50644D.
104. Ferreira, M. M.; Ramani, V. C.; Jeffrey, S. S. Circulating tumor cell technologies. *Mol. Oncol.* **2016**, *10*, 374–394, doi:10.1016/j.molonc.2016.01.007.
105. Banys, M.; Müller, V.; Melcher, C.; Aktas, B.; Kasimir-Bauer, S.; Hagenbeck, C.; Hartkopf, A.; Fehm, T. Circulating tumor cells in breast cancer. *Clin. Chim. Acta* **2013**, *423*, 39–45, doi:10.1016/j.cca.2013.03.029.
106. Esmaeilsabzali, H.; Beischlag, T. V.; Cox, M. E.; Parameswaran, A. M.; Park, E. J. Detection and isolation of circulating tumor cells: Principles and methods. *Biotechnol. Adv.* **2013**, *31*, 1063–1084, doi:10.1016/j.biotechadv.2013.08.016.
107. Galletti, G.; Sung, M. S.; Vahdat, L. T.; Shah, M. A.; Santana, S. M.; Altavilla, G.; Kirby, B. J.; Giannakakou, P. Isolation of breast cancer and gastric cancer circulating tumor cells by use of an anti HER2-based microfluidic device. *Lab. Chip* **2014**, *14*, 147–156, doi:10.1039/c3lc51039e.
108. Bitting, R. L.; Boominathan, R.; Rao, C.; Kemeny, G.; Foulk, B.; Garcia-Blanco, M. A.; Connelly, M.; Armstrong, A. J. Development of a method to isolate circulating tumor cells using mesenchymal-based capture. *Methods San Diego Calif* **2013**, *64*, 129–136, doi:10.1016/j.ymeth.2013.06.034.
109. Kirby, B. J.; Jodari, M.; Loftus, M. S.; Gakhar, G.; Pratt, E. D.; Chanel-Vos, C.; Gleghorn, J. P.; Santana, S. M.; Liu, H.; Smith, J. P.; Navarro, V. N.; Tagawa, S. T.; Bander, N. H.; Nanus, D. M.; Giannakakou, P. Functional characterization of circulating tumor cells with a prostate-cancer-specific microfluidic device. *PLoS One* **2012**, *7*, e35976, doi:10.1371/journal.pone.0035976.
110. Mikolajczyk, S. D.; Millar, L. S.; Tsinberg, P.; Coutts, S. M.; Zomorodi, M.; Pham, T.; Bischoff, F. Z.; Pircher, T. J. Detection of EpCAM-Negative and Cytokeratin-Negative Circulating Tumor Cells in Peripheral Blood. *J. Oncol.* **2011**, *2011*, 252361, doi:10.1155/2011/252361.
111. Schindlbeck, C.; Stellwagen, J.; Jeschke, U.; Karsten, U.; Rack, B.; Janni, W.; Jückstock, J.; Tulusan, A.; Sommer, H.; Friese, K. Immunomagnetic enrichment of disseminated tumor cells in bone marrow and blood of breast cancer patients by the Thomsen-Friedenreich-Antigen. *Clin. Exp. Metastasis* **2008**, *25*, 233–240, doi:10.1007/s10585-007-9137-z.
112. Mostert, B.; Kraan, J.; Sieuwerts, A. M.; Spoel, P.; Bolt-de Vries, J.; Prager-van der Smissen, W. J. CD49f-based selection of circulating tumor cells (CTCs) improves detection across breast cancer subtypes. *Cancer Lett* **2012**, *319*, doi:10.1016/j.canlet.2011.12.031.
113. Schneck, H.; Gierke, B.; Uppenkamp, F.; Behrens, B.; Niederacher, D.; Stoecklein, N. H.; Templin, M. F.; Pawlak, M.; Fehm, T.; Neubauer, H. EpCAM-Independent Enrichment of Circulating Tumor Cells in Metastatic Breast Cancer. *PLoS ONE* **2015**, *10*, doi:10.1371/journal.pone.0144535.
114. Liu, Z. Negative enrichment by immunomagnetic nanobeads for unbiased characterization of circulating tumor cells from peripheral blood of cancer patients. *J Transl Med* **2011**, *9*, 70–70.
115. Bulfoni, M.; Gerratana, L.; Del Ben, F.; Marzinotto, S.; Sorrentino, M.; Turetta, M.; Scoles, G.; Toffoletto, B.; Isola, M.; Beltrami, C. A.; Di Loreto, C.; Beltrami, A. P.; Puglisi, F.; Cesselli, D. In patients with metastatic breast cancer the identification of circulating tumor cells in epithelial-to-mesenchymal transition is associated with a poor prognosis. *Breast Cancer Res.* **2016**, *18*, 1–15, doi:10.1186/s13058-016-0687-3.
116. He, W.; Kularatne, S. A.; Kalli, K. R.; Prendergast, F. G.; Amato, R. J.; Klee, G. G.; Hartmann, L. C.; Low, P. S. Quantitation of circulating tumor cells in blood samples from ovarian and prostate cancer patients using tumor-specific fluorescent ligands. *Int. J. Cancer J. Int. Cancer* **2008**, *123*, 1968–1973, doi:10.1002/ijc.23717.

117. Seal, S. H. Silicone flotation: A simple quantitative method for the isolation of free-floating cancer cells from the blood. *Cancer* **1959**, *12*, 590–595, doi:10.1002/1097-0142(195905/06)12:3<590::AID-CNCR2820120318>3.0.CO;2-N.
118. Fischer, J. C.; Niederacher, D.; Topp, S. A.; Honisch, E.; Schumacher, S.; Schmitz, N.; Zacarias Föhrding, L.; Vay, C.; Hoffmann, I.; Kasprowicz, N. S.; Hepp, P. G.; Mohrmann, S.; Nitz, U.; Stresemann, A.; Krahn, T.; Henze, T.; Griebisch, E.; Raba, K.; Rox, J. M.; Wenzel, F.; Sproll, C.; Janni, W.; Fehm, T.; Klein, C. A.; Knoefel, W. T.; Stoecklein, N. H. Diagnostic leukapheresis enables reliable detection of circulating tumor cells of nonmetastatic cancer patients. *Proc. Natl. Acad. Sci. U. S. A.* **2013**, *110*, 16580–16585, doi:10.1073/pnas.1313594110.
119. Rosenberg, R.; Gertler, R.; Friederichs, J.; Fuehrer, K.; Dahm, M.; Phelps, R.; Thorban, S.; Nekarda, H.; Siewert, J. R. Comparison of two density gradient centrifugation systems for the enrichment of disseminated tumor cells in blood. *Cytometry* **2002**, *49*, 150–158, doi:10.1002/cyto.10161.
120. Pösel, C.; Möller, K.; Fröhlich, W.; Schulz, I.; Boltze, J.; Wagner, D.-C. Density Gradient Centrifugation Compromises Bone Marrow Mononuclear Cell Yield. *PLoS ONE* **2012**, *7*, doi:10.1371/journal.pone.0050293.
121. Müller, V.; Stahmann, N.; Riethdorf, S.; Rau, T.; Zabel, T.; Goetz, A.; Jänicke, F.; Pantel, K. Circulating Tumor Cells in Breast Cancer: Correlation to Bone Marrow Micrometastases, Heterogeneous Response to Systemic Therapy and Low Proliferative Activity. *Am. Assoc. Cancer Res.* **2005**, *11*, 3678–3685, doi:10.1158/1078-0432.CCR-04-2469.
122. Balic, M.; Dandachi, N.; Hofmann, G.; Samonigg, H.; Loibner, H.; Obwaller, A.; van der Kooi, A.; Tibbe, A. G. J.; Doyle, G. V.; Terstappen, L. W. M. M.; Bauernhofer, T. Comparison of two methods for enumerating circulating tumor cells in carcinoma patients. *Cytometry B Clin. Cytom.* **2005**, *68B*, 25–30, doi:10.1002/cyto.b.20065.
123. Andree, K. C.; Mentink, A.; Swennenhuis, J. F.; Terstappen, L. W. M. M.; Stoecklein, N. H.; Neves, R. P. L.; Lampignano, R.; Neubauer, H.; Fehm, T.; Fischer, J. C.; Rossi, E.; Manicone, M.; Basso, U.; Marson, P.; Zamarchi, R.; Lorient, Y.; Lapierre, V.; Faugeroux, V.; Oulhen, M.; Ebbs, B.; Lambros, M.; Crespo, M.; Flohr, P.; de Bono, J. S. Diagnostic leukapheresis results in a significant increase in CTC yield in metastatic breast and prostate cancer. *Am. Assoc. Cancer Res.* **2017**.
124. CANCER-ID CANCER-ID – Innovation in Medicine Available online: <https://www.cancer-id.eu/> (accessed on Oct 16, 2017).
125. Seal, S. H. A sieve for the isolation of cancer cells and other large cells from the blood. *Cancer* **1964**, *17*, 637–642, doi:10.1002/1097-0142(196405)17:5<637::AID-CNCR2820170512>3.0.CO;2-I.
126. Cho, E. H.; Wendel, M.; Luttgen, M.; Yoshioka, C.; Marrinucci, D.; Lazar, D.; Schram, E.; Nieva, J.; Bazhenova, L.; Morgan, A.; Ko, A. H.; Korn, W. M.; Kolatkar, A.; Bethel, K.; Kuhn, P. Characterization of circulating tumor cell aggregates identified in patients with epithelial tumors. *Phys. Biol.* **2012**, *9*, 16001, doi:10.1088/1478-3975/9/1/016001.
127. Sollier, E.; Go, D. E.; Che, J.; Gossett, D. R.; O’Byrne, S.; Weaver, W. M.; Kummer, N.; Rettig, M.; Goldman, J.; Nickols, N.; McCloskey, S.; Kulkarni, R. P.; Carlo, D. D. Size-selective collection of circulating tumor cells using Vortex technology. *Lab. Chip* **2013**, *14*, 63–77, doi:10.1039/C3LC50689D.
128. Marrinucci, D.; Bethel, K.; Bruce, R. H.; Curry, D. N.; Hsieh, B.; Humphrey, M.; Krivacic, R. T.; Kroener, J.; Kroener, L.; Ladanyi, A.; Lazarus, N. H.; Nieva, J.; Kuhn, P. Case study of the morphologic variation of circulating tumor cells. *Hum. Pathol.* **2007**, *38*, 514–519, doi:10.1016/j.humpath.2006.08.027.
129. Hou, H. W.; Li, Q. S.; Lee, G. Y. H.; Kumar, A. P.; Ong, C. N.; Lim, C. T. Deformability study of breast cancer cells using microfluidics. *Biomed. Microdevices* **2008**, *11*, 557–564, doi:10.1007/s10544-008-9262-8.

130. Leong, F. Y.; Li, Q.; Lim, C. T.; Chiam, K.-H. Modeling cell entry into a micro-channel. *Biomech. Model. Mechanobiol.* **2010**, *10*, 755–766, doi:10.1007/s10237-010-0271-1.
131. Shaw Bagnall, J.; Byun, S.; Begum, S.; Miyamoto, D. T.; Hecht, V. C.; Maheswaran, S.; Stott, S. L.; Toner, M.; Hynes, R. O.; Manalis, S. R. Deformability of Tumor Cells versus Blood Cells. *Sci. Rep.* **2015**, *5*, doi:10.1038/srep18542.
132. Romsdahl MM; Valaitis J; McGrath RG; McGrew EA Circulating tumor cells in patients with carcinoma: Method and recent studies. *JAMA* **1965**, *193*, 1087–1090, doi:10.1001/jama.1965.03090130015003.
133. Zheng, S.; Lin, H.; Liu, J.-Q.; Balic, M.; Datar, R.; Cote, R. J.; Tai, Y.-C. Membrane microfilter device for selective capture, electrolysis and genomic analysis of human circulating tumor cells. *J. Chromatogr. A* **2007**, *1162*, 154–161, doi:10.1016/j.chroma.2007.05.064.
134. Ntouroupi, T. G.; Ashraf, S. Q.; McGregor, S. B.; Turney, B. W.; Seppo, A.; Kim, Y.; Wang, X.; Kilpatrick, M. W.; Tsiouras, P.; Tafas, T.; Bodmer, W. F. Detection of circulating tumour cells in peripheral blood with an automated scanning fluorescence microscope. *Br. J. Cancer* **2008**, *99*, 789–795, doi:10.1038/sj.bjc.6604545.
135. Chung, Y.-K.; Reboud, J.; Lee, K. C.; Lim, H. M.; Lim, P. Y.; Wang, K. Y.; Tang, K. C.; Ji, H.; Chen, Y. An electrical biosensor for the detection of circulating tumor cells. *Biosens. Bioelectron.* **2011**, *26*, 2520–2526, doi:10.1016/j.bios.2010.10.048.
136. Desitter, I.; Guerrouahen, B. S.; Benali-Furet, N.; Wechsler, J.; Jänne, P. A.; Kuang, Y.; Yanagita, M.; Wang, L.; Berkowitz, J. A.; Distel, R. J.; Cayre, Y. E. A New Device for Rapid Isolation by Size and Characterization of Rare Circulating Tumor Cells. *Anticancer Res.* **2011**, *31*, 427–441.
137. Adams, D.; Makarova, O.; Zhu, P.; Li, S.; Amstutz, P.; Tang, C.-M. Abstract 2369: Isolation of circulating tumor cells by size exclusion using lithography fabricated precision microfilters. *Cancer Res.* **2011**, *71*, 2369–2369, doi:10.1158/1538-7445.AM2011-2369.
138. Vona, G. Isolation by size of epithelial tumor cells: a new method for the immunomorphological and molecular characterization of circulating tumor cells. *Am J Pathol* **2000**, *156*, 57–63.
139. De Giorgi, V.; Pinzani, P.; Salvianti, F.; Panelos, J.; Paglierani, M.; Janowska, A.; Grazzini, M.; Wechsler, J.; Orlando, C.; Santucci, M.; Lotti, T.; Pazzagli, M.; Massi, D. Application of a Filtration- and Isolation-by-Size Technique for the Detection of Circulating Tumor Cells in Cutaneous Melanoma. *J. Invest. Dermatol.* **2010**, *130*, 2440–2447, doi:10.1038/jid.2010.141.
140. Lecharpentier, A.; Vielh, P.; Perez-Moreno, P.; Plancharde, D.; Soria, J. C.; Farace, F. Detection of circulating tumour cells with a hybrid (epithelial/mesenchymal) phenotype in patients with metastatic non-small cell lung cancer. *Br. J. Cancer* **2011**, *105*, 1338–1341, doi:10.1038/bjc.2011.405.
141. Krebs, M. G.; Hou, J.-M.; Sloane, R.; Lancashire, L.; Priest, L.; Nonaka, D.; Ward, T. H.; Backen, A.; Clack, G.; Hughes, A.; Ranson, M.; Blackhall, F. H.; Dive, C. Analysis of Circulating Tumor Cells in Patients with Non-small Cell Lung Cancer Using Epithelial Marker-Dependent and -Independent Approaches. *J. Thorac. Oncol.* **2012**, *7*, 306–315, doi:10.1097/JTO.0b013e31823c5c16.
142. Chen, C.-L.; Mahalingam, D.; Osmulski, P.; Jadhav, R. R.; Wang, C.-M.; Leach, R. J.; Chang, T.-C.; Weitman, S. D.; Kumar, A. P.; Sun, L.; Gaczynska, M. E.; Thompson, I. M.; Huang, T. H.-M. Single-cell Analysis of Circulating Tumor Cells Identifies Cumulative Expression Patterns of EMT-related Genes in Metastatic Prostate Cancer. *The Prostate* **2013**, *73*, 813–826, doi:10.1002/pros.22625.
143. Hvichia, G. e.; Parveen, Z.; Wagner, C.; Janning, M.; Quidde, J.; Stein, A.; Müller, V.; Loges, S.; Neves, R. p. I.; Stoecklein, N. h.; Wikman, H.; Riethdorf, S.; Pantel, K.; Gorges, T. m. A novel microfluidic platform for size and deformability based separation and the subsequent molecular characterization of viable circulating tumor cells. *Int. J. Cancer* **2016**, *138*, 2894–2904, doi:10.1002/ijc.30007.

144. Hur, S. C.; Mach, A. J.; Di Carlo, D. High-throughput size-based rare cell enrichment using microscale vortices. *Biomicrofluidics* **2011**, *5*, doi:10.1063/1.3576780.
145. Mach, A. J.; Kim, J. H.; Arshi, A.; Hur, S. C.; Carlo, D. D. Automated cellular sample preparation using a Centrifuge-on-a-Chip. *Lab. Chip* **2011**, *11*, 2827–2834, doi:10.1039/C1LC20330D.
146. Hou, H. W. Isolation and retrieval of circulating tumor cells using centrifugal forces. *Sci Rep* **2013**, *3*, 1259.
147. Khoo, B. L.; Warkiani, M. E.; Tan, D. S.-W.; Bhagat, A. A. S.; Irwin, D.; Lau, D. P.; Lim, A. S. T.; Lim, K. H.; Krisna, S. S.; Lim, W.-T.; Yap, Y. S.; Lee, S. C.; Soo, R. A.; Han, J.; Lim, C. T. Clinical Validation of an Ultra High-Throughput Spiral Microfluidics for the Detection and Enrichment of Viable Circulating Tumor Cells. *PLoS ONE* **2014**, *9*, doi:10.1371/journal.pone.0099409.
148. Hofman, V.; Ilie, M. I.; Long, E.; Selva, E.; Bonnetaud, C.; Molina, T.; Vénissac, N.; Mouroux, J.; Vielh, P.; Hofman, P. Detection of circulating tumor cells as a prognostic factor in patients undergoing radical surgery for non-small-cell lung carcinoma: comparison of the efficacy of the CellSearch Assay<sup>TM</sup> and the isolation by size of epithelial tumor cell method. *Int. J. Cancer* **2011**, *129*, 1651–1660, doi:10.1002/ijc.25819.
149. Farace, F.; Massard, C.; Vimond, N.; Drusch, F.; Jacques, N.; Billiot, F.; Laplanche, A.; Chauchereau, A.; Lacroix, L.; Planchard, D.; Le Moulec, S.; André, F.; Fizazi, K.; Soria, J. C.; Vielh, P. A direct comparison of CellSearch and ISET for circulating tumour-cell detection in patients with metastatic carcinomas. *Br. J. Cancer* **2011**, *105*, 847–853, doi:10.1038/bjc.2011.294.
150. Paillet, E.; Adam, J.; Barthélémy, A.; Oulhen, M.; Auger, N.; Valent, A.; Borget, I.; Planchard, D.; Taylor, M.; André, F.; Soria, J. C.; Vielh, P.; Besse, B.; Farace, F. Detection of Circulating Tumor Cells Harboring a Unique ALK Rearrangement in ALK-Positive Non–Small-Cell Lung Cancer. *J. Clin. Oncol.* **2013**, *31*, 2273–2281, doi:10.1200/JCO.2012.44.5932.
151. Khoja, L. A pilot study to explore circulating tumour cells in pancreatic cancer as a novel biomarker. *Br J Cancer* **2012**, *106*, 508–516.
152. Morris, K. L.; Tugwood, J. D.; Khoja, L.; Lancashire, M.; Sloane, R.; Burt, D.; Shenjere, P.; Zhou, C.; Hodgson, C.; Ohtomo, T.; Katoh, A.; Ishiguro, T.; Valle, J. W.; Dive, C. Circulating biomarkers in hepatocellular carcinoma. *Cancer Chemother. Pharmacol.* **2014**, *74*, 323–332, doi:10.1007/s00280-014-2508-7.
153. Marrinucci, D.; Bethel, K.; Kolatkar, A.; Lutgen, M.; Malchiodi, M.; Baehring, F.; Voigt, K.; Lazar, D.; Nieva, J.; Bazhenova, L.; Ko, A. H.; Korn, W. M.; Schram, E.; Coward, M.; Yang, X.; Metzner, T.; Lamy, R.; Honnatti, M.; Yoshioka, C.; Kunken, J.; Petrova, Y.; Sok, D.; Nelson, D.; Kuhn, P. Fluid Biopsy in Patients with Metastatic Prostate, Pancreatic and Breast Cancers. *Phys. Biol.* **2012**, *9*, 16003, doi:10.1088/1478-3975/9/1/016003.
154. Hyun, K.-A.; Koo, G.-B.; Han, H.; Sohn, J.; Choi, W.; Kim, S.-I.; Jung, H.-I.; Kim, Y.-S. Epithelial-to-mesenchymal transition leads to loss of EpCAM and different physical properties in circulating tumor cells from metastatic breast cancer. *Oncotarget* **2016**, *7*, 24677–24687, doi:10.18632/oncotarget.8250.
155. Neves, R. P. L.; Raba, K.; Schmidt, O.; Honisch, E.; Meier-Stiegen, F.; Behrens, B.; Möhlendick, B.; Fehm, T.; Neubauer, H.; Klein, C. A.; Polzer, B.; Sproll, C.; Fischer, J. C.; Niederacher, D.; Stoecklein, N. H. Genomic High-Resolution Profiling of Single CKpos/CD45neg Flow-Sorting Purified Circulating Tumor Cells from Patients with Metastatic Breast Cancer. *Clin. Chem.* **2014**, *60*, 1290–1297, doi:10.1373/clinchem.2014.222331.
156. Möhlendick, B.; Bartenhagen, C.; Behrens, B.; Honisch, E.; Raba, K.; Knoefel, W. T.; Stoecklein, N. H. A Robust Method to Analyze Copy Number Alterations of Less than 100 kb in Single Cells Using Oligonucleotide Array CGH. *PLOS ONE* **2013**, *8*, e67031, doi:10.1371/journal.pone.0067031.
157. Polzer, B.; Medoro, G.; Pasch, S.; Fontana, F.; Zorzino, L.; Pestka, A.; Andergassen, U.; Meier-Stiegen, F.; Czyz, Z. T.; Alberter, B.; Treitschke, S.; Schamberger, T.; Sergio, M.; Bregola, G.; Doffini, A.; Gianni, S.; Calanca, A.; Signorini, G.; Bolognesi, C.; Hartmann, A.; Fasching, P. A;

- Sandri, M. T.; Rack, B.; Fehm, T.; Giorgini, G.; Manaresi, N.; Klein, C. A. Molecular profiling of single circulating tumor cells with diagnostic intention. *EMBO Mol. Med.* **2014**, *6*, 1371–1386, doi:10.15252/emmm.201404033.
158. Fabbri, F.; Carloni, S.; Zoli, W.; Ulivi, P.; Gallerani, G.; Fici, P. Detection and recovery of circulating colon cancer cells using a dielectrophoresis-based device: KRAS mutation status in pure CTCs. *Cancer Lett* **2013**, *335*, doi:10.1016/j.canlet.2013.02.015.
159. Bolognesi, C.; Forcato, C.; Buson, G.; Fontana, F.; Mangano, C.; Doffini, A.; Sero, V.; Lanzellotto, R.; Signorini, G.; Calanca, A.; Sergio, M.; Romano, R.; Gianni, S.; Medoro, G.; Giorgini, G.; Morreau, H.; Barberis, M.; Corver, W. E.; Manaresi, N. Digital Sorting of Pure Cell Populations Enables Unambiguous Genetic Analysis of Heterogeneous Formalin-Fixed Paraffin-Embedded Tumors by Next Generation Sequencing. *Sci. Rep.* **2016**, *6*, 20944, doi:10.1038/srep20944.
160. Neumann, M. H. D.; Schneck, H.; Decker, Y.; Schömer, S.; Franken, A.; Endris, V.; Pfarr, N.; Weichert, W.; Niederacher, D.; Fehm, T.; Neubauer, H. Isolation and characterization of circulating tumor cells using a novel workflow combining the CellSearch® system and the CellCelector™. *Biotechnol. Prog.* **2016**, *33*, 125–132, doi:10.1002/btpr.2294.
161. Meng, S.; Tripathy, D.; Shete, S.; Ashfaq, R.; Haley, B.; Perkins, S.; Beitsch, P.; Khan, A.; Euhus, D.; Osborne, C.; Frenkel, E.; Hoover, S.; Leitch, M.; Clifford, E.; Vitetta, E.; Morrison, L.; Herlyn, D.; Terstappen, L. W. M. M.; Fleming, T.; Fehm, T.; Tucker, T.; Lane, N.; Wang, J.; Uhr, J. HER-2 gene amplification can be acquired as breast cancer progresses. *Proc. Natl. Acad. Sci. U. S. A.* **2004**, *101*, 9393–9398, doi:10.1073/pnas.0402993101.
162. Cabel, L.; Proudhon, C.; Gortais, H.; Loirat, D.; Coussy, F.; Pierga, J.-Y.; Bidard, F.-C. Circulating tumor cells: clinical validity and utility. *Int. J. Clin. Oncol.* **2017**, *1–10*, doi:10.1007/s10147-017-1105-2.
163. Lampignano, R.; Fehm, T.; Neubauer, H. The role of CTCs in breast cancer. In *Oncogenomics*; 2018.
164. Cohen, S. J.; Punt, C. J.; Iannotti, N.; Saidman, B. H.; Sabbath, K. D.; Gabrail, N. Y. Relationship of circulating tumor cells to tumor response, progression-free survival, and overall survival in patients with metastatic colorectal cancer. *J Clin Oncol* **2008**, *26*, doi:10.1200/jco.2007.15.8923.
165. de Bono, J. S.; Scher, H. I.; Montgomery, R. B.; Parker, C.; Miller, M. C.; Tissing, H.; Doyle, G. V.; Terstappen, L. W. W. M.; Pienta, K. J.; Raghavan, D. Circulating tumor cells predict survival benefit from treatment in metastatic castration-resistant prostate cancer. *Clin. Cancer Res. Off. J. Am. Assoc. Cancer Res.* **2008**, *14*, 6302–6309, doi:10.1158/1078-0432.CCR-08-0872.
166. Mitra, A.; Mishra, L.; Li, S. EMT, CTCs and CSCs in tumor relapse and drug-resistance. *Oncotarget* **2015**, *6*, 10697–10711.
167. Mego, M. Prognostic Value of EMT-Circulating Tumor Cells in Metastatic Breast Cancer Patients Undergoing High-Dose Chemotherapy with Autologous Hematopoietic Stem Cell Transplantation. *J Cancer* **2012**, *3*, 369–380.
168. Hayes, D. F.; Cristofanilli, M.; Budd, G. T.; Ellis, M. J.; Stopeck, A.; Miller, M. C.; Matera, J.; Allard, W. J.; Doyle, G. V.; Terstappen, L. W. W. M. Circulating tumor cells at each follow-up time point during therapy of metastatic breast cancer patients predict progression-free and overall survival. *Clin. Cancer Res. Off. J. Am. Assoc. Cancer Res.* **2006**, *12*, 4218–4224, doi:10.1158/1078-0432.CCR-05-2821.
169. Hou, J.-M.; Krebs, M. G.; Lancashire, L.; Sloane, R.; Backen, A.; Swain, R. K.; Priest, L. J. C.; Greystoke, A.; Zhou, C.; Morris, K.; Ward, T.; Blackhall, F. H.; Dive, C. Clinical significance and molecular characteristics of circulating tumor cells and circulating tumor microemboli in patients with small-cell lung cancer. *J. Clin. Oncol. Off. J. Am. Soc. Clin. Oncol.* **2012**, *30*, 525–532, doi:10.1200/JCO.2010.33.3716.

170. Smerage, J. B.; Barlow, W. E.; Hortobagyi, G. N.; Winer, E. P.; Leyland-Jones, B.; Srkalovic, G. Circulating tumor cells and response to chemotherapy in metastatic breast cancer: SWOG S0500. *J Clin Oncol* **2014**, *32*, doi:10.1200/jco.2014.56.2561.
171. Helisse, C.; Berger, F.; Cottu, P.; Diéras, V.; Mignot, L.; Servois, V.; Bouleuc, C.; Asselain, B.; Pelissier, S.; Vaucher, I.; Pierga, J. Y.; Bidard, F. C. Circulating tumor cell thresholds and survival scores in advanced metastatic breast cancer: The observational step of the CirCe01 phase III trial. *Cancer Lett.* **2015**, *360*, 213–218, doi:10.1016/j.canlet.2015.02.010.
172. Schneck, H.; Blassl, C.; Meier-Stiegen, F.; Neves, R. P.; Janni, W.; Fehm, T.; Neubauer, H. Analysing the mutational status of PIK3CA in circulating tumor cells from metastatic breast cancer patients. *Mol. Oncol.* **2013**, *7*, 976–986, doi:10.1016/j.molonc.2013.07.007.
173. Pestrin, M.; Bessi, S.; Puglisi, F.; Minisini, A. M.; Masci, G.; Battelli, N.; Ravaioli, A.; Gianni, L.; Marsico, R. D.; Tondini, C.; Gori, S.; Coombes, C. R.; Stebbing, J.; Biganzoli, L.; Buyse, M.; Leo, A. D. Final results of a multicenter phase II clinical trial evaluating the activity of single-agent lapatinib in patients with HER2-negative metastatic breast cancer and HER2-positive circulating tumor cells. A proof-of-concept study. *Breast Cancer Res. Treat.* **2012**, *134*, 283–289, doi:10.1007/s10549-012-2045-1.
174. Stebbing, J.; Payne, R.; Reise, J.; Frampton, A. E.; Avery, M.; Woodley, L.; Leo, A. D.; Pestrin, M.; Krell, J.; Coombes, R. C. The Efficacy of Lapatinib in Metastatic Breast Cancer with HER2 Non-Amplified Primary Tumors and EGFR Positive Circulating Tumor Cells: A Proof-Of-Concept Study. *PLOS ONE* **2013**, *8*, e62543, doi:10.1371/journal.pone.0062543.
175. Bidard, F.-C.; Fehm, T.; Ignatiadis, M.; Smerage, J. B.; Alix-Panabières, C.; Janni, W.; Messina, C.; Paoletti, C.; Müller, V.; Hayes, D. F.; Piccart, M.; Pierga, J.-Y. Clinical application of circulating tumor cells in breast cancer: overview of the current interventional trials. *Cancer Metastasis Rev.* **2013**, *32*, 179–188, doi:10.1007/s10555-012-9398-0.
176. Melcher, C.; Schochter, F.; Albrecht, S. DETECT IV - A multicenter, single arm, phase II study evaluating the efficacy of Everolimus in combination with endocrine therapy in patients with HER2-negative, hormone-receptor positive metastatic breast cancer and exclusively HER2-negative circulating tumor cells (CTCs). *Oncol Res Treat* **2014**, *37*, 29–29.
177. Lustberg, M. B.; Balasubramanian, P.; Miller, B.; Garcia-Villa, A.; Deighan, C.; Wu, Y.; Carothers, S.; Berger, M.; Ramaswamy, B.; Macrae, E. R.; Wesolowski, R.; Layman, R. M.; Mrozek, E.; Pan, X.; Summers, T. A.; Shapiro, C. L.; Chalmers, J. J. Heterogeneous atypical cell populations are present in blood of metastatic breast cancer patients. *Breast Cancer Res. BCR* **2014**, *16*, R23, doi:10.1186/bcr3622.
178. Zhang, L.; Ridgway, L. D.; Wetzell, M. A.; Ngo, J.; Yin, W.; Kumar, D.; Goodman, J. C.; Groves, M. D.; Marchetti, D. The identification and characterization of breast cancer CTCs competent for brain metastasis. *Sci. Transl. Med.* **2013**, *5*, doi:10.1126/scitranslmed.3005109.
179. Vishnoi, M.; Peddibhotla, S.; Yin, W.; T. Scamardo, A.; George, G. C.; Hong, D. S.; Marchetti, D. The isolation and characterization of CTC subsets related to breast cancer dormancy. *Sci. Rep.* **2015**, *5*, 17533, doi:10.1038/srep17533.
180. de Wit, S.; Manicone, M.; Rossi, E.; Trap, E. K.; Lampignano, R.; Yang, L.; Oulhen, M.; Crespo, M.; Berghuis, A. M. S.; Andree, K. C.; Vidotto, R.; Tzschaschel, M.; Colomba, E.; Flohr, P.; Zamarchi, R.; Rack, B.; Alunni-Fabbroni, M.; Neubauer, H.; Fehm, T.; Farace, F.; de Bono, J. S.; Iljerman, M. J.; Terstappen, L. W. M. M. EpCAM– and EpCAM+ circulating tumor cells in metastatic breast and prostate cancer patients: a multicentre study. *Sci. Rep.* **2017**, *submitted*.
181. Home | CTCTrap Available online: <https://www.utwente.nl/en/tnw/ctctrap/> (accessed on Jul 7, 2017).
182. Preparing a Buffy Coat from Whole Blood | Human Immunology Portal.
183. Lampignano, R.; Yang, L.; Neumann, M. H. D.; Franken, A.; Fehm, T.; Niederacher, D.; Neubauer, H. A Novel Workflow to Enrich and Isolate Patient-Matched EpCAMhigh and EpCAMlow/negative CTCs Enables the Comparative Characterization of the PIK3CA Status in Metastatic Breast Cancer. *Int. J. Mol. Sci.* **2017b**, *18*, 1885, doi:10.3390/ijms18091885.

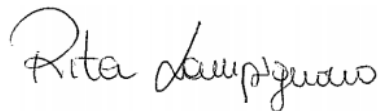
184. VyCAP Available online: <http://www.vycap.com/> (accessed on Jul 7, 2017).
185. Hollestelle, A.; Elstrodt, F.; Nagel, J. H. A.; Kallemeijn, W. W.; Schutte, M. Phosphatidylinositol-3-OH Kinase or RAS Pathway Mutations in Human Breast Cancer Cell Lines. *Mol. Cancer Res.* **2007**, *5*, 195–201, doi:10.1158/1541-7786.MCR-06-0263.
186. Kataoka, Y.; Mukohara, T.; Shimada, H.; Saijo, N.; Hirai, M.; Minami, H. Association between gain-of-function mutations in PIK3CA and resistance to HER2-targeted agents in HER2-amplified breast cancer cell lines. *Ann. Oncol. Off. J. Eur. Soc. Med. Oncol. ESMO* **2010**, *21*, 255–262, doi:10.1093/annonc/mdp304.
187. Klein, C. A.; Schmidt-Kittler, O.; Schardt, J. A.; Pantel, K.; Speicher, M. R.; Riethmüller, G. Comparative genomic hybridization, loss of heterozygosity, and DNA sequence analysis of single cells. *Proc. Natl. Acad. Sci. U. S. A.* **1999**, *96*, 4494–4499.
188. Deutsch, T. M.; Riethdorf, S.; Nees, J.; Hartkopf, A. D.; Schönfisch, B.; Domschke, C.; Sprick, M. R.; Schütz, F.; Brucker, S. Y.; Stefanovic, S.; Sohn, C.; Pantel, K.; Trumpp, A.; Schneeweiss, A.; Wallwiener, M. Impact of apoptotic circulating tumor cells (aCTC) in metastatic breast cancer. *Breast Cancer Res. Treat.* **2016**, *160*, 277–290, doi:10.1007/s10549-016-3997-3.
189. Spiliotaki, M.; Mavroudis, D.; Kapranou, K.; Markomanolaki, H.; Kallergi, G.; Koinis, F.; Kalbakis, K.; Georgoulas, V.; Agelaki, S. Evaluation of proliferation and apoptosis markers in circulating tumor cells of women with early breast cancer who are candidates for tumor dormancy. *Breast Cancer Res. BCR* **2014**, *16*, doi:10.1186/s13058-014-0485-8.
190. Kallergi, G.; Konstantinidis, G.; Markomanolaki, H.; Papadaki, M. A.; Mavroudis, D.; Stournaras, C.; Georgoulas, V.; Agelaki, S. Apoptotic Circulating Tumor Cells in Early and Metastatic Breast Cancer Patients. *Mol. Cancer Ther.* **2013**, *12*, 1886–1895, doi:10.1158/1535-7163.MCT-12-1167.
191. Rossi, E.; Basso, U.; Celadin, R.; Zilio, F.; Pucciarelli, S.; Aieta, M.; Barile, C.; Sava, T.; Bonciarelli, G.; Tumolo, S.; Ghiotto, C.; Magro, C.; Jirillo, A.; Indraccolo, S.; Amadori, A.; Zamarchi, R. M30 Neoepitope Expression in Epithelial Cancer: Quantification of Apoptosis in Circulating Tumor Cells by CellSearch Analysis. *Clin. Cancer Res.* **2010**, *16*, 5233–5243, doi:10.1158/1078-0432.CCR-10-1449.
192. Markou, A.; Farkona, S.; Schiza, C.; Efstathiou, T.; Kounelis, S.; Malamos, N.; Georgoulas, V.; Lianidou, E. PIK3CA Mutational Status in Circulating Tumor Cells Can Change During Disease Recurrence or Progression in Patients with Breast Cancer. *Clin. Cancer Res.* **2014**, *20*, 5823–5834, doi:10.1158/1078-0432.CCR-14-0149.
193. Gasch, C.; Oldopp, T.; Mauermann, O.; Gorges, T. M.; Andreas, A.; Coith, C.; Müller, V.; Fehm, T.; Janni, W.; Pantel, K.; Riethdorf, S. Frequent detection of PIK3CA mutations in single circulating tumor cells of patients suffering from HER2-negative metastatic breast cancer. *Mol. Oncol.* **2016**, *10*, 1330–1343, doi:10.1016/j.molonc.2016.07.005.

# Appendix

## **A. Statement**

Hiermit erkläre ich, Rita Lampignano, dass ich die vorliegende Dissertation selbstständig verfasst und bei keiner anderen Universität bzw. Fakultät in der vorgelegten oder einer ähnlichen Form eingereicht habe. Für die Anfertigung der Dissertation habe ich keine anderen als die angegebenen Hilfsmittel verwendet. Die Stellen, die anderen Arbeiten dem Wortlaut oder dem Sinn nach entnommen sind, wurden unter Angabe der dazugehörigen Quelle kenntlich gemacht.

Düsseldorf, den 07. November 2017

A handwritten signature in black ink, reading "Rita Lampignano". The signature is written in a cursive, flowing style.

Rita Lampignano

## **B. List of Abbreviations**

ER	Oestrogen Receptor
PR	Progesterone Receptor
AR	Androgen Receptor
HER2/neu	Human Epidermal growth factor Receptor 2
PI3K	Phosphatidylinositol 3-Kinase
BRCA1/2	BReast CAncer 1/2, early onset
RTK	Tyrosine Kinase Receptor
PTEN	Phosphatase and Tensin homolog
RAS	RAt Sarcoma
RAF	Rapidly Accelerated Fibrosarcoma
PIK3CA	Phosphatidylinositol 3-Kinase Catalytic subunit Alpha
RBD	RAS-Binding Domain
mTOR	mammalian target of rapamycin
EpCAM	Epithelial Cell Adhesion Molecule
MMPs	Matrix MetalloProteinases
EMT	Epithelial Mesenchymal Transition
CTC	Circulating tumour cell
PD-L1	Programmed Death-Ligand 1
MET	Mesenchymal Epithelial Transition
PB	Peripheral Blood
FDA	Food and Drug Administration
mBC	metastatic Breast Cancer
WBC	White Blood Cells
RBC	Red Blood Cells
EGFR	EstroGen Receptor Factor
CDCP1/CD318	CUB domain-containing protein 1
DLA	Diagnostic LeukApheresis
FACS	Fluorescence-Activated Cell Sorting
DEP	DiElectroPhoresis
PFS	Progression-Free Survival
OS	Overall Survival
DTC	Disseminated Tumour Cell
RPMI 1640	Roswell Park Memorial Institute 1640 Medium
HEPES	4-(2-hydroxyethyl)-1-piperazineethanesulfonic acid
STR	Short Tandem Repeat
DMSO	Dimethyl Sulfoxide

PBS	Phosphate Buffered Saline
rpm	revolutions per minute
RT	Room Temperature
DAPI	4',6-diamidino-2-phenylindole
PE	PhycoErythrin
APC	AlloPhycoCyanin
BSA	Bovine Serum Albumine
PerCP	PERidinin-Chlorophyll-Protein complex
PCR	Polymerase Chain Reaction
EDTA	EthyleneDiamineTetraacetic Acid
FITC	Fluorescein IsoThioCyanate
CY5	Cyanine 5
BF	Bright Field
WGA	Whole Genome Amplification
TAE	Tris base/Acetic acid/EDTA
dNTP	DeoxyNucleotideTriPhosphate
ssDNA	Single Strand DNA
NC	No Cell control buffer
WT	Wild-Type
vs.	versus
c.a.	circa
h	hours
L	litre
mL	millilitre
µl	microlitre
nl	nanolitre
min	minute
° C	Celsius degree
nm	nanometre
ng	nanogramme
M	Molar
mM	milliMolar
e.g.	exempli gratia
i.e.	id est

### C. List of Figures

Figure 1. The Hallmarks of Cancer.....	1
Figure 2. Tumour progression and heterogeneity .....	2
Figure 3. The human female breast .....	4
Figure 4. The formation of an invasive carcinoma .....	4
Figure 5. The simplified PI3K pathway .....	7
Figure 6. The PIK3CA oncogene.....	8
Figure 7. The invasion-metastasis cascade .....	10
Figure 8. The dissemination and colonization of tumour cells .....	11
Figure 9. The epithelial to mesenchymal transition.....	12
Figure 10. Frequency and size of CTCs compared to blood cells .....	14
Figure 11. Whole blood centrifuged on a density gradient.....	27
Figure 12. Workflow #1 for CTC-enrichment and detection .....	28
Figure 13. The VyCAP™ filtration device .....	29
Figure 14. VyCAP™ slide holder.....	32
Figure 15. Workflow #2 for CTC-enrichment, detection and isolation .....	34
Figure 16. <i>The Parsortix™ system</i> .....	35
Figure 17. The CellCelector™ micromanipulator.....	36
Figure 18. Ampli1™ WGA steps.....	41
Figure 19. Validation of the immunostaining #1 on cytospins.....	46
Figure 20. Validation of the immunostaining #1 on the microsieve .....	48
Figure 21. Patient-matched EpCAM <sup>high</sup> and EpCAM <sup>low/negative</sup> CTCs collected from blood samples with CellSearch® and VyCAP™ .....	50
Figure 22. Two EpCAM <sup>high</sup> and one EpCAM <sup>low/negative</sup> CTC collected from blood samples via CellSearch® and via VyCAP™, respectively.....	51
Figure 23. Patient-matched EpCAM <sup>high</sup> and EpCAM <sup>low/negative</sup> CTCs collected from DLA samples with CellSearch® and VyCAP™ .....	53
Figure 24. Two EpCAM <sup>high</sup> and one EpCAM <sup>low/negative</sup> CTC collected from DLA samples via CellSearch® and via VyCAP™, respectively.....	54
Figure 25. Validation of immunostaining #2 on cytospins .....	55
Figure 26. Validation of immunostaining #2 inside Parsortix™ cassette .....	57
Figure 27. Patient-matched EpCAM <sup>high</sup> and EpCAM <sup>low/negative</sup> CTCs enriched in blood samples with CellSearch® and Parsortix™ .....	59

Figure 28. Counts of EpCAM <sup>high</sup> and EpCAM <sup>low/neg</sup> CTCs compared with a linear regression test .....	60
Figure 29. Isolated EpCAM <sup>low/negative</sup> cells and EpCAM <sup>high</sup> cells .....	61
Figure 30. Representative Gel-Electrophoresis of WGA-QC PCR products .....	62
Figure 31. Comparison of high integrity WGA products of EpCAM <sup>high</sup> and EpCAM <sup>low/negative</sup> CTCs sorted from 13 patients.....	64
Figure 32. Representative pictures of gel-electrophoresis of PIK3CA exons 9 and 20 PCR products of amplified genomes of CTCs .....	65
Figure 33. Representative PIK3CA Exons 9 and 20 sequencing profiles within CTCs and cell lines.....	68
Figure 34. Comparison of recovery rates of MCF-7 cells achieved via VyCAP™ and via Parsortix™ systems.....	75
Figure 35. Tumour cell/leukocyte ratio in blood samples processed via VyCAP™ and Parsortix™ devices.....	76

#### **D. List of Tables**

Table 1. PI3Ks inhibitors in clinical trials .....	9
Table 2. Immunostaining mastermix #1 .....	30
Table 3. Amount of MCF-7 cells spiked per each spiking experiment .....	31
Table 4. The immunostaining mastermix #2. ....	37
Table 5. Amount of MCF-7 cells spiked per each spiking experiment. ....	38
Table 6. PIK3CA exons 9 and 20 PCR primers.....	43
Table 7. Thermal cycler program of PIK3CA exons 9 and 20 PCRs.....	43
Table 8. Thermal cycler program of ExoSAP-IT® cleaning protocol. ....	44
Table 9. PIK3CA exons 9 and 20 sequencing primers.....	45
Table 10. Amount of MCF-7 cells spiked and enriched per each spiking experiment. ....	47
Table 11. Clinical features of patients' primary tumours.....	49
Table 12. Clinical features of patients' primary tumours.....	52
Table 13. Amount of MCF-7 cells spiked, captured and harvested per each spiking experiment. ....	56
Table 14. Clinical features of patients' primary tumours.....	58
Table 15. CTCs processed for WGA show different integrity of their amplified genomes .....	63
Table 16. Amplified genomes of CTCs processed for PIK3CA exons 9 and 20 PCRs may not exhibit the presence of the respective amplicon .....	66
Table 17. Mutational analysis of PIK3CA hotspot regions in exons 9 and 20 within patient-matched EpCAM <sup>high</sup> and EpCAM <sup>low/negative</sup> CTCs.....	67



## **E. Acknowledgments**

I would like to thank Prof. Dr. Neubauer, Prof. Dr. Fehm and Dr. Niederacher for the possibility to join their research group, for their supervision and for being involved in many interesting projects, which led me to the achievement of my PhD. I thank Prof. Dr. Urlacher for the co-supervision and last but not least, the whole research lab for welcoming me and for the great practical help and moral support they have always provided me: Marina, Martin, Johanna, Liwen, André, Ellen, Franziska, Doro, Nora, Dagmar, Ulla, Leonard. Nothing would have been possible without you!

Many sincere thanks!

## **F. Scientific Curriculum Vitae**

### **PhD at the Heinrich-Heine-University (HHU), Düsseldorf**

---

- 11/2014 – 11/2017 **Institute for Obstetrics and Gynaecology of the University Hospital of Düsseldorf**  
Prof. Dr. T. Fehm, Prof. Dr. H. Neubauer (Supervisor)  
PhD in Biology  
Final degree: Dr. rer. nat.  
Main Topic: Enrichment, isolation and molecular characterization of circulating tumour cells in metastatic breast cancer patients, for treatment strategies optimization
- 11/2014 – 11/2017 PhD student of the Düsseldorf School of Oncology and of the Interdisciplinary Graduate and Research Academy Düsseldorf

### **Academic Studies at the “Aldo Moro” University, Bari, Italy**

---

- 06/2014 – 09/2014 **Italian State Examination for Biologists**  
Final degree: officially certified Biologist
- 10/2011 – 03/2014 **Master’s degree in Medical Biotechnology and Molecular Medicine**  
Final degree: Master of Science
- 10/2007 – 07/2011 **Bachelor’s degree in Health and Pharmacology Biotechnology**  
Final degree: Bachelor of Science

### **Internships**

---

- Veterinary Clinics and Animal Productions Unit, Department of Emergency and Organ Transplantations of the “Aldo Moro” University, Valenzano (BA), Italy**  
Prof. Dr. M.E. Dell’Aquila
- 09/2013 – 03/2014 Master’s thesis  
Topic: Holding immature oocytes in meiotic inhibitor-free medium: effects on nuclear chromatin, bioenergy parameters and embryonic development after ICSI in a large animal model
- 09/2010 – 07/2011 Bachelor’s thesis  
Topic: “Valutazione dell'attività mitocondriale e livelli intracellulari dei ROS embrioni murini vitrificati” - *Evaluation of mitochondrial activity and ROS levels in vitrified mouse embryos*

## Publications

---

**Lampignano R**, Yang L, Neumann M, Franken A, Fehm T, Niederacher D, Neubauer H. A novel workflow to enrich and isolate patient-matched EpCAM<sup>high</sup> and EpCAM<sup>low/negative</sup> CTCs enables the comparative characterization of the PIK3CA status in metastatic breast cancer. *Int J Mol Sci.* 2017, 18, 1885.

**Lampignano R**, Schneck H, Neumann M, Fehm T, Neubauer H. Enrichment, isolation and molecular characterization of EpCAM<sup>negative</sup> circulating tumor cells. *Adv Exp Med Biol.* 2017, 994, 181–203.

**Lampignano R**, Fehm T, Neubauer H. The role of CTCs in breast cancer. *Oncogenomics. Expected in January 2018.*

de Wit S, Manicone M, Rossi E, Trap EK, **Lampignano R** et al. EpCAM– and EpCAM+ circulating tumor cells in metastatic breast and prostate cancer patients: a multicentre study. *Sci Rep.* 2017, *Submitted.*

## Speeches at Congresses

---

**8. Wissenschaftliches Symposium der Kommission Translationale Forschung (11/2016)** Molecular insights in EpCAM<sup>low/negative</sup> CTCs non-detectable by the CellSearch® system in metastatic breast cancer.

**32. Deutscher Krebskongress (02/2016)** Enrichment, detection and isolation of EpCAM<sup>negative</sup> circulating tumor cells of breast cancer combining Parsortix© system and CellCelector™ micromanipulator.

## Posters at Congresses

---

**3rd ACTC Advances in Circulating Tumour Cells (10/2017)** Enrichment, isolation and PIK3CA mutational analysis of patient-matched EpCAM<sup>low/negative</sup> and EpCAM<sup>high</sup> CTCs in metastatic breast cancer patients.

**19th International AEK Cancer Congress (04/2017)** Characterization of the PIK3CA status within EpCAM<sup>low/negative</sup> CTCs in metastatic breast cancer.

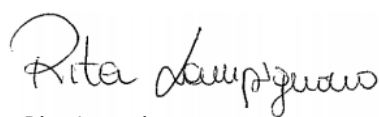
**62. Deutsche Gesellschaft für Gynäkologie und Geburtshilfe (10/2016)** How to isolate and characterize EpCAM<sup>negative</sup> circulating tumor cells in metastatic breast cancer.

**36. Deutsche Gesellschaft für Senologie (05/2016)** A novel label-free workflow to enrich and isolate single EpCAM<sup>negative</sup> circulating tumor cells in metastatic breast cancer.

**10th ISMRC International Symposium on Minimal Residual Cancer (03/2016)** The combination of Parsortix© system and CellCelector™ micromanipulator enables the characterization of EpCAM<sup>negative</sup> circulating tumor cells in breast cancer.

**7. Wissenschaftliches Symposium der Kommission Translationale Forschung (10/2015)** Detection of EpCAM<sup>negative</sup> circulating tumor cells by using VyCAP filters technology.

Düsseldorf, 07.11.2017



Rita Lampignano